A Novel Sand Control Testing Methodology to Simulate Radial Flow regime in SAGD Wells

by

Phuong Hoang Nguyen

A thesis submitted in partial fulfilment of the requirements for the degree of

Master of Science

in

Petroleum Engineering

Department of Civil & Environmental Engineering
University of Alberta

Abstract

Sand control devices (SCDs) such as Slotted Liners (SLs) have been playing a crucial role in sand production for Steam Assisted Gravity Drainage (SAGD) operations. Lately, optimizing and selecting the proper design of SCDs in the laboratory to quantify and qualify the SCD's performance is gaining significant attention from the industry.

Researchers have been investigating and developing sand control testing setups to evaluate the performance of different SCDs under varying well conditions. Many laboratory sand control apparatuses with various procedures have been introduced, such as the pre-packed Sand Retention Test (SRT) and Scaled Completion Test (SCT). Notably, these current testing facilities employ a linear flow regime, which does not represent the actual SAGD conditions where the fluid towards the well follows radial flow geometry. Little effort has been spent on examining how sand production and fines migration change in conjunction with the radial flow geometry rather than the linear flow regime.

This thesis introduces and describes a Full-scale Completion Testing (FCT) facility accompanying its testing protocol. The assembly aims to emulate the radial-flow conditions observed in SAGD production wells. Rather than conducting the laboratory testing with disk-shaped screen coupons employed in current testing facilities, the FCT employs cylindrical-shaped screens that allow replicating the flow geometry in the near-coupon region much more closely to the actual in-situ conditions. The assembly is considered an advanced facility to evaluate the performance of SCDs under radial-flow conditions regarding sand retention and plugging performance.

Many single-phase tests with brine flow were carried out to mitigate the facility's limitations through numerous improvements identified after each experimental work. Based on the

experimental results obtained from successful tests, the flow distribution around the screen was determined to be uniform by investigating the pressure distribution and fines concentration inside the sand pack. Two identical tests verified the testing repeatability in terms of differential pressures, fines production, and sanding levels. The facility can confidently assess the sand retention efficiency under the radial flow regime, which is a more representative testing condition than linear flow.

According to comparisons performed between the vertical and horizontal tests, it is noticeable that pressure readings, permeability, and fines production follow similar trends with small variations in these two positions. Regarding cumulative sand production, lesser sanding levels were observed regarding the horizontal direction than the vertical one. Additionally, lower fines migration was noticed in radial-flow tests than linear-flow experiments, which can be attributed to lower velocities and weaker drag forces far from the liner, which is the nature of radial flow configuration.

The study elaborates on the real SAGD flow geometry around the sand control device using the innovative FCT experimental setup and testing procedure, allowing assessing the liner performance under more realistic testing conditions. Testing results obtained from the assembly can be utilized to complement and validate the current testing procedures, which mostly incorporate the linear flow geometry. The facility and operational procedures could be custom-built based on any objectives and motivations concerning SCDs.

Dedication

This dissertation is dedicated to my dearest family.

Acknowledgments

I want to express my sincere appreciation to Dr. Alireza Nouri for his valuable guidance, support, and kind help throughout my master's program. I much appreciate the opportunity to pursue my research under Dr. Nouri's supervision. He has always been accessible and willing to help me with my research. I have learned from him the skill of critical thinking and a rigorous attitude towards research.

I would like to express my deepest gratitude to my family. I much appreciate their unconditional love and support for me. I also want to thank my friends, including Luis, Gene, Martin, and Vincent, for supporting me even during the most challenging time.

I also want to thank my colleagues Dr. Mohammad Haftani, Dr. Mahmood Salimi, Arian Velayati, Rahman Miri, José Bitencourt Zimmermann, and Chenxi Wang. Especially, I am thankful to Dr. Mohammad Haftani for his countless bits of help and assistance in this research.

I gratefully acknowledge RGL Reservoir Management Inc and NSERC for funding this research.

Table of Contents

List of Tables

List of Figures

List of Symbols and Abbreviations

Symbols

A_c	Total surface area of a coupon
C_w	Wellbore circumference
Q_{lab}	Injection rate in the laboratory scale
Q_{field}	Production rate in the field scale
Q_w	Brine flow rate
P_e	External pressure
P_w	Wellbore pressure
l_w	SAGD well length
k	Permeability
μ_w	Water viscosity
h	Thickness
r_e	External radius
r_w	Wellbore radius
α	Non-contributing liner connection
β	Slot plugging potential

Abbreviations

CHOPS	Cold Heavy Oil Production with Sand
CSS	Cyclic Steam Stimulation
CNRL	Canadian Natural Resources Limited
CFD	Computational Fluid Dynamics

DAQ	Data Acquisition
FCT	Full-Scaled Completion Test
OFA	Open Flow Area
PSD	Particle Size Distribution
PPS	Precise Punched Screens
SL	Slotted Liner
SAS	Stand-alone Screen
SAGD	Steam Assisted Gravity Drainage
SCD	Sand Control Device
SRT	Sand Retention Test
SRTS	Sand Retention Test with Stress
SCT	Scaled Completion Test
WWS	Wire-Wrapped Screen

Chapter 1: Introduction

1.1 Background

Canada's proven heavy oil reserves are estimated to be around 171 billion barrels, which are one of the largest oil reserves in the world (Natural Resources Canada, 2019). The surface oil sands, which is feasible by mining, are roughly 20% of the total oil sands area. Thus, non-minable resources must be recovered by in-situ techniques (CAPP, 2020). In-situ thermal recovery by Steam Assisted Gravity Drainage (SAGD) accounted for nearly 60% of total bitumen production in 2018 (CAPP, 2020). This technique is presently preferred as the primary method for in-situ heavy oil production.

SAGD is a bitumen extraction process employing two horizontal wells in a target reservoir. High-pressure, high-temperature steam is injected into the injection well to heat the heavy oil and bitumen and reduce its viscosity. By way of gravity, low viscosity emulsion composed of melted bitumen and condensate water flows toward the bottom well before being pumped out to the surface (Butler, 1992).

Sand production is considered to be a significant problem in SAGD operations due to the unconsolidated formation where SAGD is operated. Sand Control Devices (SCDs) are installed to prevent sand production in the SAGD process while controlling the inflow of reservoir fluids into the wellbore to the surface. Slotted Liner (SL), Wire-Wrapped Screen (WWS), and Punched Screen (PS) are the main completion tools to control the sanding in sand prone formations (Zhang, 2017; Montero et al., 2018).

The most current popular SCD options are slotted liners and wire wrapped screens (Sheng, 2013). A slotted liner is a pipe with multiple longitudinal slots spread along the length and around the circumference of the pipe. A wire wrapped screen consists of a perforated structural pipe to provide unimpeded flow and a specially shaped wire wound around it. The gaps between the wire wraps provide the sand control.

The primary purpose of any SCDs is to give sand retention at the designed levels and allow the reservoir inflow while discharging fines to avoid slot plugging (Bennion et al., 2009). SCDs vary in many aspects from open flow area, manufacturing, retention, and cost. The optimum SCDs for

a given problematic situation is one that reduces sand production to acceptable levels with minimal inflow resistance at the lowest economic cost.

Conventionally, the design criteria for SCDs had been either based on empirical correlations or field experience. However, a growing interest in employing sand control laboratory testing has been seen observed in recent years, which aims to aid in the selection and design of SCDs for SAGD operations. Sand control laboratory testing is considered to be a cost-effective and accurate approach to select suitable sand control applications for a given process. Also, the experiments help researchers to obtain the necessary information to implement comprehensive numerical simulation and design studies.

Typically, the primary motivation of sand control testing is to try to replicate near-wellbore conditions as much close as possible. The experiments are simplified to a certain extent by employing some simplifying assumptions for practicality. Test assumptions should always be re-evaluated if possible, to increase testing's reliability when applying in the real world.

1.2 Problem Statement

Selecting optimum SCDs through sand control experiments has been investigated for years since 1938 (Coberly, 1938). However, researchers started focusing on employing sand control testing in the SAGD context for just about a decade (Bennion et al., 2009). Many laboratory setups under different conditions have been set up to either study performance of SCDs or obtain an understanding of various testing parameters on the SCD performance. However, to simplify the laboratory experiments, some simplifying assumptions have been made, aiming to reduce the complexity of the real-world conditions. In detail, the linear flow configuration rather than the radial one has been established as the primary flow regime inside the sand pack. Regarding the linear flow, with the placement of the coupon at the bottom of the sand pack, the testing facilities could only partially simulate the top position of the liner.

Little focus has been given towards the radial flow regime, representing the real SAGD wells. Most research works in the past (Markestad et al., 1996; Ballard and Beare, 2003, 2006; Bennion et al., 2009; Romanova et al., 2014; Devere-Bennett, 2015; Wang et al., 2018, 2020a, 2020b, 2021; Montero et al., 2018; Fattahpour et al., 2018) have been based on experiments considering the linear flow. Unlike the unchanged velocity profile along the sand pack in most testing facilities

employing the linear flow configuration, the profile of radial flow velocity follows an exponential trend. In the radial flow regime, flow velocity increases more rapidly when it comes closer to the liner because the open area to flow decreases when approaching the wellbore. As a result, the magnitude of the drag forces generated by fluid velocities with the radial flow geometry is different compared to the linear flow. Overall, the impacts of the radial flow regime on screen performance have not been investigated thoroughly.

This study employs a Full-scale Completion Testing (FCT) facility to assess the performance of the slotted liner regarding a radial-flow condition. Following that, suggestions for testing improvements are also presented to troubleshoot the FCT setups being identified from the experimental works. In the experiments, consistent sand preparation and packing methods were used to ensure consistency for the experiments. Various sand control experiments with a single-phase brine have been performed to provide better understandings of the effect of the radial flow configuration on sand production. Within the thesis, the impacts of the radial flow geometry on sand production and fines migration are investigated.

1.3 Research Objectives

A novel testing facility is commissioned into the laboratory to evaluate the effects of the radial flow on the SCD performance both in the vertical and horizontal directions. Single-phase scenarios of brine injection for slotted liners are performed, and testing results are investigated to improve the equipment. After each experiment, the setup designs are studied to identify the limitations of the device accompanying modifications to mitigate the testing deficiencies in terms of the setup and test procedure. The improvements are proven by repeating the tests and reducing the primary sources of errors. The ultimate purpose of the facility's modifications is to establish a uniformly radial fluid injection, which is verified by checking the pressure distribution and fines concentration inside the sand pack. Also, test repeatability is determined by a couple of identical tests.

The thesis also analyzes the impacts of the radial flow on produced sand and fines migration inside the sand pack. The study aims to evaluate how permeability and pressure drop are distributed concerning the radial flow regime. Besides, the comparison between the vertical and horizontal testing conditions is investigated to highlight the impacts of different flow conditions on the

experimental results. It is more representative to resemble in-situ conditions in the laboratory incorporating the radial flow regime rather than the linear flow.

1.4 Research Hypothesis

It is common knowledge that the flow regime around the SAGD wellbore is radial but not linear. Conducting the testing considering the radial flow should provide more accurate results compared to the linear one. However, performing this type of testing requires more time and cost, and these experiments are considered to be much more complicated.

Concerning radial flow conditions, the pressure drop is much higher than the linear flow regime due to flow convergence under the same conditions. Slots on the liner cause the flow towards the slot to deviate in the region close to the liner. Therefore, flow streamlines towards the well generate additional pressure gradients, increasing the likelihood of sand production. Ignoring the radial flow regime in most of the experimental works in the past would lead to the underestimation of pressure drops. Besides, it is essential to account for the force combination adjacent to the liner. The gravity force acting on sand particles in the near-coupon region for a vertical liner helps the particles remain in their places. While for a horizontal liner, gravity helps to destabilize the grains at the liner top while preventing the sand production at the liner bottom.

The level of fines migration concerning the radial flow configuration is supposed to be much more non-uniform compared to the linear flow in which the flow velocity is constant along the sand pack. The differences in terms of fines migration between two flow regimes can be attributed to the magnitude of drag forces generated. In the linear flow regime, the expectation is to observe fines migration occurring over the entire length of the sand pack. On the other hand, concerning the radial flow geometry, owing to the weaker drag forces generated by smaller fluid velocities at far distances away from the liner, fewer particles could be detached and displaced towards the liner.

Besides, in the comparison between the vertical and horizontal directions, the total sand produced in the horizontal configuration is expected to be lower than the vertical one, owing to the higher plugging potential of the upward flow around the liner. In other words, the plugging issue occurring regarding the horizontal condition is supposed to be more severe than the vertical one.

1.5 Research Methodology

The thesis attempts to get the FCT facility commissioned. The apparatus is considered to be advanced equipment in the assessment of the sand production process in oil sands to replicate the conditions of the SAGD production wells. The testing device is capable of conducting experiments under the radial flow regime in both vertical and horizontal directions. The improvements have been made over the setup from testing to testing to address the facility's deficiencies. The research steps are performed as follows:

1. Review SCDs' performance in a comparison between radial and linear flow.
2. Commission the testing facility in the laboratory for the case where the liner is in the vertical position.
3. Identify the limitations regarding the testing setup along with corresponding improvements over the equipment.
4. Test and check the repeatability of the modified experimental setups. The facility is verified to be more representative of the actual conditions of SAGD wells. Besides, the equipment can confidently provide a uniform radial inflow towards the sand control screen.
5. Use the assembly with the liner in the horizontal condition, which is a closer representation of SAGD production wells.
6. Identify the limitations concerning the new design of the machinery under the horizontal direction along with corresponding attempts and efforts to mitigate them.

1.6 Significance of the Work

Designing slotted liners play an essential role in the performance of the production well in SAGD operations. The improper design would cause massive sand production, low flow efficiency, and liner erosion. Therefore, in oil sands reservoirs, the optimum design of the SCDs is critical work in attempts to reduce the sand production and increase the reservoir productivity for SAGD producers. Many sand control testing apparatuses have been utilized to assess the performance of SCDs. However, current testing facilities are employing the linear flow regime, which is not the actual flow geometry around the wellbore.

This research introduces a full-scale completion testing methodology for performing sand control laboratory testing incorporating the radial flow regime to mimic more realistic SAGD producer

wells under laboratory conditions. A cylindrical-shaped screen is employed in the equipment instead of a disk-shaped screen coupon, which enables to capture better the actual SAGD operations. Utilizing the facility helps to evaluate the SCDs' performance more practically.

Besides, the study provides detailed knowledge to run the facility properly through a standard operating procedure outlined. Evaluation of slotted liner performance regarding the radial flow condition gives better understandings concerning the influence of flow regime on the sand retention and plugging tendencies. The research also presents difficulties and challenges while performing the experimental tests under both vertical and horizontal conditions with accompanying modifications to tackle them.

1.7 Thesis Structure

The thesis consists of 5 chapters:

- Chapter 1 provides a general overview of the problem and introduces the scope of the work and methodology to address the issue.
- Chapter 2 presents a literature review on the SAGD regarding the radial flow and stand-alone screens and compares the linear and radial flow.
- Chapter 3 outlines in detail the experimental setup, testing material, testing plan, and testing procedure.
- Chapter 4 presents how improvements in the testing facility are implemented via experimental works. This chapter explains how modifications are identified to troubleshoot the equipment's deficiencies, showing the extent of difficulties in carrying out the test. The testing repeatability is verified. Also, the comparison of experimental results between the vertical and horizontal directions is performed.
- Chapter 5 summarizes outstanding contributions as well as ideas and suggestions for future studies.

Chapter 2: Literature Review

2.1 Introduction

Canada has the third-largest oil reserve in the world, where 170 billion barrels of oil can be recovered economically with today's technology, and 165 billion barrels are located in the oil sands (CAPP, 2019). Because 97% of the proven oil reserves are in unconsolidated oil sands (CAPP, 2020), dealing with sand production is a vital task. Three main techniques have been used widely to exploit oil resources: (1) in-situ mining for the depth of under 50m, (2) primary production, and (3) thermal operations.

For shallow reservoirs buried within the depth of around 50m, the standard technology employed is open-pit mining by operators like CNRL and Canadian Oil Sands Ltd. (Robert and Abbakumov, 2014). Exploiting the reserves with the mining technique has some limitations relating to the potential restrictions of the facility. The method can only be applied economically for shallow deposits, accounting for less than 20% of Alberta's bitumen production (CAPP, 2020). Besides, oil sands mining requires landscape alterations and extensive water usage, which affect the environment.

Regarding the primary production, the technology is Cold Heavy Oil Production with Sand (CHOPS). The drawback of this technique is high operational cost reaching up to 15-20% of the whole project (Dusseault, 2002). This high cost is due to processing produced solids with a low ultimate recovery of around 10% (Dusseault, 2002).

Currently, 80% of oil sands reserves recovered is carried out through thermal in-situ operations (CAPP, 2020) such as Cyclic Steam Stimulation (CSS) and Steam Assisted Gravity Drainage (SAGD) (Zhang et al. 2007). The primary objective of these techniques is to provide heat to the unconsolidated formations to improve the mobility of the heavy oil in place, and therefore facilitate the heavy oil production towards the surface.

Concerning the CSS technique, the operation involves injecting steam into a well, then a soaking period followed by the production period (Bybee, 2003). CSS is more environmentally friendly than mining because it requires minimal landscape dislocation. Also, the ratio of water to produced oil is about 1:1, and the ultimate recovery could reach around 25% (Jimenez, 2008). However, the

high injection steam pressure during the injection period can cause cyclic and thermal stresses arising around the wellbore, potentially resulting in the failure of the wellbore (Albahlani and Babadagli, 2008).

The SAGD technology, which is the focus of this research, is the most important recovery technique for exploiting bitumen in Alberta. The SAGD processes cause the lowest negative impact on the landscape and require a smaller amount of water for oil production compared to open-pit mining (Lightbown, 2017). Furthermore, SAGD operations show a high ultimate recovery of 50% or more and outperform other in-situ techniques (Handfield et al., 2009).

SAGD operations comprise of two technologies (Figure 2-1). The first one is to inject a large volume of steam into the formation of interest. The second technology is two horizontal wells of a separation distance of approximately 5 meters, which are parallel. The upper wells act as a steam injector, and the lower ones serve as the production well. Injecting steam would create a vapor champer rising in the formation, allowing contact between cold bitumen with high viscosity and hot steam. Because of the contact, the bitumen would be heated, and its viscosity then reduces to a low magnitude of 8-20 cp (Devere-Bennett, 2015). By decreasing heavy oil viscosity, oil would be able to flow with the support of gravity towards the producing well in which a mixture of oil and brine can be pumped to the surface thanks to the artificial lift technique. Typically, the operating temperature during the SAGD operations ranges from 150℃ to 270℃ (Irani, 2013).

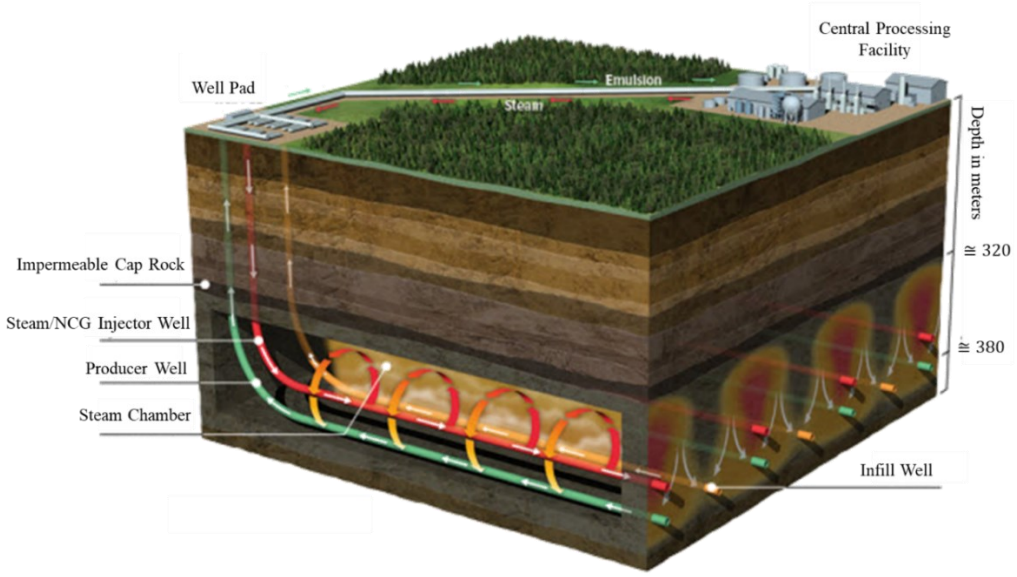

Figure 2-1. Schematic of the idealized SAGD operations

When production is in progress, a sub-cool being maintained between the injector and producer is around $20 - 40^{o}C$ (Edmunds, 2000; Gates and Leskiw, 2010), forming a pool of liquid around the producer called the steam trap. The steam trap is crucial in SAGD operations because it helps to prevent steam breakthrough from occurring in the injector. The steam breakthrough results in high potentials of massive sand production (Gates and Leskiw, 2010). However, many SAGD wells have experienced steam breakthrough episodes owing to poor drilling (Brooks and Tavakol, 2012), operational practices (Irani, 2013), and completion design. Because most bitumen reservoirs are found in loosely consolidated or unconsolidated reserves, sand control screens must be installed to prevent sand production.

2.2 Sand Production in SAGD

Sanding is encountered in many wells during the production phase. Wellbore integrity is put at high risk when excessive sand production occurs. Sand production could also lead to loss of productivity and mechanical failure of downhole equipment and surface facility. These problems add up to the total production cost.

In the petroleum industry, sanding problems have existed since the beginning of oil production (Matanovic et al., 2012). Oil sands reservoirs are typically unconsolidated with negligible compressive strength and high sanding potential (Penberthy and Shaughnessy, 1992). Sanding occurs when the oil flow velocity is high enough to overcome inner forces that hold grains together (Penberthy and Shaughnessy, 1992).

Another potential contributor to sanding is the steam hammering effect during the start-up period. Steam hammer may disturb the near-wellbore region and destroy inner-granular cohesive bonds, resulting in excessive sand production (Irani, 2013). The steam hammer occurs when a rapid condensation takes place as the liquid phase isolates steam. High enough heat transfer may take place, which causes the vapor void to collapse, producing a massive pressure shock (Irani, 2013).

As previously reported in the literature, sand production higher than 3-4% of produced mass can harm surface devices (Burton et al., 2005). Moreover, produced sand concentrations above 1% can be problematic to the functionality of Electrical Submersible Pumps (ESP), as reported by Devere-Bennett (2015).

Different combinations of physical forces that are gravitational force and hydrodynamic forces, including drag force and pressure gradient force, act on sand grains around the wells (Figure 2-2). Concerning the vertical wellbore, hydrodynamic forces (Fd) are the forces pushing the grains toward the liner. In contrast, gravity force (W) tends to hold the grains in their place, as demonstrated in Figure 2-2a.

Regarding horizontal wellbores, the role of gravity force depends on its position with respect to the wellbore (Figure 2-2b). For example, the gravity and drag forces supplement each other to displace the sand grains located above the screen into the wellbore. Conversely, the gravity force resists the hydrodynamic forces at the screen bottom and reduces the ability to produce sand. Therefore, it is essential to consider the flow configurations and their effects on not only sanding but also fines migration as well as plugging tendencies in the sand control testing.

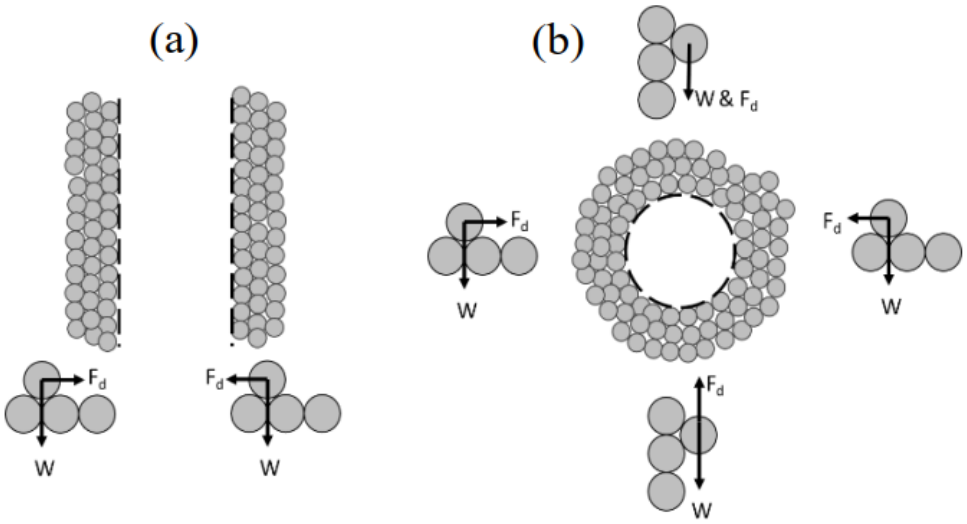

Figure 2-2. The forces acting on particles around the a) vertical and b) horizontal wellbore in an unconsolidated oil sand reservoir, after Haftani et al. (2020)

2.3 Stand-alone Screens (SASs)

Many designs of sand control devices have been devised and developed in the oil and gas industry. In the scope of this study, only stand-alone sand control devices that have been employed for SAGD wells will be discussed. They are Slotted Liners (SLs), Wire-Wrapped Screens (WWSs), and Precise Punch Screens (PPSs). Slotted liners and wire-wrap screens are most widely employed

(Sheng, 2013). For the slotted liners, they are the least expensive and are considered to be suitable selections for thermal projects with low flow rates (Bellarby, 2009).

Selection of SCDs involves many contributing elements such as reliability, cost, productivity impairment, sand quality (PSD), reservoir heterogeneity and characterization, fines content, the potential cost of reparation and workover, expected production, and company policies (Suman et al., 1985). It can be very detrimental to the economics of the recovery process if stand-alone screens are selected inappropriately, which leads to their failure causing either well sanding or plugging.

2.3.1 Slotted Liners (SLs)

In slotted liners, slots with a certain length, distribution density, and geometry are cut into a solid pipe. They are relatively inexpensive sand control solutions being implemented in low economics and well-sorted sand reservoirs where production is at a low rate, and oil viscosity is high (Kaiser et al., 2000; Matanovic et al., 2012). The main reason why slotted liners have been commonly used in SAGD is that they offer good mechanical integrity and come with a low cost per foot when comparing to other sand control devices for horizontal well completion (Sheng, 2013). Besides, the slotted liners have the advantage of providing a variable slot density to optimize the inflow or outflow distribution (Kaiser et al., 2000).

Open Flow Area (OFA) is the total area of slots divided by the total surface area (Matanovic et al., 2012). SLs provide the lowest OFA in comparison with other stand-alone screens (Montero, 2019). Generally, slots' specifications deliver OFA between 1 to 3% depending on the slot density and the slot width (Spronk et al., 2015). However, the maximum OFA is restricted to 1.5%, considering mechanical integrity (O'Hara, 2015).

Slot width and geometry are decisive factors that determine slot plugging, affecting the slotted liner lifetime (Sheng, 2013). There are three main slot geometries involving straight, keystone, and rolled/seamed tops, shown in Figure 2-3. Straight cut type with a uniform width across the liner thickness is machined by a single blade plunge providing the same width along the slot. The keystone shaped slots have a larger inner width than the outer width being manufactured by two blades plugging at different angles at specified aspect ratios (external width/internal width). This shape provides a mechanism that lowers plugging tendencies by creating the easier passage of

produced sand grains and fines (Bennion et al., 2009; Fermaniuk, 2013). The rolled top or seamed slots have varying slot width across the liner thickness. This type is an improved version of the straight cut slot where the application of longitudinal stresses on the surface of the outer side of the slot causes it to deform plastically around 1mm inwards.

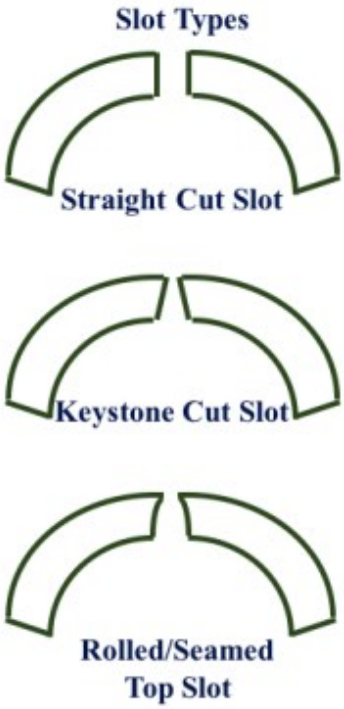

Figure 2-3. Different slot configurations for the slotted liners, after Guo et al. (2018)

Another problem contributing to the plugging potential of the slotted liner is corrosion (Romanova and Ma, 2013). Developments in a coating such as High-Phosphorus Ni-P coating have displayed promising results in terms of a decrease in corrosion and scaling, prolonging the lifetime of the liners, as reported by Sun et al. (2018).

SCDs provoke a transformation of the flow streamlines in the near-coupon region (Kaiser et al., 2002). This phenomenon is called flow convergence (Figure 2-4), which plays a vital role in determining the inflow repairment and screen performance. An additional pressure drop caused by flow convergence can increase fines migration, which reduces the retained permeability (Mahmoudi et al., 2017a).

Kaiser et al. (2000) claimed that the impact of slot density is much more considerable on inflow resistance than slot width and open area (Kaiser et al., 2000). This statement emphasizes the significance of slot spacing in the design of SLs.

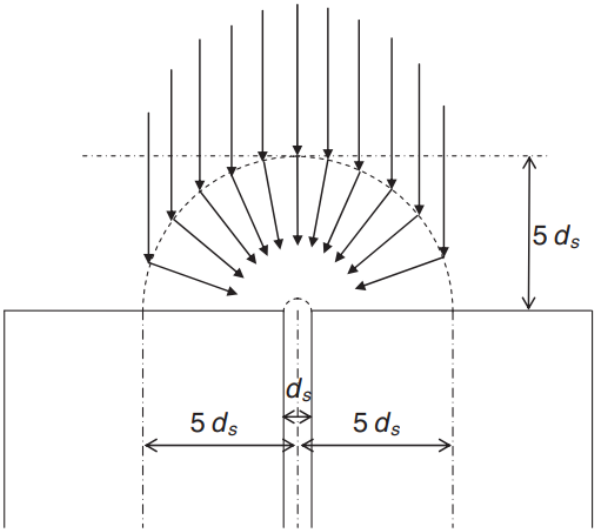

Figure 2-4. Schematic of the flow convergence toward a wire-wrap screen, after Chanpura et al. (2011)

Besides, according to Computational Fluid Dynamics (CFD) studies implemented on slotted liners, it was reported that an OFA higher than 3% would not impact the flow distribution within the SAGD wells and the reservoir (Sivagnanam et al., 2017). Recent studies have indicated that slotted liners with the low OFA render higher plugging issues compared to WWS (Romanova and Ma, 2013; Romanova et al., 2014; Wang et al., 2020a).

2.3.2 Wire-Wrapped Screens (WWSs)

The wire-wrapped screen was initially introduced by Layne and Gerwick (1973). Wire-wrapped screens are made of a continuous triangular or trapezoidal cross-sectional stainless-steel wire being wrapped and welded onto ribs or rods which are attached to a base pipe (Figure 2-5). AISI 304L or 316L steel wire is employed to fabricate the outer wire jackets to provide a corrosion-resistant feature (Romanova et al., 2014).

The OFA of WWSs ranging from 6 to 12%, depending on the slot size, wire thickness, and the screen percentage per joint, surpasses the 1-3% OFA provided by SLs (Spronk et al., 2015). The high OFA allows less resistance to flow and reduces flow velocities at the sand bridges, resulting

in a lower level of sanding problems (Suman et al., 1983; Bellarby, 2009). Nonetheless, it is worth noting that the higher OFA of WWSs does not guarantee better screen performance than SLs (Fattahpour et al., 2018), although WWSs typically work better than SLs for the same formation properties.

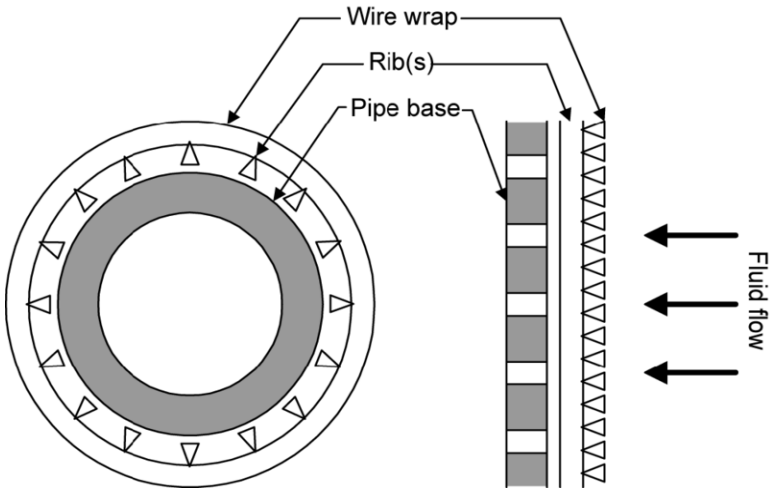

Figure 2-5. Wire-wrapped screens, after Zhang (2017)

Besides, the distance between wire slots in WWSs is smaller, decreasing the influence of flow convergence (Kaiser et al., 2002). WWSs are often more costly than SLs owing to the material and the design (Fattahpour et al., 2018). The lower cost explains why SLs are sometimes selected over WWSs in SAGD operations (Fattahpour et al., 2018).

2.3.3 Precise Punched Screens (PPSs)

Recently, PPSs have gained more attention in the thermal recovery context, owing to its relatively high OFA and low cost (Matanovic et al., 2012; Spronk et al., 2015; Fattahpour et al., 2018). In the punched screens, a punched filtration jacket made of stainless steel is welded onto a carbon-steel perforated base pipe (Figure 2-6). The jacket gives a strong corrosion-resistant feature, and the base pipe provides mechanical integrity. Its application easily allows the formation fluids to flow into the screen through punched slots while preventing the formation sand from entering the filtration jacket. It is reported that the PPSs are durable against corrosion (Yang and Macaraeg, 2013). Recently, laboratory testings have been performed to compare the performance between PPS and SL. It is found that PPSs lower plugging potential due to its OFA ranging from 6-14%, which is at least three times higher than SLs (Zhang, 2017; Wang et al., 2021). In addition, another

finding is that PPSs present better resistance to liner collapse, owing to at least four times the mechanical strength higher than SLs (Zhang, 2017).

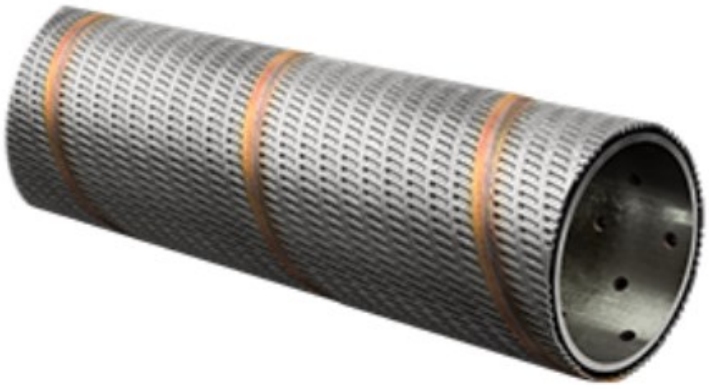

Figure 2-6. Precise Punched Screen, after RGL Reservoir Management Inc (2018)

2.3.4 Failure of Sand Control Screens

In ideal situations, SCD's installation should have no impact on wellbore productivity (Parlar et al. 2016). In real-world conditions, the utilization of SCDs in the oil sands reserves has been encountering different risks, which result in failures of the screen. The loss of the intended purpose of the devices would lead to catastrophic sanding production, accompanying a substantial decrease in oil production. The primary failure sources of any SCDs are plugging, corrosion, erosion, and collapse.

Erosion can occur at any free surface within the sand formation. Regarding the wellbore employing the SCDs, the screen wires or slots can be worn by high inflow velocities, damaging the original design. For cases where plugging of the slots and near-screen porous media occurs, the effects of erosion are getting worse (Hamid and Ali 1997; Gillespie et al. 2009). Besides, the steam breakthrough can cause erosive damage to the sand control liner, yielding a massive amount of sand production (Toma et al. 1988; Das, 2005). The productivity impairment can result from the plugging of the screen slots caused by corrosion (Bennion et al., 2009; Romanova and Ma, 2013).

Recently, the significance of the plugging issue in SAGD operations has been underlined by some researchers (Romanova et al., 2014; Fattahpour et al., 2016). Many detrimental problems consisting of reduction of the wellbore productivity, the increase of the steam-oil ratio, higher potential of steam breakthrough, and prevention of a uniform growth of the steam chamber, which are caused by the rise of the pressure differential between the well-pair (Bennion et al., 2009), have

been attributed to the slot plugging (Romanova et al., 2014). In the past researches, it is reported that the plugging owing to sand grains is unlikely to happen (Bennion et al., 2009; Chanpura et al., 2012; Romanova and Ma, 2013). The main issues adding up to the plugging problems of the liner are corrosion, scales, and clay particles trapped in the slots (Romanova and Ma, 2013). The illustration of how clay films develop inside the slots can be seen in Figure 2-7. WWSs employing stainless steel such as AISI 304L, and 316L can provide strong resistance to corrosion (Romanova et al., 2014). Conversely, the carbon-steel base pipe can experience severe corrosion (Mahmoudi et al., 2018).

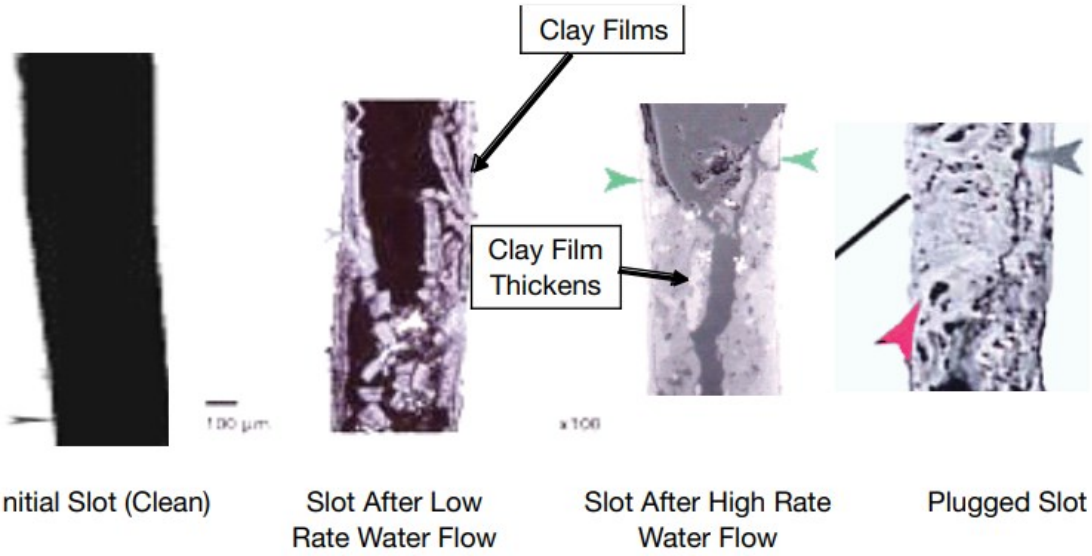

Figure 2-7. The photo illustration of the evolution of clay films inside the slots over time, after Bennion et al. (2009)

Another factor affecting the sand control ability of the SCDs is integrity loss in the base pipe compromised by the flow of high-velocity wet steam in the steam breakthrough (Mahmoudi et al., 2018). Besides, screen plugging can occur owing to screens installed in poorly conditioned mud, the mixture of mud particles with formation sand, filter cake mixed with formation sand, mixing of coarse and fine sands from different zones, and clay or shale mixed with formation sand (Chanpura et al., 2012).

2.4 Sand Control Evaluation in Testing Types

Experimental setups have been implemented lately to assist in the optimum selection of SCDs for given conditions, such that there is an acceptable solid retained in conjunction with a minimum

loss in wellbore productivity. The laboratory testing is designed to represent field conditions as much close as possible to assess the performance of screens under lab conditions. Its primary objective is to measure the total amount of produced sand and flow impairment based on screen/sand pack permeability measurements. Usually, the flow resistance is evaluated in terms of pressure drops or retained permeability. The retained permeability is the ratio of final permeability at the area close to the SCD over the initial permeability of the top section (Mahmoudi et al., 2016). The retained permeability is used to quantify the extent of permeability reduction.

Sand control evaluation tests include scaled and full-scale liner tests (Montero et al., 2018). There is no existing standard operating procedure for any sand control testing types. As a result, there are current differences in various aspects such as height, diameter, sand preparation, fluid and flow characteristics, phase ratios, and measurements encountered in the published literature (Montero et al., 2018).

The main goal of the sand control testing is to aid in choosing the optimum sand control screens for specific reservoir conditions, controlling the sand production below the acceptable threshold. Technically, drawing a conclusion on which the screen provides the best performance based on results is quite clear and straightforward. The most problematic issue is to determine its reliability through dependency on assumptions.

2.4.1 Current Sand Control Experimental Tests

The downhole conditions in a well are reproduced in scaled tests to a certain level to evaluate relevant physical phenomena. Usually, they are small and straightforward types of equipment that can run many relatively inexpensive tests, providing more insights into the performance of the sand control completions. Scaled tests involve the slurry and pre-packed tests in sand control studies (Montero et al., 2018).

2.4.1.1 Slurry Tests

Ballard et al. (1999) introduced a slurry sand retention setup, which involved a screen coupon placed in a flow loop, and a mixture of sand slurry in a viscous fluid (mainly brine with polymer) at low concentration (0.1% by volume) pumped into an empty cell towards the screen. During the test, the differential pressure across the coupon was recorded. Initially, the pressure drop across the screen coupon is low but significantly goes up when the sand and fines accumulate over it due

to the formation of a filter cake. A schematic of the typical slurry test consisting of a slurry preparation component, test cell, and effluent collection component is shown in Figure 2-8.

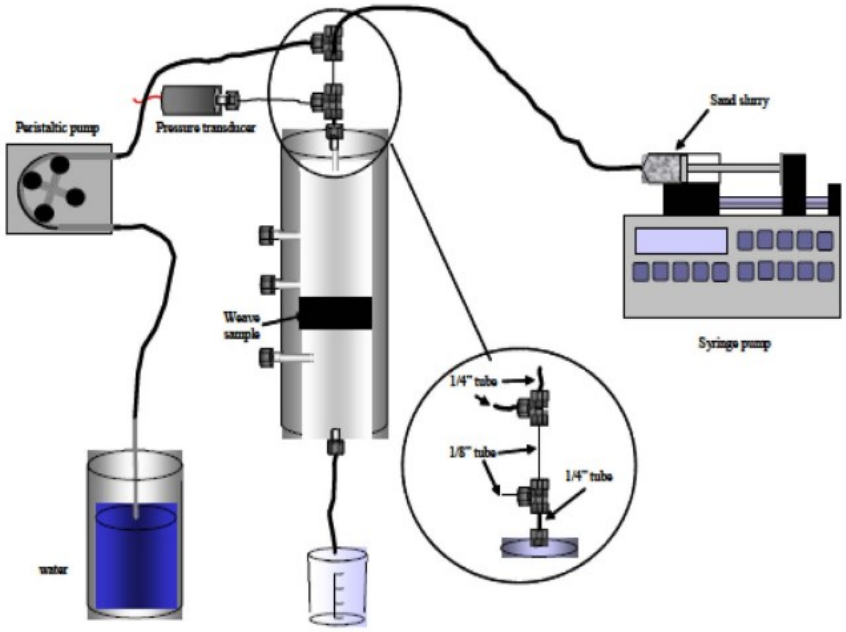

Figure 2-8. Scheme of slurry-type sand retention testing, after Montero et al. (2018)

Figure 2-9 illustrates a schematic illustration of two possible scenarios of the borehole. The slurry test aims to simulate particle flow in the annular gap between the screen and the wellbore at low concentrations (Ballard and Beare, 2003 and 2006; Chanpura et al., 2011) (Figure 2-9a). Table 2-1 outlines the acceptance criteria of SCDs regarding the slurry tests. It is worth mentioning that slurry tests are not able to capture the actual SAGD conditions. It is because, during preheating stages, the unconsolidated formation reasonably collapses onto the SCD, closing the annular space (Fattahpour et al., 2016; Montero et al., 2018).

As mentioned previously, the slurry tests are not ideal for mimicking SAGD production wells. However, the slurry experiment can be used to evaluate the scab liner (Montero et al., 2018). Installing scab liners is a standard solution to remedy the damage induced by failed SCD by setting up a new SCD inside the damaged zone. In such a circumstance, particles distributed in the production fluids come to the secondary SCD. Thus, slurry testing may be carried out appropriately to assess the sand control performance under this case. Specific aspects, for instance, particle concentration and flow rates, must be appropriately investigated in the laboratory to get accurate testing results under the designed SAGD conditions.

Table 2-1. Summary of the SCDs criteria in slurry tests

Source	Sand Production	Screen Plugging	Produced Particle Size
Hodge et al., 2002	≤ 0.12 lbm/ft^2 of flow area	$\geq 50\%$ retained screen permeability	-
Adams et al., 2009	≤ 0.15 lbm/ft^2 of flow area	$\geq 50\%$ retained screen permeability	-
Williams et al., 2006	$\leq 6\%$ in effluent	<100 psi across sand pack and screen	$D_{50} \leq 50$ µm
Constien and Skidmore, 2006	≤ 0.12 lbm/ft^2 of flow area	$\geq 50\%$ retained screen permeability	$D_{50} \leq 50$ µm

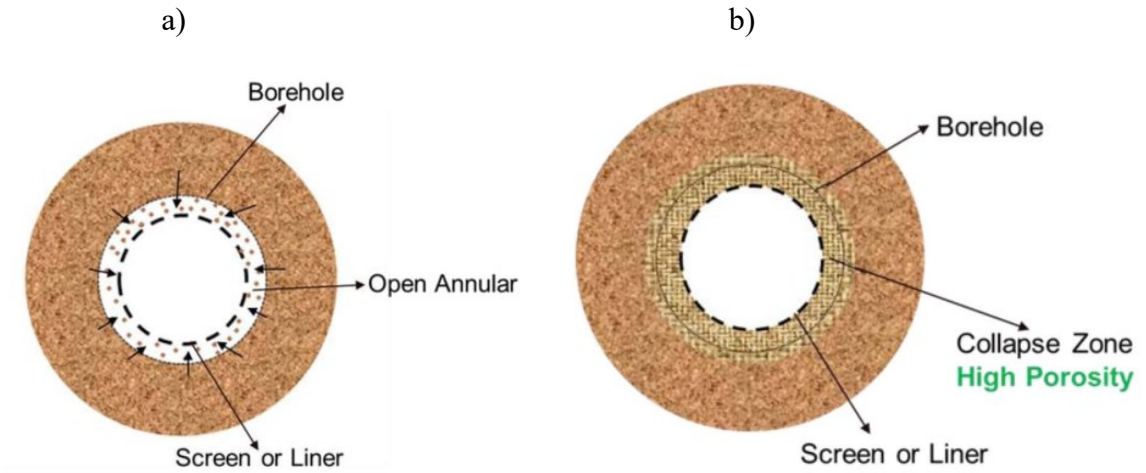

Figure 2-9. Two types of borehole conditions: a) the annular slurry flow in the annular gap simulated in the slurry test, and b) sand collapse over the SCD simulated by pre-packed SRT, after Montero et al. (2018)

2.4.1.2 Pre-Packed Tests

For pre-packed sand control testing, the sand sample is poured inside a test cell and then packed in a layer-by-layer method. A coupon is placed directly at the bottom of a sand pack. The fluids follow linear flow geometry through the sand pack from the top towards the coupon. The sand pack is more representative of the actual SAGD wells because the sand face more likely collapses

over the liner, which leads to the closure of the annular gap during the start-up stage (Chanpura et al., 2011; Fattahpour et al., 2016).

The pre-packed tests resemble the case where a rapid collapse of formation sand takes place over the SCD, filling the space between the formation and the screen (Chanpura et al., 2011). The annular space is filled with loose sand generating a high porosity region (Figure 2-9b). The liner installed in this situation is in touch with a high-permeability porous medium (Guo, 2018). In unconsolidated reservoirs, the commencement of flow is powerful enough to fail the rock around the wellbore (Ballard and Beare, 2003 and 2006; Chanpura et al., 2011). For heavy oil-bearing sands, collapse is induced by many factors such as rock-fluid thermal expansion, drag forces, and bitumen melting surrounding the SAGD wellbore (Fattahpour et al., 2016).

The pre-packed Sand Retention Test (SRT) procedure consists of a coupon installation representative of the downhole liner. Next, a sand pack preparation is conducted by placing sand over the coupon and packing it with gentle taps in the cell to provide a consistent permeability and porosity medium along the testing cell. A porous disc is put on the top of the sand pack to provide a uniform injection throughout the test. Then, the sand pack is saturated by a low injection rate from the bottom towards the sand pack to avoid a premature plugging potential of the sand sample during the saturation phase. A certain amount of stress or load is applied during the saturation phase to prevent the fluidization of the sand pack because of the counter-gravity drag force exerted by the saturating fluid (Ballard and Beare, 2003). When saturation is completed, the test is proceeded by injecting fluids at different flow rates from the top of the sand pack linearly towards the SCD. There are two approaches to do the main injection phase: constant pressure differential and constant flow rate (Montero et al., 2018). The produced sand is collected throughout the test. Either the flow rate or pressure drop is calculated after the test to evaluate the SCD performance.

Prepack setup can vary significantly depending on the way how they represent the SCD in SAGD operations. The variations in terms of design and procedure are based on the size of the facility, sand pack preparation technique, SCD device, fluid properties, number of injection phases and the order of fluid phases and their associated rates, stress magnitude applied and its anisotropy, and flow geometry towards the liner coupon (Montero et al., 2018).

Regarding the pre-packed experiment, pressure measurements play a crucial role. Pressure ports are installed along the cell wall and inside the testing cell at specific distances away from the test

coupon to capture pressure evolution during the test. Pressure measurements give knowledge about how permeability inside the sand pack evolves during the flow test. Therefore, it provides insights into the flow conditions, plugging issues, and fines migration as well.

The setups are classified into three main categories: conventional SRT, SRT with stress, and full-scale tests. Each group will be described in detail in the following sections.

Conventional Pre-Packed Sand Retention Test (SRT)

A sand control testing is classified as conventional if there is no confining stress being applied over the test, and only linear flow occurs. A typical schematic representation of the pre-pack SRT setup is displayed in Figure 2-10. The assembly commonly comprises a fluid injection unit, including compressors and pumps, a core holder, a sand and fines collection unit, a back-pressure column, and a measurement system. The setup can mimic the initial phase of the collapse zone over the SCD, where the near-liner region is made up of high-porosity formation sand, and the effective stress in this zone is nearly zero (Montero et al., 2018).

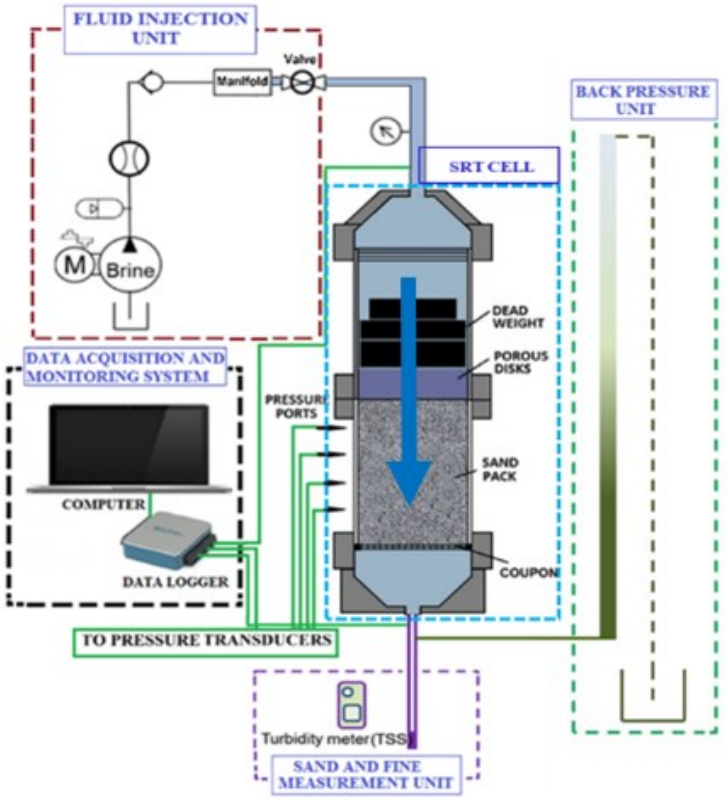

Figure 2-10. Scheme of pre-packed SRT, after Haftani et al. (2019)

Pre-packed SRT with Stress (SRTS)

The setup of SRTS has similar features with the conventional SRT, but the facility can apply confining stresses on the sand pack. A schematic of a typical SRTS setup is depicted in Figure 2-11. The application of stress levels enables the simulation of different stages in the SAGD well life cycle. Typically, stresses around the SCD initially are at low magnitude at the early stages of production stages. Over time, the stress gradually increases along with the expansion of the steam chamber. The build-up of stress occurs due to many phenomena such as reservoir thermal expansion, shear dilation, and poroelastic sand expansion (Fattahpour et al., 2016). Most SRTS setups used in the SAGD context only apply axial stress (Bennion et al., 2007 and 2009; Romanova et al., 2014; Devere-Bennett, 2015; O'Hara, 2015), which restricts the control of the confining horizontal stress over the sand pack. A more improved facility capable of applying independent levels of stress in different directions was developed by Fattahpour et al. (2016). The setup was utilized to assess the influence of confining stress (Guo et al., 2018) and anisotropic stress (Wang et al., 2018) on SCD performance.

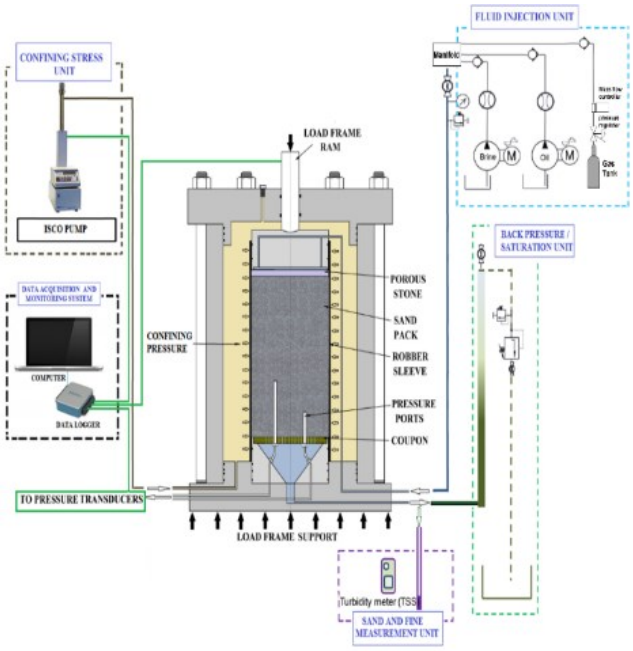

Figure 2-11. Scheme of pre-packed SRT with stress, after Wang et al. (2018)

2.4.2 Experimental Equipment with Radial Flow Regime

The main limitation of the conventional SRT and SRTS is linear flow geometry in both setups, which is not representative for SAGD producers where radial flow dominates the near-wellbore

region. The testing facility employing the radial flow is Full-Scale Completion Testing (FCT), as demonstrated in Figure 2-12. The FCT facility is relatively new in the field of sand testing, capable of capturing the SAGD well conditions more closely. The flow in the FCT experiment follows a radial geometry, which is in contrast to linear flow in the SRT test.

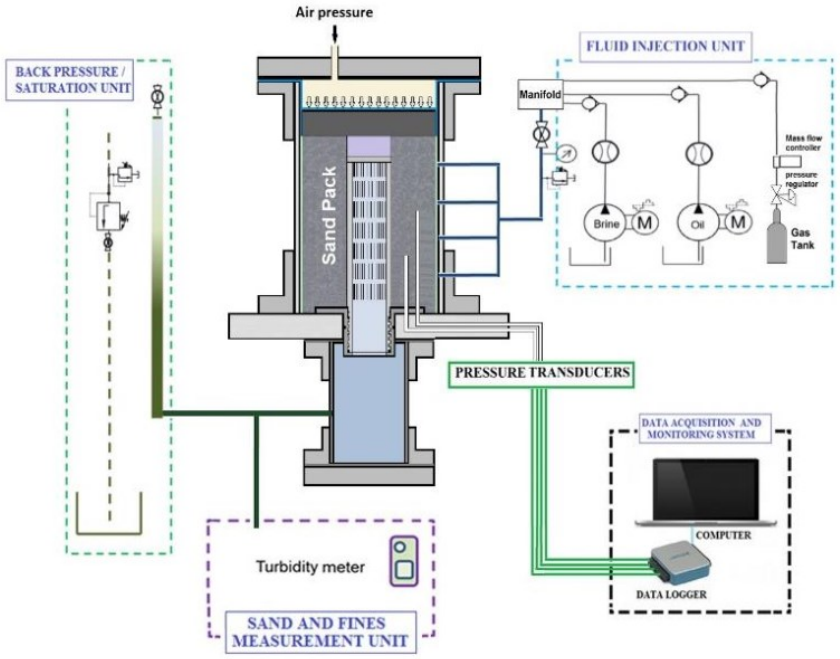

Figure 2-12. Full-scale Completion Test Facility (FCT), after Haftani et al. (2020)

Concerning the radial flow regime, flow velocity increases rapidly when approaching more closely to the liner because the open area to flow decreases as the wellbore is approached. Hence, it is expected that there is a lower level of fines migration far from the liner due to the weaker drag forces generated by lower fluid velocities (Valdes and Santamarina, 2006). Besides, thick radial bridges can be developed at a certain radial distance away from the outlet due to the fine particles retardation as the flow converges (Valdes and Santamarina, 2006). These radial bridges would increase the stability of the formation and reduce the production of solid particles.

Dating back to the early 1900s, Chenault (1938) carried out some testing employing radial-flow cell assembly. The tests were purposely designed to compare flow rates with and without screens for conventional well operations. A testing schematic is shown in Figure 2-13. A sample of screens is mounted in the center of the removable sand basket. After oil leaves the screen sample, it flows towards a countercurrent-flow settling tank with a conical bottom and terminates in a burette for

collecting sand. The overflowing oil passes through a collecting trough and flows to a suction tank for re-circulation. One limitation of the setup is no capability of applying axial loading over the sand pack. Another limitation possibly causing some erroneous testing results is that sand might not have enough time in the settling tank for settling down and terminating in the burette. High-velocity oil flow may carry some sand to the collecting trough, impacting the amount of sand production collected after the test.

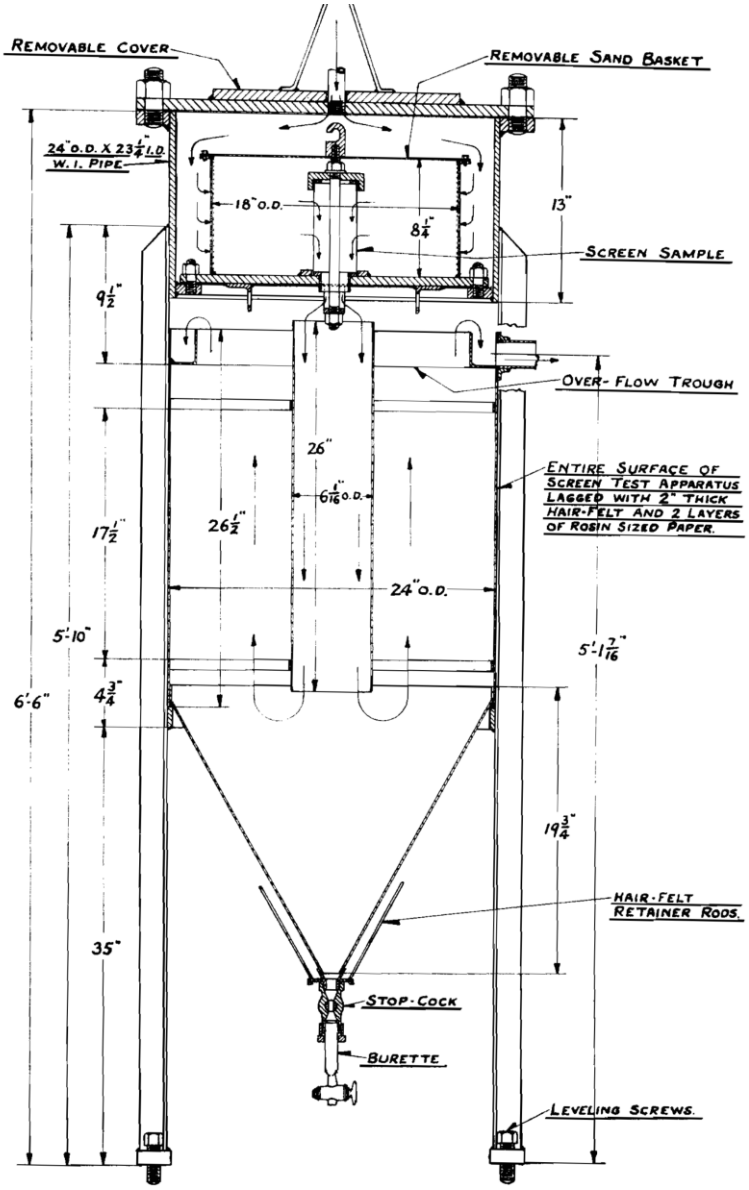

Figure 2-13. The screen testing chamber and sedimentation tank, after Chenault (1938)

Subsequently, Qi (2004) devised a large-scale experimental apparatus for simulating sand production. The fluid injection followed a radial-flow regime in the setup. The author came up

with the relationship between fluid viscosity, flow rate, and sand production. The study conducted multiple tests to compare the performance of pre-packed screens versus gravel packing.

Papamichos et al. (2001) studied the effects of external stresses and flow rates on sand production by using a testing setup employing the radial flow with a hollow cylinder specimen (Figure 2-14). The hollow cylinder specimen was accommodated in the center of the testing cell surrounded by high permeability gravel. The fluid was injected via the top piston and then distributed inside the packed gravel before passing through the specimen. The testing equipment did not incorporate any sand control devices. The setup of the fluid injection unit does not confidently provide a uniform radial flow toward the specimen. In detail, most of the flow might pass through the bottom part of the specimen to the inner hole due to gravity.

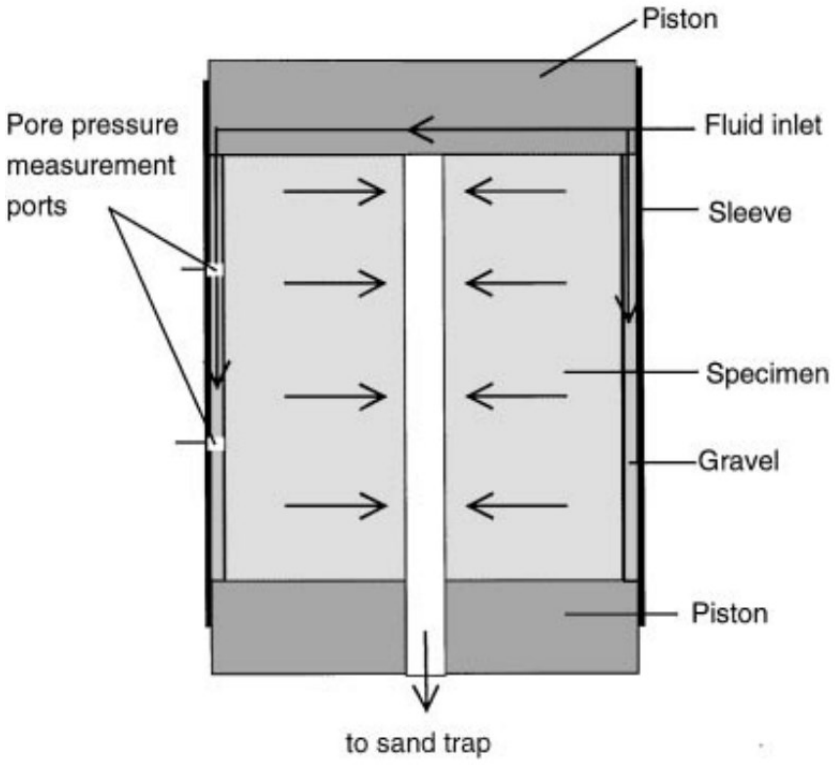

Figure 2-14. Schematic of the testing setup with a hollow cylinder specimen, after Papamichos et al. (2001)

Nouri et al. (2005) conducted hollow cylinder tests where a high injection rate was delivered from the outer surface of the specimen toward the central hole to study the sanding level and failure of the perforation in the formation surrounding the wellbore. The experiment was conducted on

weakly-consolidated sandstones. The testing facility involves an axial loading unit, flow vessels, sanding measurement unit, and instrumentation. Figure 2-15a illustrates a schematic of the consolidation chamber used by Nouri et al. (2005). The flow was delivered to four vessels through a manifold to small holes in the circumference of a platen to provide a radial inward flow (Figure 2-15b). One limitation of the equipment is the limited number of inlets. Four inlets in the circumference of the platen bottom do not guarantee to render the uniform radial inflow through the outer surface of the specimen. The facility's second limitation is that most of the outlet flow may come from the specimen bottom where the fluid is injected. The top of the specimen may not have any flow provided low flow rates.

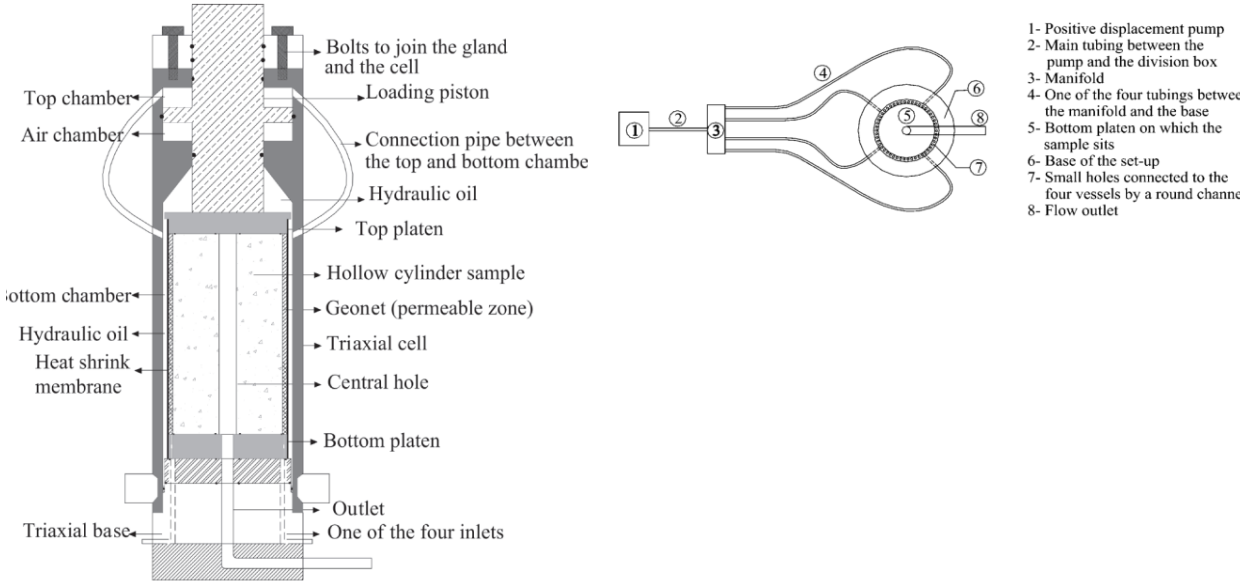

Figure 2-15. Schematic of the configuration of a) the consolidation chamber, and b) the fluid flow vessels, after Nouri et al. (2006)

Afterward, Jin et al. (2012) assessed the performance of several sand control screens for gas wells via developing a large-scale laboratory test apparatus. The radial gas flow was simulated in the study. Throughout the study, the impacts of pressure and flow rates on sand stability were investigated. Figure 2-16 displays a schematic of the testing apparatus, which includes the data monitoring unit, injection unit, experimental cylinder, and sand collection unit. There are two fluid ports connected from the injection component to the outer boundary of the cylinder. The limited number of injection ports is problematic for developing the uniform flow distributed inside the sand pack.

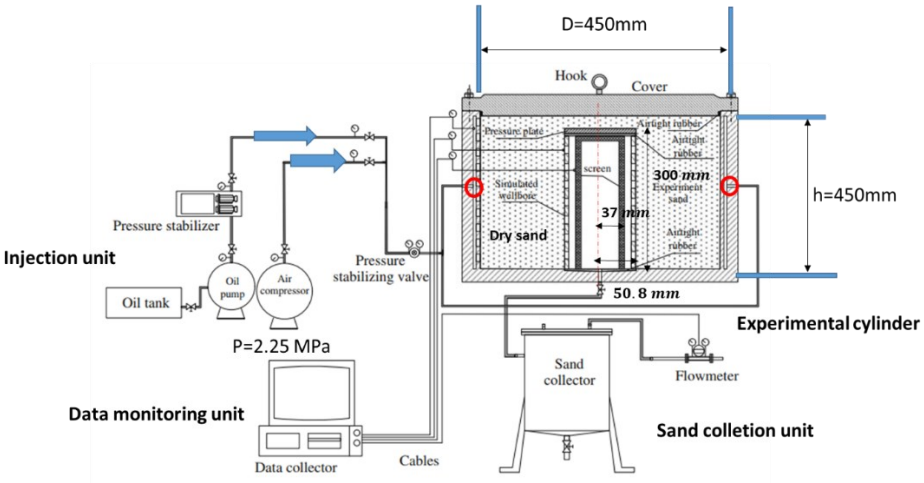

Figure 2-16. Schematic of the sand control experimental equipment, modified after Jin et al. (2012)

Dong et al. (2017) developed a new experimental setup to assess the overall performance of mechanical screens (Figure 2-17). The sand slurry was carried by fluid flowing radially towards a screen sample via two injection ports to simulate the process of sand retaining. Based on the experimental results, a set of indexes was devised to describe the screen performance. The calculation method was also developed to effectively select an optimum screen type with a small number of experimental testing. The equipment's primary limitation is the limited number of injection points, which might result in a high level of non-uniform flow distribution in the region close to the screen sample.

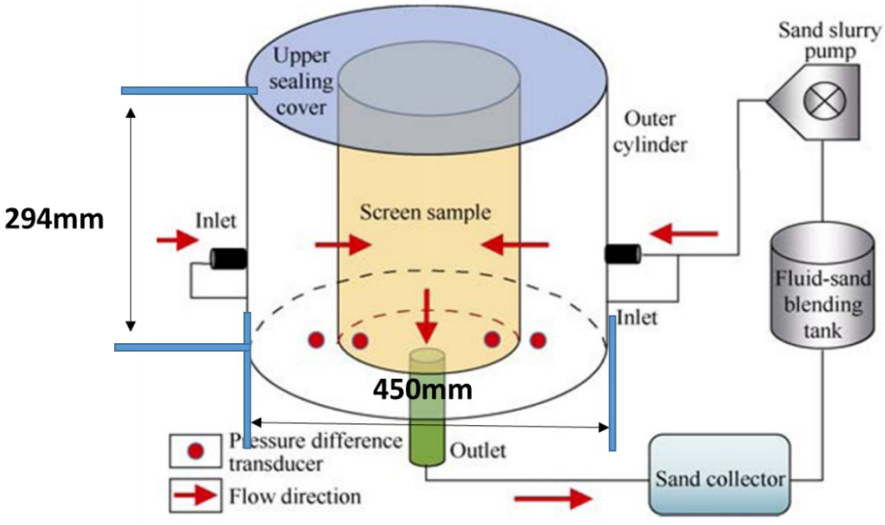

Figure 2-17. Schematic of the testing apparatus, modified after Dong et al. (2017)

Similarly, Ma et al. (2020) developed an experimental setup to evaluate screen performance. Figure 2-18 shows a schematic of the sand control testing facility investigated by Ma et al. (2020). In the research, a sand slurry was radially injected into the cell towards the screen from two injection ports located at the outer side of the testing cell. The study aimed to investigate sand control screens' performance by processing sand control simulation unit, analyzing formation parameters, determining pressure drops through the sand retaining medium, and calculating the oil-production index. The testing setup cannot confidently provide the uniform injection due to the limited number of fluid ports.

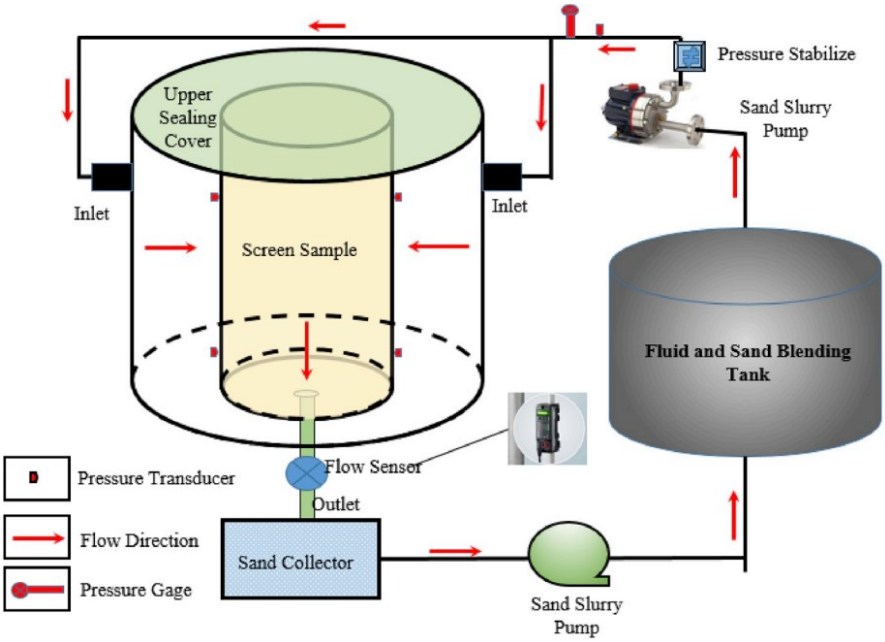

Figure 2-18. Schematic of the sand control testing apparatus, after Ma et al. (2020)

Anderson (2017) introduced a novel large-scale apparatus and testing procedure to validate previous scaled tests. A schematic of the testing equipment developed by Anderson (2017) is presented in Figure 2-19. Rather than using a single-slot coupon, the author employed a cylindrical screen with 7 inches in diameter. The screen was installed at the bottom of the sand pack. In the setup, sand was packed over the top part of the screen as a curved coupon. Approximately 50kg of sand was accommodated in the test to ensure a representative sample. The fluids were injected from top to bottom towards the tested screen. The study purported to compare the small-scale testing results on the single-slot coupon that had been done before with the ones obtained from the large-scale testing equipment. Anderson (2017) concluded that the results obtained from small- and large-scale testing facilities show a good agreement. The assumption regarding the setup is

that the flow regime is radial when it approaches more closely to the liner. However, due to the same cross-sectional area along the packed sand, the radial flow could not be fully established. In detail, the flow geometry is linear for most parts of the sample except that the flow streamlines deviate from a linear trajectory in the region close to the curved coupon.

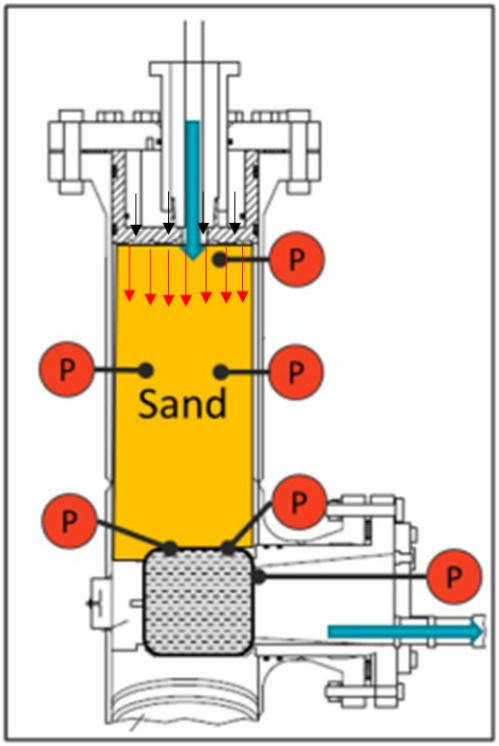

Figure 2-19. Schematic of the large scale testing apparatus, modified after Anderson (2017)

A detailed review of the existing testing setups presented above has shown that the radial flow regime has not been thoroughly studied in the thermal recovery context. Even though the researchers have been trying to replicate the radial flow, their testing apparatuses show some limitations in establishing the uniform fluid injection. It is of prime importance to assess the screen performance concerning the fully developed radial flow configuration, which is more representative of the SAGD wells.

2.5 Comparison between the Liner (SRT) and Radial (FCT) Flow Geometries

2.5.1 Flow Geometry

In the SRT facility, the flow regime is linear, flowing from the top of the cell to the bottom. In the linear flow geometry, flow velocity in sections away from the coupon is constant when the flow is

stabilized. Thus, the pressure gradient is the same along the testing sample except for adjacent to the coupon where the flow streamlines converge. The convergent fluid flow adjacent to the coupon is expected to increase the flow velocity (Mahmoudi et al., 2017a). On the other hand, the flow velocity increases rapidly for the radial flow regime when it comes closer to the wellbore (Figure 2-20). Hence, the pressure gradient is larger, with a decreasing distance from the liner.

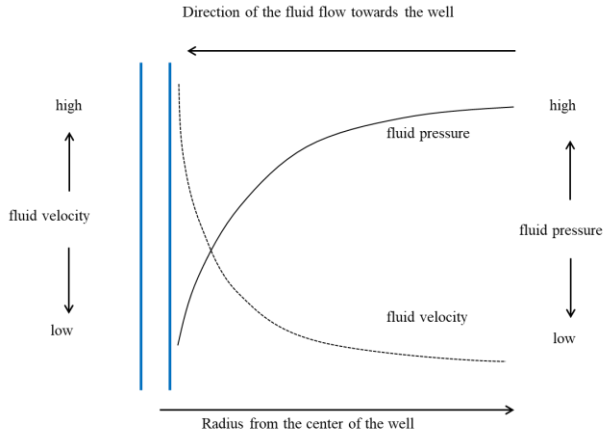

Figure 2-20. The profile of pressure and fluid velocity versus radius

Figure 2-21 shows a schematic of the inflow for a typical reservoir with isotropic permeability. It is evident that the flow regime in the vicinity of the SAGD producers is radial, not linear. The SRT captures the vertical flow only at the top side of the SAGD wells, where the flow velocity is most likely the highest one. SRT testing is proposed in simulating the worst-case scenarios (Fattahpour et al., 2020) to assess if excessive sand production will occur. The inability to replicate the correct flow geometry is a deficiency of the SRT testing.

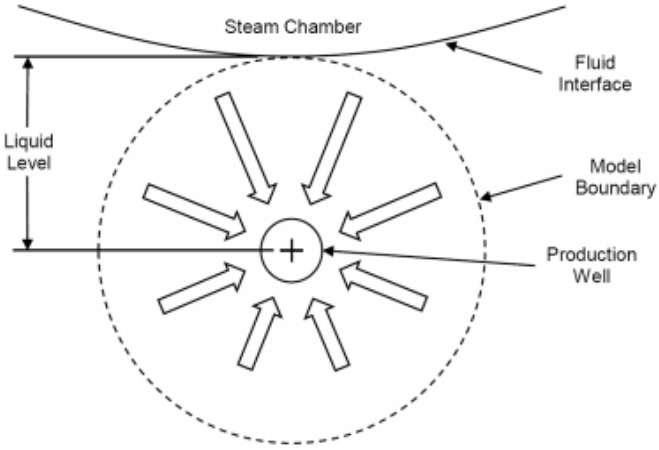

Figure 2-21. Flow around the wellbore in SAGD operations, after Taubner et al. (2016)

Additionally, the upward flow in the SRT experiment cannot be studied due to the linear stream from the top of the sand pack towards the coupon. In other words, only the top side of the horizontal well is simulated with the current SRT facilities. Matanovic et al. (2012) discussed the importance of the upward flux and claimed the upward flow increases plugging potential. Therefore, considering the radial flow geometry in the experimental tests is essential, which is a more representative testing condition.

2.5.2 Seepage Forces

Valdes and Santamarina (2006) discussed the impacts of varying velocity on fines migration and sand production in the radial flow configuration. For the far region where the flow velocity is low, no particle transport is anticipated. When the fluid velocity goes up in the middle zone with intermediate radial distances, the gravity force prevails. For the near field, drag forces become dominant ones applying on particles. On the other hand, concerning the linear flow regime, seepage forces are the same at regions away from the coupon except for the vicinity of the coupon where the flow convergence occurs.

The evolution of seepage forces in the radial flow geometry is different from those of the linear flow regime. The seepage forces in porous media play a crucial role in flow-driven particle migration. Hence, accounting for the actual flow regime in the sand-retention testings is necessary for simulating the conditions of the borehole more closely.

2.5.3 Fines Concentration

Figure 2-22 shows the fines concentration distribution in an SRT test. The top of the sand pack shows the largest amount of migrated fines. The middle region displays a small change in terms of fines transportation because the region receives some fines released from the top and loses some fines to the lower zone at the same time. The near-coupon area illustrates a rise in fines accumulation. These observations are typical in the SRT experiments.

On the other hand, fines migration follows a different pattern concerning the radial flow regime. At large radial distances to the liner, the low fluid velocity is not sufficient enough to move fines. Also, instead of the highest fines concentration being in the near-coupon area, fines accumulate mostly at a characteristic radial distance away from the liner, forming a radial arch (Valdes and

Santamarina, 2006), as displayed in Figure 2-23. Hence, employing the FCT facility incorporating the radial flow configuration is necessary for studying fines migration.

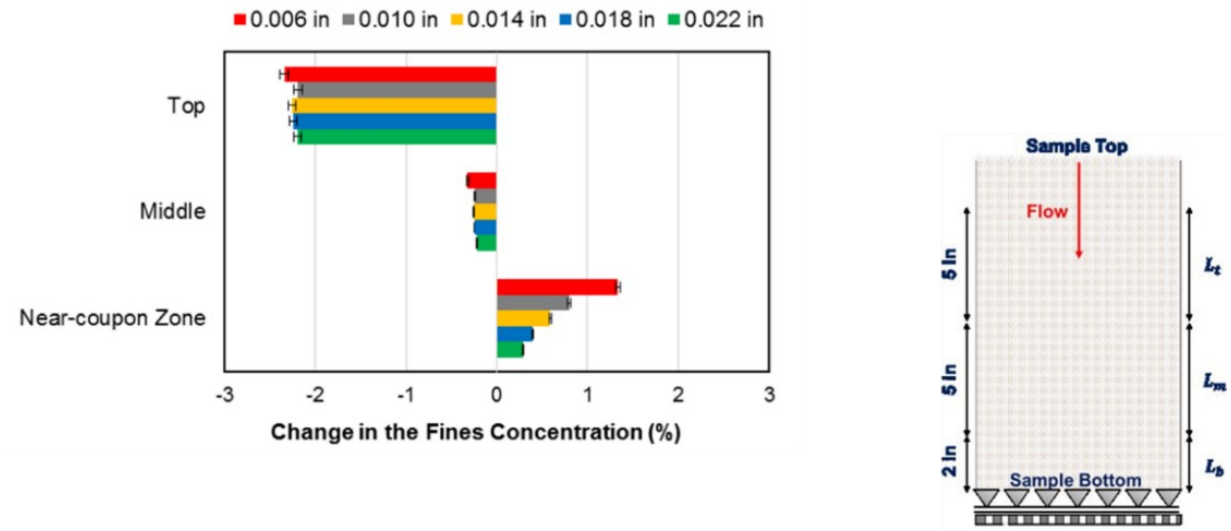

Figure 2-22. Change in fines concentration along the sand pack, after Montero (2019)

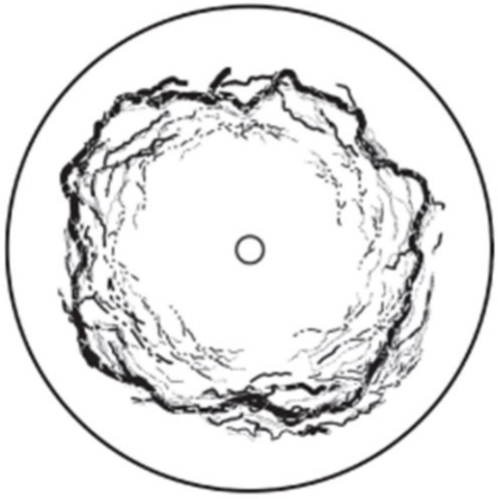

Figure 2-23. Fines concentration in radial flow after the evolution of annular clogging ends, after Valdes and Santamarina (2006)

2.5.4 Flow Convergence

The convergence of flow streamlines near the screen is illustrated in Figure 2-24. Chanpura et al. (2011) found that the pressure drop associated with the flow convergence in the linear flow could be 1.5 times more than the case without considering the flow convergence. Since the contribution of the flow convergence to the total pressure drop can be considerable, considering the flow

convergence in the testing is essential for mimicking the field conditions. Determining the magnitude of the flow convergence incorrectly in the total pressure drop would lead to an erroneous permeability calculation. The reported permeability would be lower than actual if ignoring the flow convergence (Chanpura et al., 2011).

Besides, it is reported that the pressure drop through open slots is negligible compared to that induced by the flow convergence regardless of the slot dimension (Kaiser et al., 2002). The extent of the affected zone due to the flow convergence is controlled by slot spacing, which is expressed by the correlation following a linear relationship (Kaiser et al., 2002) (Figure 2-24).

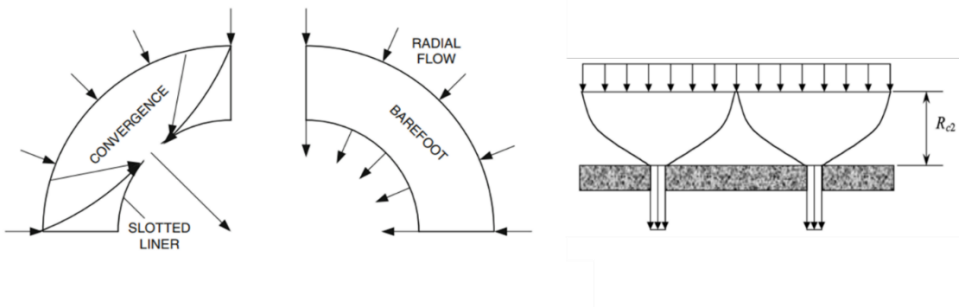

Figure 2-24. Radial flow convergence illustration, after Kaiser et al. (2002)

The slot lengths in different columns are different in slotted liner coupons employed in the SRT (Figure 2-25). The flow-convergence zone is not fully developed for the top and bottom columns of the coupon. The affected zone around the coupon due to flow convergence is illustrated in Figure 2-26. The flow geometry of the fluid flow can be divided into four main components: the linear flow through slots, the radial flow induced by multiple slots, the radial flow caused by slot unit angular distribution, and the radial flow far away from the liner (Furui, 2004). In the analytical model to calculate a skin buildup due to flow convergence, each circle's radius caused by the convergence of flow streamlines around each slot is half of the slot unit width (Mahmoudi et al., 2017a).

On the other hand, the FCT test is performed using cylindrical-shaped screens, as shown in Figure 2-27. The slotted liner allows the flow geometry around the slots to be fully established, as displayed in Figure 2-28. Regarding the cylindrical-shaped screens, the radius of the influence due to the flow convergence, which is characterized as a series of radial flow regions, is a function of the liner radius and the number of slots per column (Furui et al., 2005). These parameters cannot

be accounted for with the disk-shaped screen coupon in which the number of slots per column is not the same, and the impact of the liner radius cannot be considered.

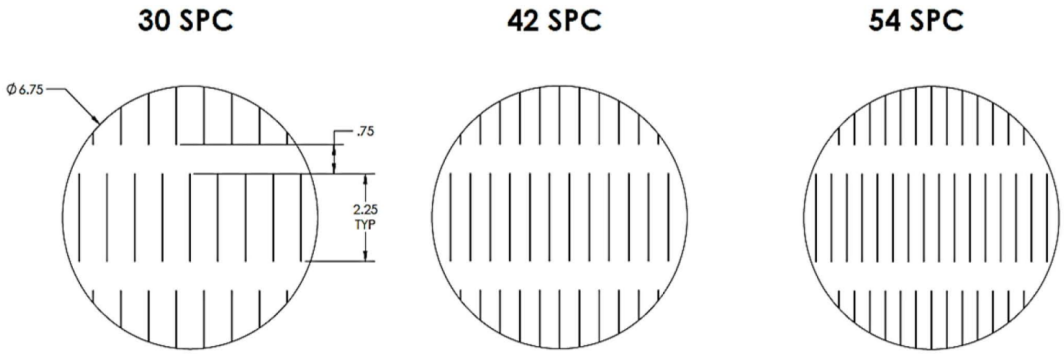

Figure 2-25. Schematic of the flat coupon, after Mahmoudi et al. (2017a)

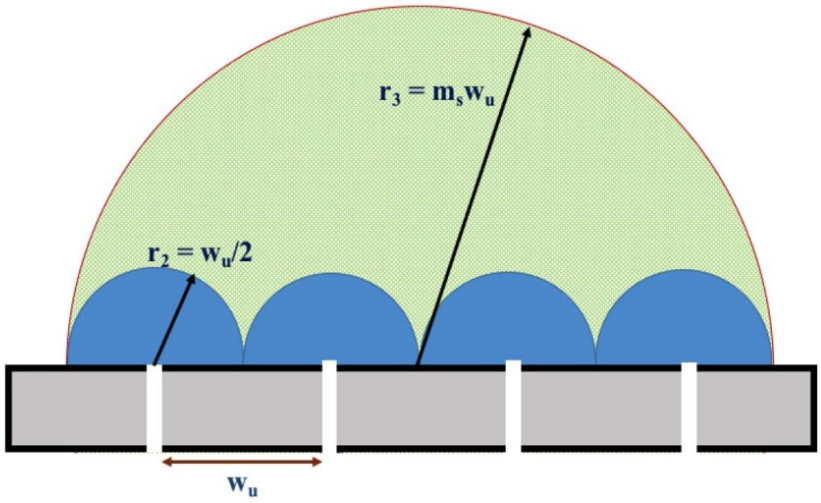

Figure 2-26. The flow geometry around the tested liner coupon, after Mahmoudi et al. (2017a)

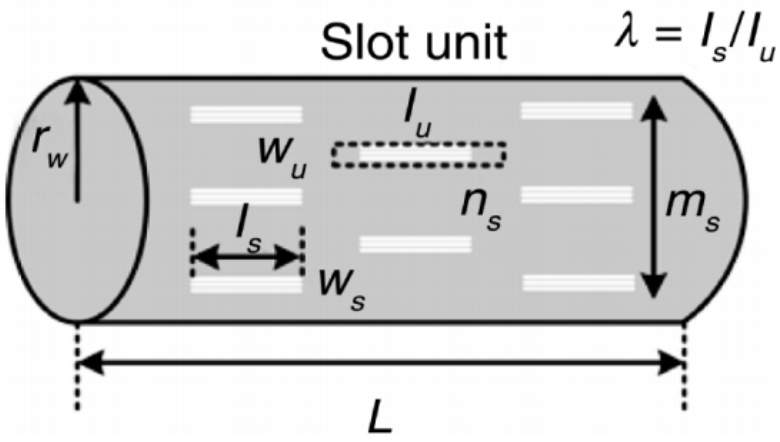

Figure 2-27. Schematic of the slotted liner, after Furui et al. (2005)

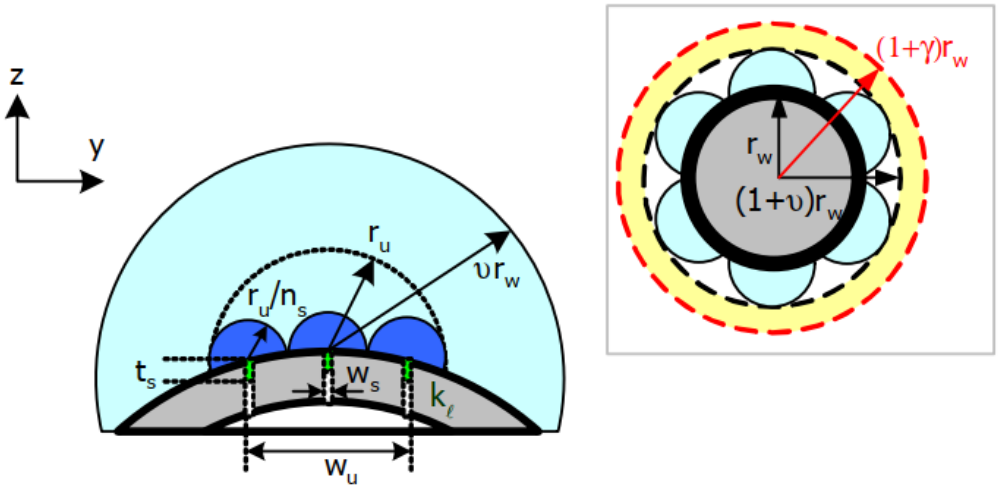

Figure 2-28. The flow geometry around the slotted liner, after Furui (2004)

Different extents of the flow-convergence regions induced by multiple slots between the flat coupon and cylindrical liner lead to different impacts on inflow impairment. In conclusion, the FCT facility with cylindrical screens presents a higher potential capability to represent the field cases more realistically than the SRT test employing the flat coupons.

2.6 Summary

The backgrounds in SAGD operations, as well as sand control, were presented in this chapter. Different sand control experimental tests reported in the literature were introduced, and their limitations in terms of the testing setup were discussed. The differences between the SRT and FCT testing in terms of the flow geometry, seepage forces, fines concentration, and flow convergence were elaborated.

The detailed review of the existing experimental setups for sand retention tests in the past indicates that most of the equipment incorporating the radial flow geometry have been mainly developed for conventional well applications. Concerning the thermal recovery context, the radial flow regime has not been thoroughly investigated. It is of supreme importance to assess the screen performance under the radial flow geometry to represent the SAGD wells more closely. Although many researchers have developed novel testing apparatuses employing the radial flow configuration, the testing setups still present some limitations regarding the uniformity of the flow distribution.

The thesis will describe the FCT facility and testing procedure for sand control testing in the SAGD context in the next chapter. The equipment is introduced as an advanced testing facility for better simulation of the SAGD reservoirs with the radial flow regime. Several challenges were encountered while developing the testing facility and operating procedure before their final versions were adopted.

Chapter 3: Experimental Setup and Testing Procedure

3.1 Introduction

This study employs the Full-scale Completion Test (FCT) facility to simulate the downhole conditions in the SAGD production wells. The FCT setup allows assessing the sand control screens in terms of sand retention in the presence of the radial flow regime. The FCT is an advanced testing facility to mimic the SAGD production wells with more representative conditions. This chapter will focus on the design of the main components of the testing facility and the testing procedure as well.

3.2 Testing Materials

All FCT tests in the thesis were performed using representative sand classes from the McMurray Formation. In the study, the replication of the DC-I type of Particle Size Distribution (PSD) from the McMurray Formation is achieved by mixing two commercial sands and one commercial clay that are Sil 1, LM70, and Helmer Kaolinite. Figure 3-1 presents the cumulative size distribution of the commercial sands and clay.

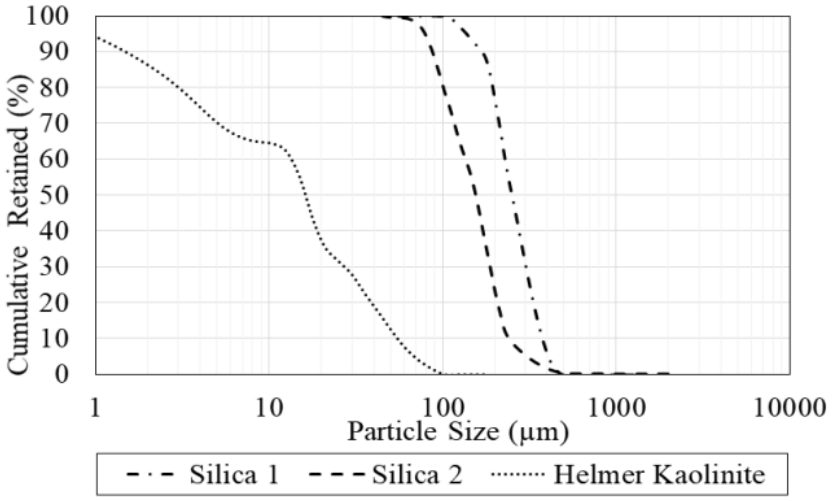

Figure 3-1. Particle size distribution for two commercial sands and one commercial clay

Abram and Cain (2014) categorized the McMurray Formation into four main groups. In detail, DC-I is considered as the finest sand, and DC-IV is regarded as the coarsest one. The mixtures of commercial sands display a reasonable agreement with the formation sands, as shown in Figure

3-2. Generally, synthetic samples provide a reasonable replication of the formation sands. The DC-III deviates 25 microns from the actual formation sand, while the DC-II and DC-I display a deviation of ±50 and ±55 microns, respectively (Montero, 2019). Table 3-1 provides characteristic points of the synthetic DC-I. Table 3-2 presents the composition of the DC-I replicated in the lab.

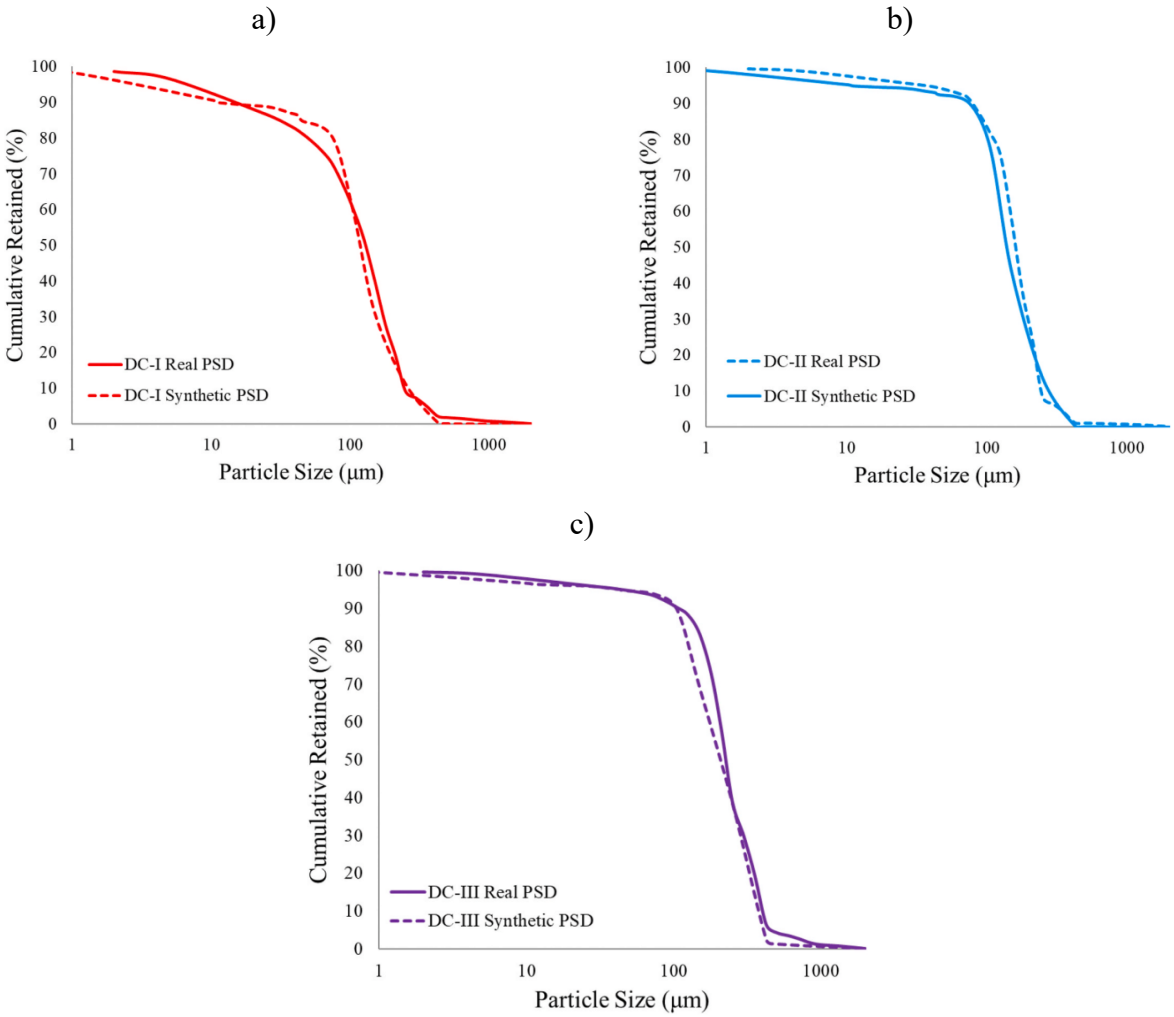

Figure 3-2. PSD curves for a) original DC-I and replicated DC-I, b) original DC-II and replicated DC-II, and c) original DC-III and replicated DC-III from the commercial sands, after Wang et al. (2021)

Table 3-1. Characteristics of synthetic DC-I

D90	D70	D50	D10	% fines	Uniformity Coefficient	Sorting Coefficient
25	80	135	232	14.5	5.9	9.3

Table 3-2. The composition of the DC-I

Silica 1 (Sil 1)	Silica 2 (LM 70)	Helmer Kaolinite
15.5%	70%	14.5%

Figure 3-3 compares the PSD of the DC-I type between Abram and Cain (2014), the replicated sample determined by the calculation from combining different commercial sands, and four samples extracted from the sand pack preparation. The figure shows a good agreement between these curves measured by different methods.

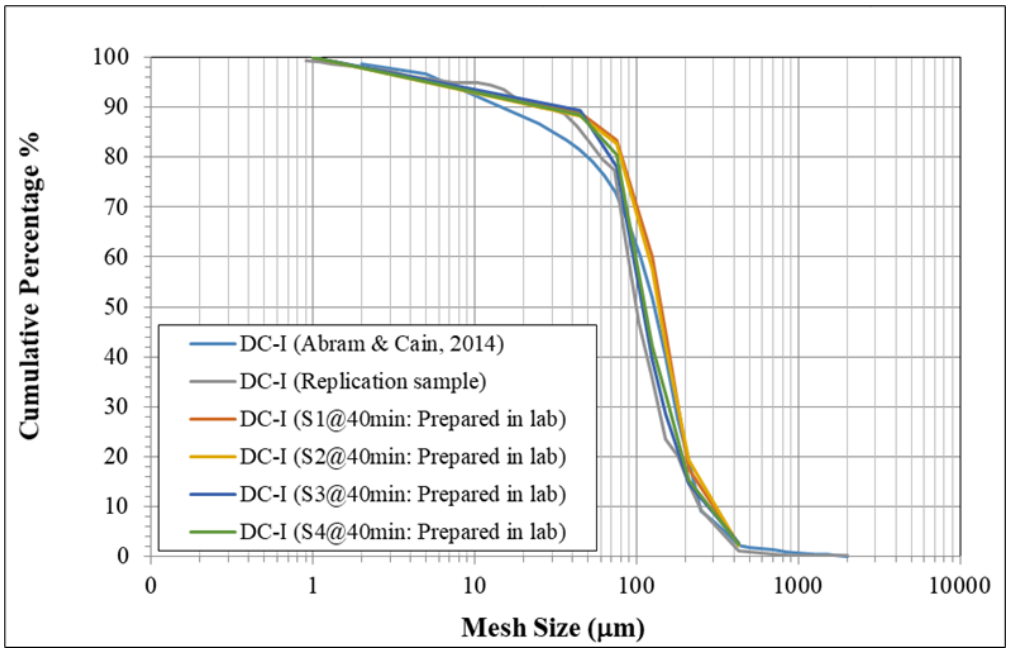

Figure 3-3. Comparing the DC-I PSD from different methods

3.3 Experimental Setup

Schematics of the FCT setups for the liner's vertical and horizontal positions can be seen in Figure 3-4 and Figure 3-5, respectively. The FCT facility comprises of five major components, namely: (1) sand pack cell, (2) fluid injection unit, (3) data acquisition and monitoring group, (4) sand and fines measurement unit, and (5) back-pressure unit. The testing facility can conduct the sand retention tests employing the liner in both the vertical and horizontal directions. In this research, eight tests were carried out regarding the vertical liner, and three tests were performed concerning the horizontal liner. The following parts give further details on each component of the apparatus.

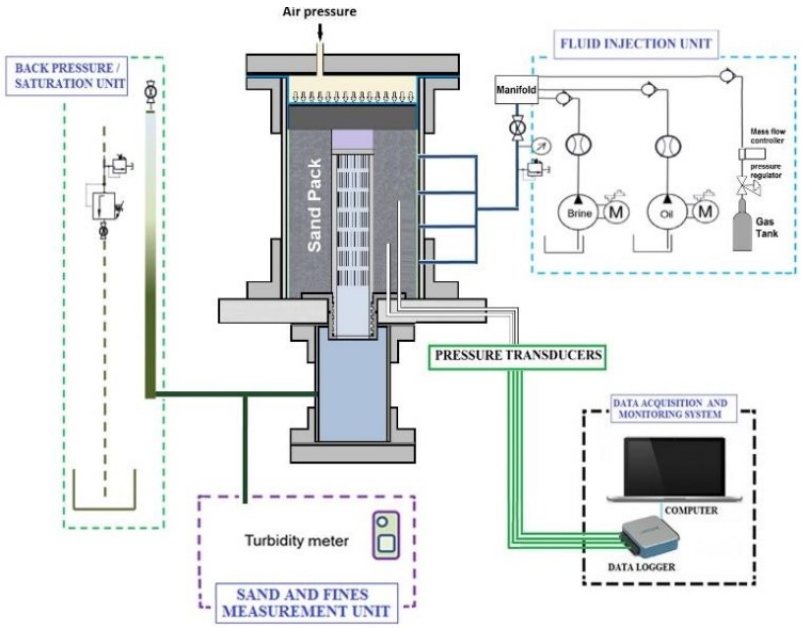

Figure 3-4. Full-scale Completion Test Facility (FCT) in the vertical position of the liner, after Haftani et al. (2020)

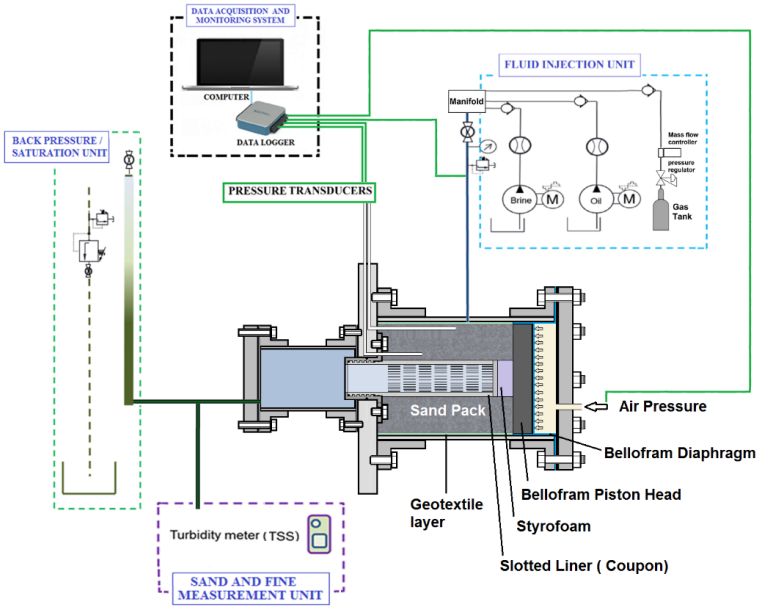

Figure 3-5. Full-scale Completion Test Facility (FCT) in the horizontal position of the liner

3.3.1 Sand Pack Cell

Figure 3-6 shows a schematic of the sand pack cell. The FCT cell is a hollow cylinder with an inside diameter of 12 inches and a height of 19 inches. Sand is packed, and a slotted liner coupon

with an outer diameter of 3.5 inches and a height of 12 inches is installed inside the equipment's cell. The device enables researchers to assess the performance of different SCDs by installing any liner or screen (e.g., slotted liner, wire-wrapped screen, or punched screen) with a diameter of 3.5 inches at the center of the cell.

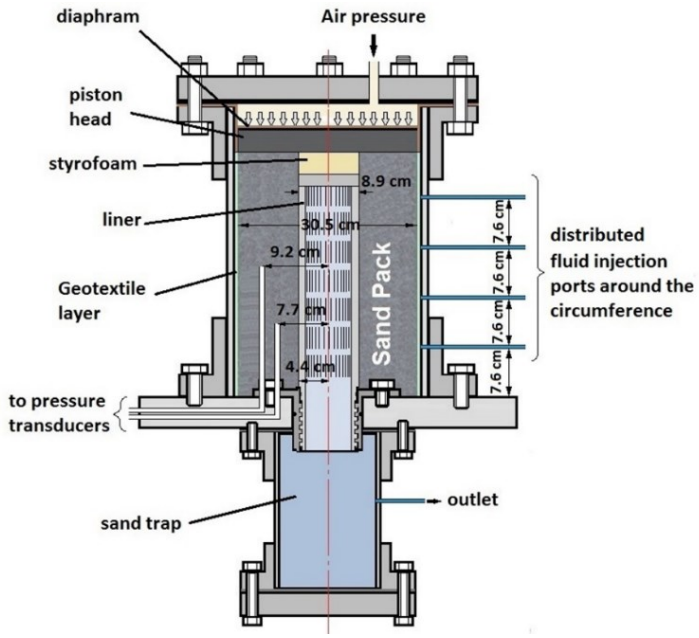

Figure 3-6. Schematic diagram of the equipment's cell

With the FCT cell, a large amount of sand can be packed layer by layer by employing a moist tamping technique around the liner. A diaphragm is installed at the top of the sand pack. The FCT cell, body, and flanges are made of PVC materials. The use of PVC pipe limits the FCT cell's maximum operating pressure to about 40 psi, considering appropriate safety factors.

The axial load applied upon the sand pack is generated by the air supply. The main reasons to apply the axial pressure are to prevent channeling in the sand pack, avoid sand fluidization during the saturation phase, and act as the normal stress on the screen in the fluid injection. Also, to record pressure evolution in the sand pack during the flow test, different pressure ports with different heights are employed.

Figure 3-7 illustrates the FCT cell used in the laboratory. Flowlines installed around the FCT cell are used for delivering fluid into the sand pack towards the liner. A pipe is installed at the top of the cell to facilitate the de-airing of the sand pack during the saturation phase to ensure the sand pack can be fully saturated.

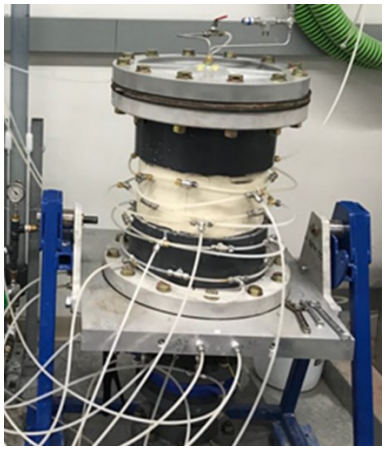

Figure 3-7. The photo illustration of the FCT cell in the vertical FCT test

The aluminum base plate with a hole at the center where placing the liner is displayed in Figure 3-8. The purpose of the hole is to screw the slotted liner. Besides, the hole is a path where the produced fluids, sand, and fine particles can go through to a sand trap. The sand trap is set up below the base plate to collect the produced sand during the testing. The FCT cell can be rotated either vertically or horizontally, based on the objective of the test.

Figure 3-8. The photo illustration of the base plate with the slotted liner

3.3.2 Fluid Injection Unit

The pumping system consists of two triplex metering pumps for brine injection, as shown in Figure 3-9. The output flow rate from these two pumps is controlled by setting up the stroke length and adjusting the pump frequency through a Variable Frequency Drive (VFD). Two 100-liter tanks are being used to feed the pumps. Before running the test, each pump needs to be calibrated to figure out the best-chosen setting to achieve any designed flow rate.

Figure 3-9. The photo illustration of the two triplex metering pumps

Figure 3-10 displays fluid injection ports with the liner being in the vertical position. Four injection rows of the fluid ports surround the FCT cell. Each row has four injection ports located in the cell's circumference, purporting to inject the fluid radially through the sand pack towards the liner. The total number of injection ports is 16. Four flowlines are connected from the pumps to the system of the injection inlets. Each flowline is connected to one injection row to ensure the same amount of injected fluid at different elevations of the FCT cell.

Figure 3-10. The photo illustration of the fluid injection ports in the vertical FCT test

Some modifications were made regarding the fluid injection unit with the horizontal liner (Figure 3-11). A flow manifold was added in the system with eight flowlines coming out of its top (Figure 3-12), and the injection inlets in the FCT cell was connected directly to the flow manifold before the pumps. When rotating the FCT cell to the horizontal direction, a set of two injection ports located at the same level is connected and injected by only one flowline. Therefore, the total number of flowlines needed is 8 to deliver brine to 16 fluid ports.

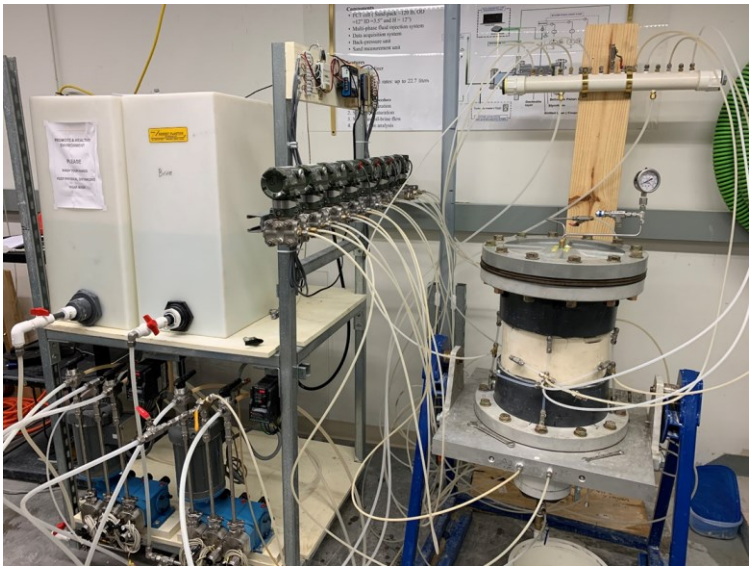

Figure 3-11. The photo illustration of the fluid injection system in the horizontal position

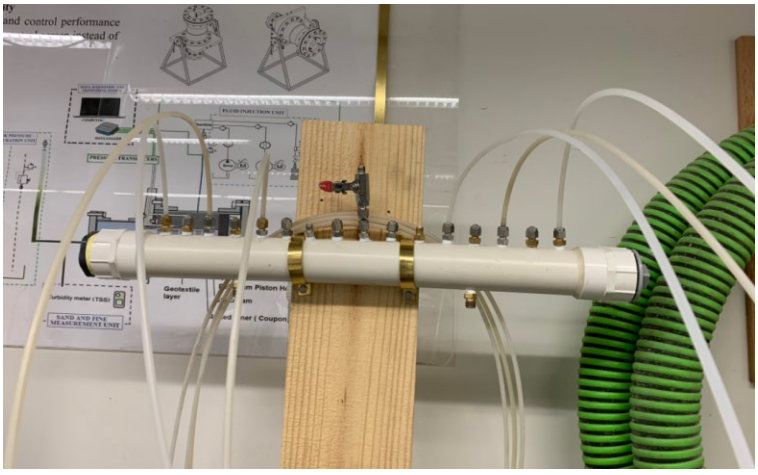

Figure 3-12. The photo illustration of the flow manifold

3.3.3 Data Acquisition and Monitoring Group

The data acquisition and monitoring group includes differential pressure transducers and a data acquisition system (LabVIEW). Figure 3-13 shows differential pressure transducers installed for

the experiments performed in the vertical direction. The pressure transducers with 0.25% accuracy are utilized to keep track of the pressure evolution in the sand pack at different locations around the liner to investigate permeability variations throughout the test due to fines migration and determine the uniformity of the flow distribution in the FCT cell.

Figure 3-13. The photo illustration of the differential pressure transducers

In the research, six and seven pressure transducers are set up for the vertical and horizontal FCT tests, respectively. These transducers are connected to narrow steel pipes installed inside the sand pack at three elevations of 3.5, 6.5, and 9.5 inches from the base plate and two radial distances of 3 and 3.6 inches from the center of the liner (Figure 3-14). The configuration of the pressure ports allows validating the flow distribution's uniformity inside the sand pack by comparing the pressure differentials near the slotted liner.

Determining the uniformity of the flow distribution inside the sand pack is essential to verify whether an experiment is successful. In ideal cases where the same amount of fluid is injected from the outer side of the sand pack, pressure readings at the pressure ports located at the same radial distances from the vertical liner should be similar. Figure 3-15 displays a schematic of the pressure ports on the base plate with their letters and numbers regarding the vertical FCT tests. Ports with A and B letters are located at a radial distance of 3.6'' referred to as far ports and 3'' referred to as close ports from the liner center, respectively. Numbers 1, 2, and 3 indicate the vertical locations of the pressure ports at levels of 9.5'', 6.5'', and 3.5'' from the bottom,

respectively. For example, port A1 is located far from the liner at the height of 9.5'' from the bottom.

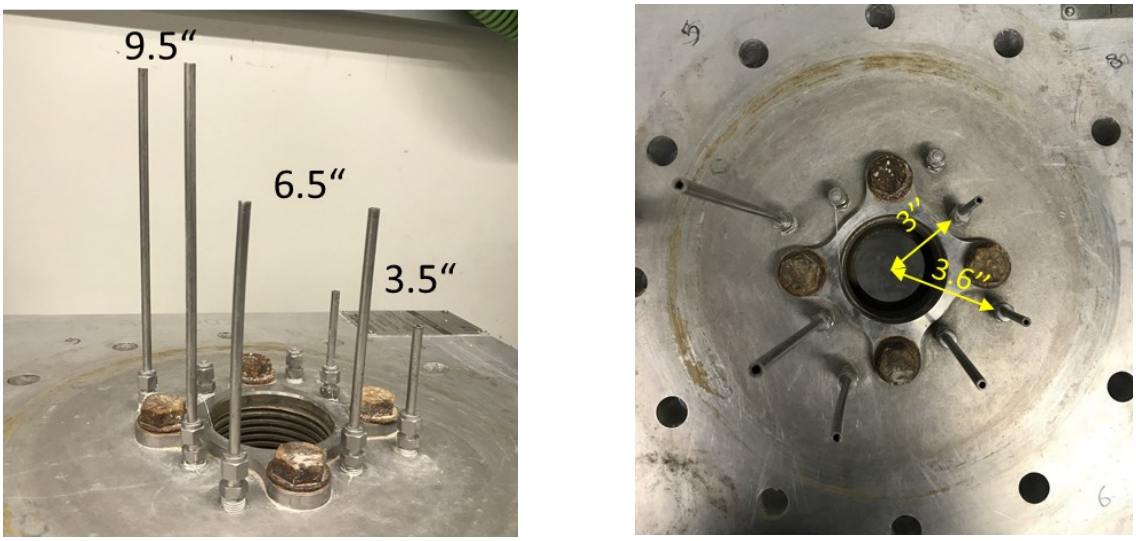

Figure 3-14. The photo illustration of the pressure ports in the lab for the vertical FCT tests

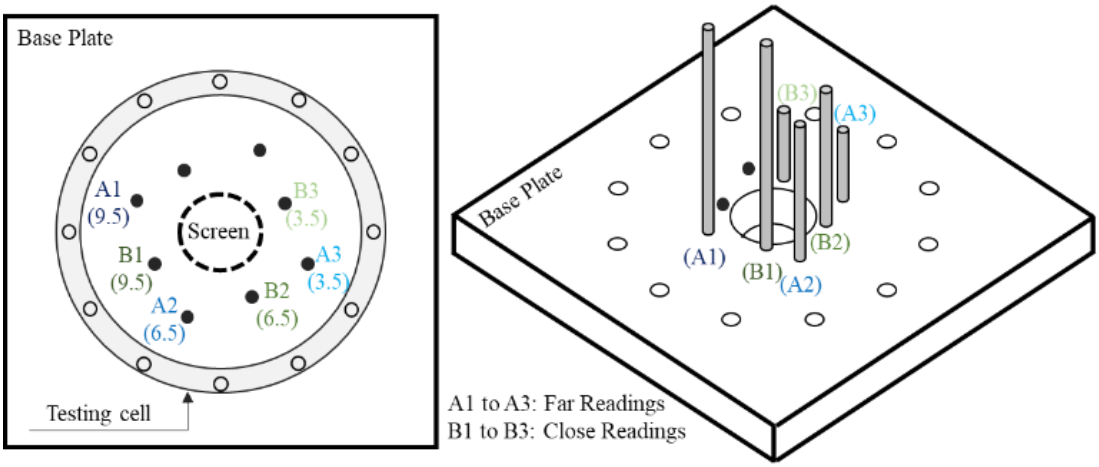

Figure 3-15. Schematic of the pressure port locations around the liner and their labels; top and side view (the numbers below each label is the height of the pressure port in inches) in the vertical tests, after Haftani et al. (2020)

Two additional pressure ports were set up for the horizontal direction of the FCT testing. Initially, two different pressure transducers were added to the system. However, because of problems relating to the Data Acquisition (DAQ), one of the two added pressure transducers cannot function adequately. Consequently, seven out of eight pressure ports are included in the system to track the pressure evolution around the liner in the horizontal FCT experiments. A schematic of the pressure

port locations with their labels and numbers concerning the horizontal experiments is demonstrated in Figure 3-16. Ports A4 and B4 are the additional ones added to the monitoring system. Since the FCT cell is rotated along the base plate's axis, ports A2 and B2 become the top part of the cell, while ports A4 and B4 are the bottom ones.

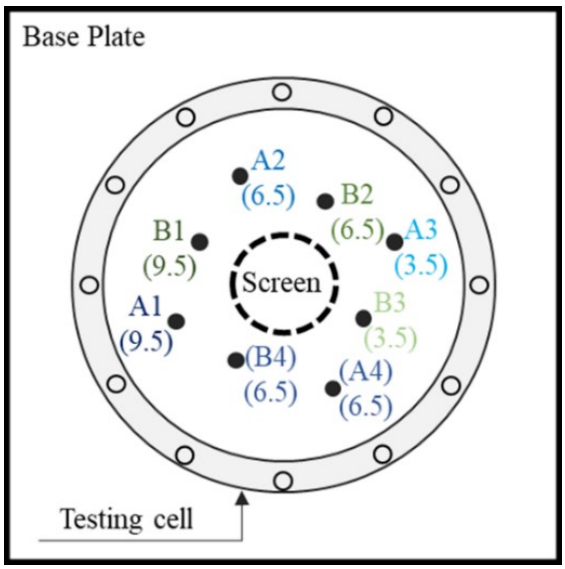

Figure 3-16. Schematic of the pressure port locations around the liner and their labels; top and side view (the numbers below each label is the height of the pressure port in inches) in the horizontal tests (top view of the base plate where it is rotated)

During the flow test, the differential pressures between the pressure ports and the liner are measured using the differential pressure transducers. The DAQ device is employed to collect signals transmitted from LabVIEW Signal Express software's pressure transducers. The volume of produced fluid coming out of the back-pressure column in 2 minutes is measured using graduated cylinders, and then the flow rate can be calculated by dividing the fluid volume by the interval. The flow rate is measured every 10 minutes on average during the flow test to control the injection rate.

3.3.4 Sand and Fines Measurement Unit

The sand and fines measurement unit comprises the sand trap used to monitor the produced sand during the test (Figure 3-17). The sand trap is installed at the center of the base plate bottom, as shown in Figure 3-18. A metering needle valve is connected to the sand trap to control the flow rate coming out of a pipe, aiming to avoid disturbing the fluid pressure in the sand pack while

collecting effluent samples from the sand trap to measure the concentration of produced fines. Fines are particles smaller than 44 microns (Abram and Cain, 2014). The PSD of produced fines can be measured using a laser particle size analyzer.

Moreover, the mass of the produced fines is estimated by a turbidimeter device that can be calibrated employing standard bottles with known turbidity. The relationship between readings of turbidity meter and fines concentration is linear. The total amount of produced fines for each stage is determined by multiplying the fluid volume produced per stage with the concentration of produced fines in that stage.

Figure 3-17. The photo illustration of the sand trap

Figure 3-18. The photo illustration of the sand trap in the system

3.3.5 Back Pressure Unit

As shown in Figure 3-19, the back-pressure unit is primarily used to generate minor back-pressure (3.25 psi) on the sand pack during the saturation and flow phases. For the saturation phase, a low injection rate is pumped into the sand pack through the back-pressure column to prevent the viscous fingering and channeling phenomena.

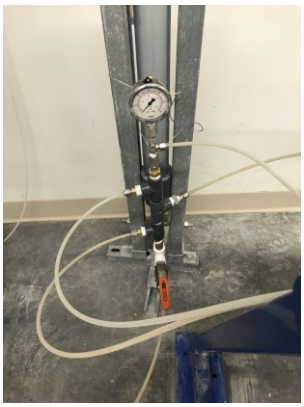

Figure 3-19. The photo illustration of the back-pressure column

3.4 Testing Procedure

3.4.1 Flowing Fluid

Bennion et al. (2009) showed that pH and salinity could considerably influence the mobilization, flocculation, and deflocculation of clays in the SAGD context. Over time, condensed water mixes with formation water, resulting in a gradual decrease in the produced water salinity when more melted bitumen and water are produced. On the other hand, the pH level observes a gradual increase when more condensate with caustic nature is injected (Bennion et al., 2009). Acidic gases such as carbon dioxide decrease the pH of formation water (Bennion et al., 2009). The typical initial formation salinity ranges from less than 4,000-100,000 ppm (Cowie, 2013) to 1,500-5,000 ppm for the SAGD production wells (Peterson et al., 2007).

Mahmoudi (2016) analyzed the significance of brine salinity and pH on the clay mobilization in the SAGD wells. The retained permeability is lower regarding lower salinities while the value goes up concerning lower pH levels. Within the thesis, Sodium Chloride brine with a salinity of 400 ppm and a pH of 7.9 is prepared as the injection fluid. Sodium and chlorides were examined to be the dominant ions in water produced from SAGD wells (Montero, 2019). Many studies have

shown that for SAGD wells, 400 ppm is the lowest salinity value, and 7.9 is an average pH level (Mahmoudi, 2017; Birks et al., 2017; Haftani et al., 2019).

3.4.2 Slotted Liner

The experiments in the thesis employed a rolled top slotted liner with a diameter of 3.5 inches and a height of 12 inches (Figure 3-20). The aperture sizes are 0.028 seamed to 0.022 inches. Four columns of slots are manufactured, including 18 slots per each column. Employing the multi-slot liner in the laboratory testing enables us to capture the inter-slot interactions.

Figure 3-20. The photo illustration of the rolled top slotted liner

3.4.3 Setup and Liner Assembly Phase

Before a packing procedure, a verification step of the cleanliness of the apparatus is required. It is needed to clean the machinery with water, pressurized air, and appropriate detergent. The work has to be explicitly done in the following parts: a) the sand trap connection, b) the flowlines, and c) pressure ports. Besides, the liner must be washed and cleaned before gauging the slot size. Also, a connection from the triplex metering pumps to the back-pressure column is checked. After fulfilling the column, the volume of brine is released to rinse the back-pressure pipe. It is essential to have all O-rings inspected to examine if there is any damage to them, and further action required to replace them if necessary.

Moreover, it is required to put a mesh inside the pressure ports to avoid any sand entering. Subsequently, the liner is screwed carefully to the FCT table. Afterward, one gasket is utilized to

seal the cell, followed by placing it on the base plate. Marks on the FCT cell must be adjusted to match with other marks on the base plate to keep consistent relative positions of the injection ports and pressure ports, ensuring consistency in comparing the testing results. Later, nuts are tightened in the order from 1 to 12 strictly.

3.4.4 Sand Pack Preparation

In the sand pack preparation, the dry commercial sands and clay are mixed to achieve a uniform particle distribution similar to that of the McMurray Formation. The compositional fractions of the existing clay materials in the core samples from the McMurray Formation's oil sands are 64.5%, 23.3%, and 11.3% for kaolinite, illite, and smectite, respectively (Devere-Bennet, 2015).

In the thesis, the DC-I type of PSD is replicated by mixing two commercial sands and one commercial clay. The detailed composition of a tested sand mixture is shown in Table 3-3. The shape factors, including sphericity, angularity, and aspect ratio of the commercial sands in the sand pack preparation, are reasonably comparable to those of the field sands (Mahmoudi, 2017). Thus, the mixture replicated in the lab could represent the formation sands for large-scale testing (Mahmoudi, 2017). The XRD analysis of the commercial clay indicates 67wt% of kaolinite, 28wt% of illite, and 5% of quartz. The composition is comparable to the one reported by Devere-Bennet (2015), except that it is missing the smectite clay.

Table 3-3. The composition for a dry sand-mixture of the DC-I

LM125 (gr)	Sil-1 (gr)	Helmer Kaolinite (gr)
26,600	5,890	5,510

38 kg of dry commercial sands and clay are prepared via two batches for one experiment. Each batch, including 19 kg of the dry sample, is mixed thoroughly in a mixture for around 10 minutes to reach a uniform mixture with the desired PSD (DC-I). After that, 10% wt of brine (1.9 kg) is added for each batch and mixed in the mixer for another 10 minutes to produce a uniformly moist sand-mixture sample.

Figure 3-21a displays the installation of the FCT cell before packing the sand. A moist tamping method is employed to pack the sand layers. Two layers of geotextile wrap a mesh before being put inside the FCT cell to ensure the uniform fluid injection from the sand pack's outer side. Next,

twelve uniform sand layers in the sequence are packed. A small rod is employed to flatten the surface of the sand. Each layer has a height of 1.4 in and weight of 3,656g on average predetermined respect to target porosity of 37% and grain-specific gravity. After packing each layer, its surface is slightly scratched to avoid discontinuity between packed layers. Before the packing goes to layer #10, a de-airing tube is installed on the cell (Figure 3-21b).

After finishing the sand packing phase, the de-airing tube is put neatly on the sand pack top before placing a specially designed diaphragm on the top of the sand pack. The diaphragm edges must be right at the cell top gasket rim to secure the diaphragm in place and prevent any leaks from occurring (Figure 3-21c). A top flange is then installed before tightening the nuts in a cross fashion to avoid over-torque and damage to it. Next, another gasket is put on the top of the sand trap, and then the sand trap is installed at the base plate bottom. Figure 3-21d shows the complete cell assembly in the vertical test.

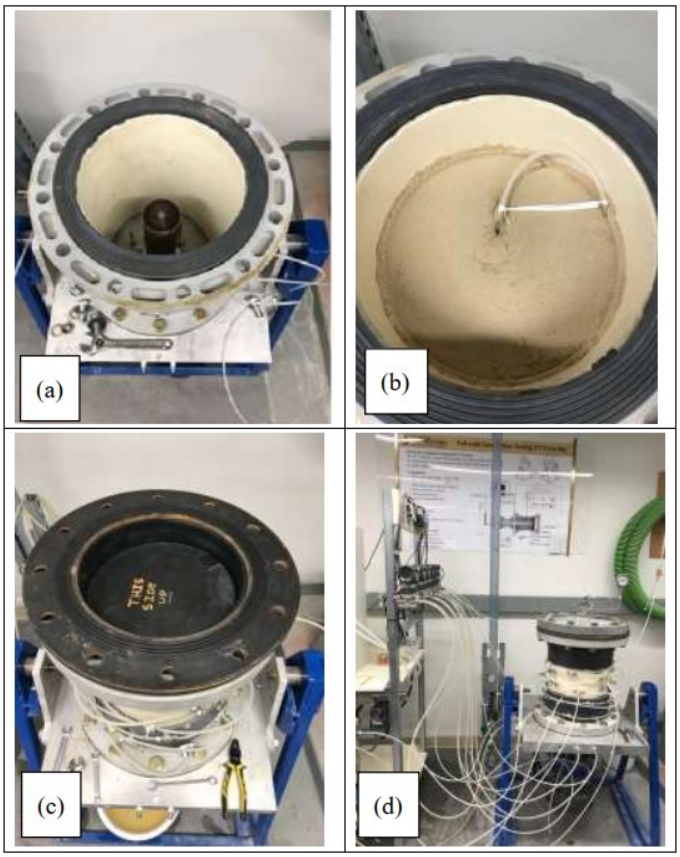

Figure 3-21. Sand packing phase and cell assembly: a) the FCT cell before the packing phase, b) the installation of the de-airing tube, c) the installation of the diaphragm, and d) the vertical FCT cell after packing the sand.

Later, 20 psi axial stress is applied over the sand pack using the air supply to pressurize the diaphragm. The air pressure is maintained for 5 minutes to check if any leaks are present in the system. If the air pressure drops more than one psi, it is essential to depressurize and remove the top flange. The investigation would be repeated and troubleshot until no leaks are spotted.

3.4.5 Saturation Phase

The sand pack is saturated by pumping brine at 8,000 cc/hr through the back-pressure column. De-airing the cell and pressure measurement tubes must be done to ensure the sand pack is fully saturated. The start time of fluid injection is recorded. Based on the past experimental works, it takes almost 3-4 hours to saturate the sand pack with brine thoroughly.

In the end, the outlet is checked if any bubbles are produced. Besides, the flow rate at the outlet is measured to see whether it gets stabilized. All air bubbles existing in the pressure measurement tubes connected from the FCT cell to the transducers must be removed to ensure all the pressure transducers operate precisely. The cell is left overnight in the vertical position for the vertical FCT tests. Regarding horizontal FCT experiments, the cell is rotated horizontally.

After completing the saturation phase, the connection between the back-pressure column and the pumps is closed to isolate it, opening the pumps' flow path to the sand pack. It is reminded that the saturation phase is performed with axial pressure applying over the sand pack to ensure no fluidization occurs.

3.4.6 Brine Injection

The brine injection scheme in the laboratory can be devised by scaling down the field production rate by the following equation:

$$\frac{Q_{lab}}{Q_{fielf}} = \frac{A_c}{l_w\left(1-\frac{\alpha}{100}\right)C_w}\frac{1}{\left(1-\frac{\beta}{100}\right)} \tag{3.1}$$

where Q_{lab} is the brine flow rate in the lab (bbl/day), Q_{field} is the typical production rate in the field (bbl/day), A_c is the total surface area of a coupon (ft^2), l_w is the SAGD well length (ft), α is non-contributing liner connection (%), C_w is the wellbore circumference (ft), and β is the slot plugging potential (%).

The typical production rate is 2,000-4,000 bbl/day for the SAGD wells with a length of 700-1000 m. Thus, the well liquid flux employing a 7-inch slotted liner is in the range of 0.33-0.95 bbl/day/ft^2. The range would be 0.30-0.87 bbl/day for the liner with an area of 0.92 ft^2. Plugging of sand control screens owing to many factors such as scale deposition, corrosion products, and fouling by fines deposition can render the slot plugging up to 90% (Romanova and Ma, 2013; Montero et al., 2018). Also, the non-contributing sections, because of liner connections of the sand control completion, could make up around 20% of the well length. Thus, taking into account the non-contributing sections and different plugging levels, the flow rates at the laboratory scale are calculated to emulate the SAGD production flux in this thesis (Figure 3-22). Table 3-4 details the flow rate for each stage.

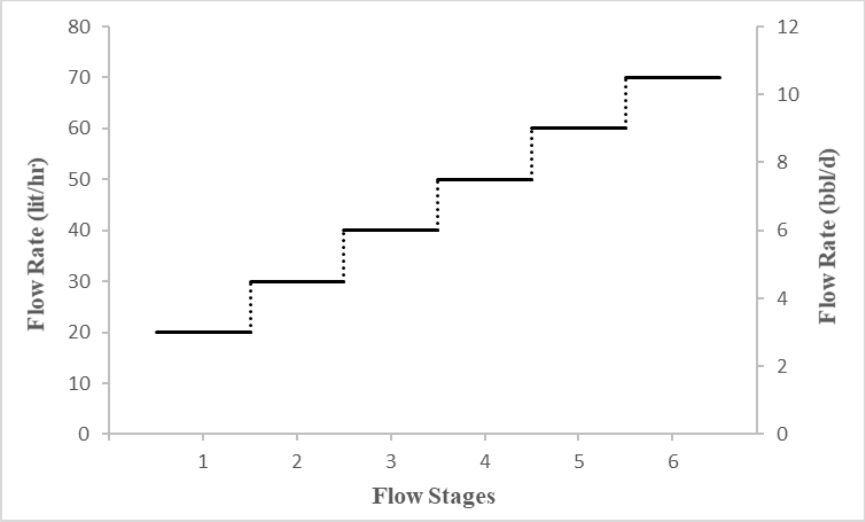

Figure 3-22. The flow rates for single-phase brine injection during the FCT tests

Table 3-4. Detailed flow rates during the flow test

Flow stage	Flow rate (cc/hr)	Flow rate (lit/hr)
1	20,000	20
2	30,000	30
3	40,000	40
4	50,000	50

5	60,000	60
6	70,000	70

The VFD frequency is set up corresponding to each stage, as demonstrated in Table 3-5. The VFD frequency and ramp-up time rise following increases in the flow rate. Once the VFD frequency is 10, the acceleration time is set on 720 to apply the ramp-up in the injection stage.

Table 3-5. The VFD and ramp-up time for each stage

Stage No.	1	2	3	4	5	6
Flow rate (cc/hr)	20,000	30,000	40,000	50,000	60,000	70,000
VFD	9	13.5	18.1	22.9	27.6	32.1
Ramp up time (min)	1.8	2.7	3.62	4.58	5.52	6.42
Ramp up rate (lit/hr/min)	11.1	11.1	11.0	10.9	10.9	10.9

At the beginning of each flow stage, the DAQ application software is started. Following that, valves between the brine tanks and pumps are open. Next, the two pumps start operating simultaneously. During the flow ramp-up period, one effluent sample is collected. When the flow gets stable, the injection rate is reported, and another effluent sample is collected. The pressure variations inside the cell are recorded during the ramp-up and flow-stabilized periods.

Each flow stage is carried out for around 15 minutes. At the end of each stage, the program is stopped recording, and the two pumps are turned off to stop the fluid injection. All data is saved into files on either a desktop computer or google drive. All these steps are repeated to complete six injection stages. Lastly, the valves between the brine tanks and pumps are closed.

3.4.7 Sampling

After performing all the liquid flow stages, the back-pressure column is drained, followed by draining the cell. All the lines from the cell, including injection lines and pressure measurement lines, are then disconnected. When the sample is completely drained, the axial load is released slowly. Eventually, the top flange is open for sampling.

Two types of samples collected after the test are vertical and horizontal samples for fines concentration measurement inside the sand pack, as displayed in Figure 3-23. Regarding the horizontal samples, three horizontal cores from the front and three ones from the back view of the sand pack at three different elevations of 3.5'', 6.5'', and 9.5'' from the bottom are extracted from the sand pack using a split core barrel. Three samples are extracted from each horizontal core at the distances from the outer liner surface of 0-0.8'', 0.8-1.6'', and 1.6-2.4''. The horizontal samples are labeled using four terms including location (F for the front, B for the backside), level (B, M and T for 3.5'', 6.5'', and 9.5'' from the bottom), and radial distance (C for 0-0.8'', M for 0.8-1.6'', and F for 1.6-2.4'' from the outer liner surface). Regarding the horizontal FCT test, the horizontal cores are also extracted at the left and right sides of the sand pack (L for the left side and R for the right side) (Figure 3-24). Also, one extra horizontal sample is extracted from each horizontal core located at the interval with a radial distance of 2.4''- end from the outer liner surface, labeled as F2.

Concerning the vertical samples, two vertical cores are taken. One is far from the liner at the front view of the sand pack; another is from the backside adjacent to the liner (Figure 3-23). Five samples are extracted from each vertical core at the distances of 3.5'', 6.5'', 9.5'', 12'', and 14'' from the bottom. The length of each vertical sample is 1''. The vertical samples are labeled using sample type (V for vertical samples), location (F for front and B for backside), level (B, M, T, T1, and T2 for vertical distances from the bottom of 3.5'', 6.5'', 9.5'', 12'', and 14'').

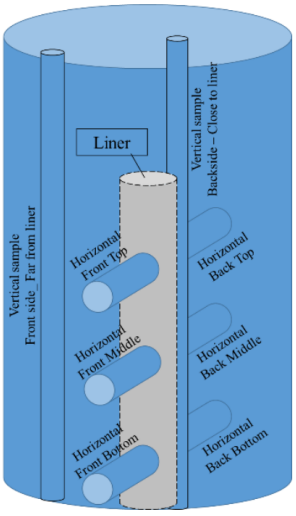

Figure 3-23. Schematic of the sampling configuration regarding the vertical testing condition, after Haftani et al. (2020)

Figure 3-24. The photo illustration of the sampling phase regarding the test performed in the horizontal direction of the sand pack cell

Figure 3-25 depicts detailed steps for taking core samples from the sand pack in the vertical FCT tests. The nuts are opened by the order to remove the top flange before taking out the gasket and diaphragm (Figure 3-25a). Next, the mesh is removed from the sand pack (Figure 3-25b). The horizontal cores are collected from the front and back views (Figure 3-25c). Subsequently, the vertical cores are taken, as shown in Figure 3-25d. For the horizontal FCT tests, the horizontal cores are also taken from the left and right views.

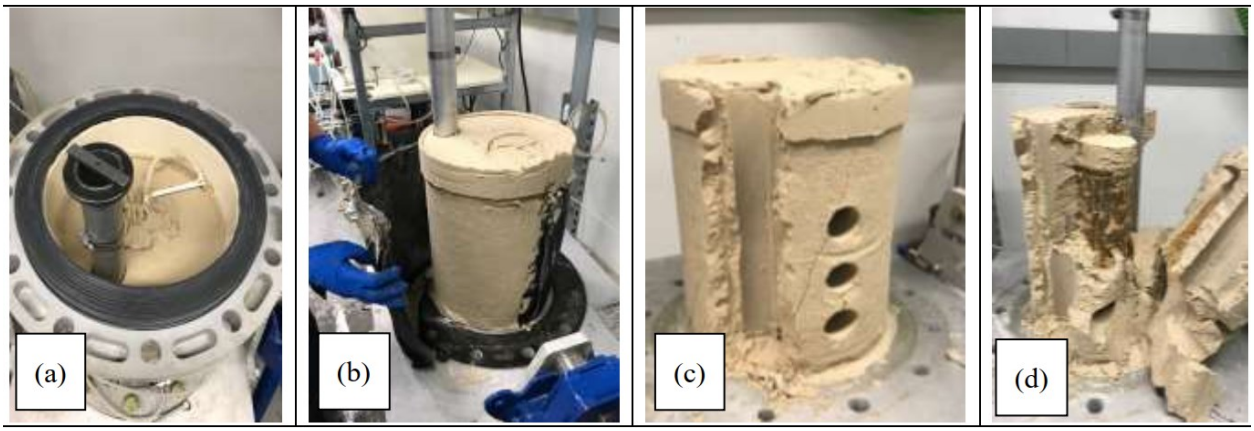

Figure 3-25. Sampling steps in the vertical FCT tests. a) The removal of the top gasket, b) The sand pack after removing the mesh, c) Three horizontal cores from the front view and the vertical core at the front, and d) the vertical core at the back.

When all samples are collected, they are put carefully into small cups appropriately labeled according to their origins. The cups are placed in an oven at 100°C for 6 hours to vaporize all the

liquid inside them. Each dry sample and its container are then weighted (Table 3-6). Later, each sample is crushed slowly by mortal and pastel and then mixed with water thoroughly using a blender. The mixture is then dumped into a specially designed sieve with a mesh size of 44 μm to separate sand and fines. Next, the sand is washed out of the sieve into the container. After that, the cup containing the wet sand is dried one more time in the oven at 100°C for at least 6 hours. Thereafter, the cup with the dry sand is weighed and recorded.

Table 3-6. The sample of the wet sieving data

Date:				
Sample Name	Weight of cup (gr)	Weight of dry sand & cup (gr)	Weight of sand & clay (gr)	Weight of washed clay (gr)

3.4.8 Produced Sand and Fines

After completely draining the FCT cell, the sand trap is disconnected carefully and slowly due to its heavyweight. Two samples of the produced sand during the fluid injection and the saturation phase are collected. All sands around the liner are removed by shaving the liner, as displayed in Figure 3-26.

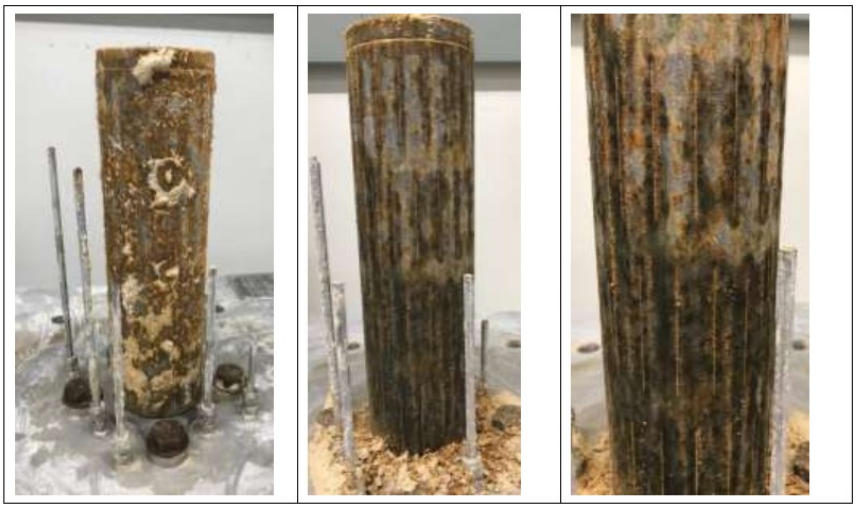

Figure 3-26. The photo illustration of the liner before and after cleaning

A picture of the liner with a flashlight is taken to check whether any plugging is inside the slots. It is more helpful to use a magnifier to examine all slots for any plugging inside them. Ultimately, the liner is opened, and two other samples that are produced sand inside the liner and the slots are

collected. Cups containing the wet sands are dried using the oven at 100°C for at least 6 hours before being weighed. For the produced fines measurement, the samples in small bottles collected during the saturation and flow stages are shaken and then put into the chamber to measure each sample's turbidity.

3.5 Conclusion

The chapter outlined the final version of the experimental setup and operating procedure regarding the FCT test in both the vertical and horizontal positions. Following the standard testing procedure strictly is vital for the success of the laboratory experiment.

In the next chapter, the thesis will elaborate on all the FCT experiments carried out with both the vertical and horizontal liner. Initially, the testing facility showed many deficiencies in generating uniform fluid injection. Numerous improvements to troubleshoot challenges and shortcomings in the testing setup and testing procedure were implemented through experimental works before reaching their final versions.

Chapter 4: Detailed Improvements of the FCT Setup

4.1 Introduction

The FCT facility is a new testing setup for evaluating the SCD performance with the radial flow regime. It is an advanced apparatus for simulating SAGD operations more closely than the SRT equipment.

Chenault (1938) presented testing results with a radial-flow cell apparatus for conventional well operations, which compares flow rates considering cases with and without sand control screens. Qi (2004) conducted multiple tests to compare the performance of pre-packed screens versus gravel packing via developing a large-scale experimental device incorporating the radial-flow regime in sand production. Papamichos et al. (2001) and Nouri et al. (2005) carried out hollow cylinder tests to study the sanding level and failure of the perforation in the near-wellbore formation when injecting a high flow rate from the outer surface of the specimen towards the central hole.

Jin et al. (2012) assessed the performance of several sand control screens for gas wells by developing large-scale laboratory equipment capable of emulating the radial flow, studying the effects of pressure and flow rates on sand stability. Dong et al. (2017) devised a set of indexes with the calculation method to assess the screen performance employing a novel experimental device with the radial inward flow. Anderson (2017) introduced a novel large-scale apparatus using a cylindrical screen to validate previous small-scale testing results with a single-slot coupon. They claimed a good agreement in the testing results from small- and large-scale testing facilities. Ma et al. (2020) developed an experimental facility to evaluate the screen performance in which a sand slurry injected follows a radial geometry towards the screen from the outer boundary.

In summary, most of the facilities incorporating the radial flow have been established mainly for conventional wells. The radial flow regime has not been thoroughly studied in the thermal recovery context. The FCT facility employs the radial flow configuration and can be considered a major advancement over the past research works. Nonetheless, running the FCT setup is not an easy task, requiring many attempts to mitigate the original FCT setup's limitations. This chapter will outline several FCT tests accompanying its results and discussions. All modifications implemented to improve the FCT setup and testing procedure through experiment practices will also be presented.

4.2 Summary of the Tests

There are twelve tests in total within the thesis, including eight vertical, one flow calibration, and three horizontal tests. The liner's position, modifications, and purposes of the experiments are outlined in Table 4-1. The first five experiments are unsuccessful because of some limitations in the setup. Test V6 is marked as the first successful experiment. The next two identical tests (Test V7 and V8) were performed to assess the repeatability. Test H9 was carried out with the liner being in the horizontal direction. Next, a flow calibration test was performed to address pump issues that were faced in Test H9. After tackling the pumps' problems, two more experiments (Test H10 and H11) were conducted in the horizontal direction. The following parts give further details on each experiment.

Table 4-1. The summary of remarks for the experiments

Test Name	Position of the liner	Remarks
Test V1	Vertical	- Refining FCT standard testing procedure - Replicating the DC-III type PSD from the McMurray Formation - Manual mixing of commercial sands
Test V2	Vertical	- Removing the flow manifold in the flow injection unit - Replicating the DC-II type PSD from the McMurray Formation - Installing more pressure transducers
Test V3	Vertical	- Replicating the DC-I type PSD from the McMurray Formation - Wrapping the mesh by two layers of geotextile for better fluid injection
Test V4	Vertical	- Introducing a pressure regulator - Troubleshooting many limitations regarding the setup
Test V5	Vertical	- Introducing a flow ramp-up

		- Applying a new sand packing method to achieve lower porosity of the sand pack
Test V6	Vertical	- Removing the pressure regulator - Using a mixer to produce a uniformly sand-mixture sample
Test V7 and V8	Vertical	- Assessing the repeatability of the test results
Test H9	Horizontal	- Designing a new configuration of the fluid injection unit
Flow Calibration Test	SRT	- Examining the operation of the pumps with the SRT facility
Test H10	Horizontal	- Re-designing the configuration of the fluid injection unit
Test H11	Horizontal	- Extending each flow stage of the injection test for a more extended period

4.2.1 Initial Testing Setup

The fluid injection unit is demonstrated in Figure 4-1, having only three rows of fluid ports to deliver brine from a small flow manifold. Figure 4-2 displays the FCT cell in the lab. Figure 4-3 presents a schematic of the pressure ports inside the sand pack around the liner. Only three pressure transducers were set up to keep track of ports B3, A2, and A3.

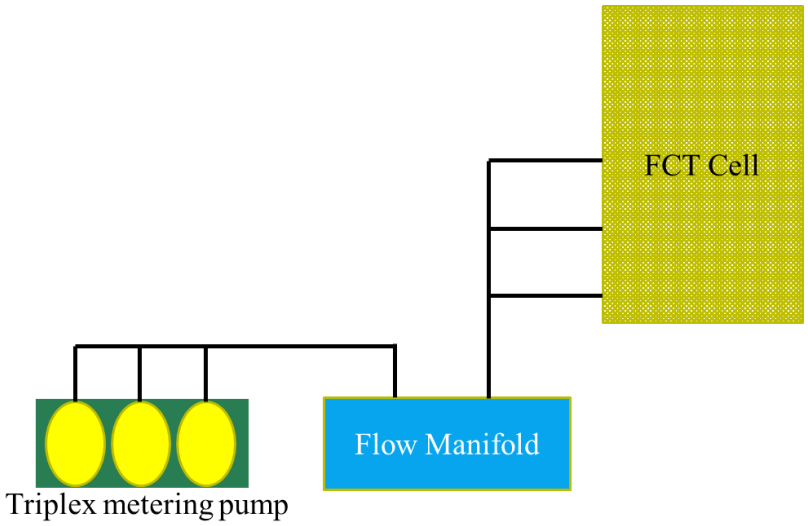

Figure 4-1. Schematic of the fluid injection unit

The dry commercial sands were mixed manually to achieve a uniform particle distribution in the packing preparation. 36 kg of the dry sand sample with 10% wt of brine (the salinity of 400 ppm and the pH of 7.9) was prepared and then mixed to generate a moist sample. The moist sand sample was packed into the FCT cell in a layer-by-layer method to achieve a uniform porosity of about 47%. At this time, the study employed the DC-III PSD type for the testing program. Also, the mesh was wrapped by one layer of geotextile.

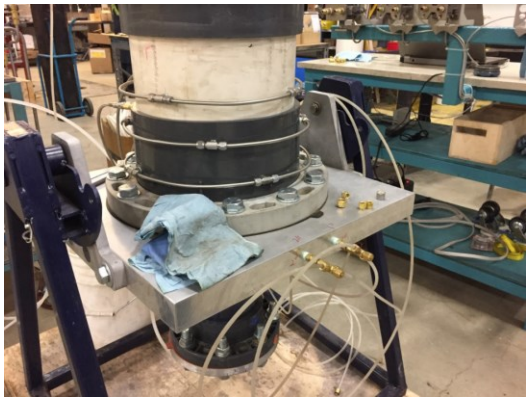

Figure 4-2. The photo illustration of the FCT cell

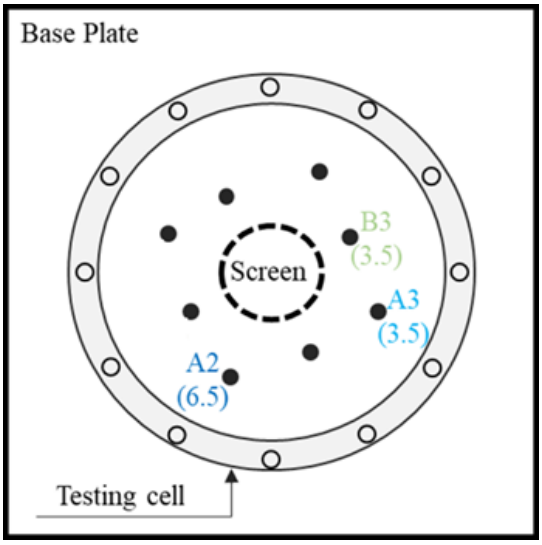

Figure 4-3. Schematic of the pressure port locations around the liner and their labels

4.2.2 Vertical FCT

4.2.2.1 Test V1: DC-III with manual mixing of materials

The experiment employed the DC-III PSD type. One more injection row was installed to generate flow at the top of the sand pack, as shown in Figure 4-4. Four injection rows were configured along

the height of the FCT cell. Each row had four injection ports located in the cell's circumference, attempting to provide the radial flow injection towards the sand pack. There were 16 fluid ports in total. The FCT cell was connected to the small flow manifold before the triplex metering pumps. There were four flowlines from the manifold at different elevations connected to the FCT injection points, as displayed in Figure 4-5.

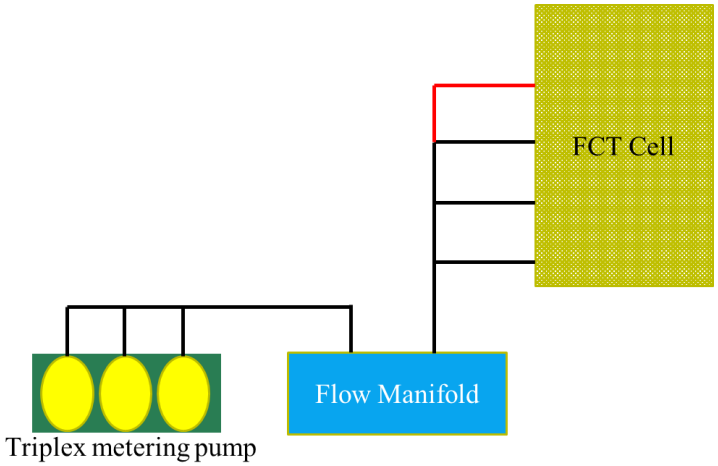

Figure 4-4. Schematic of the new fluid injection unit

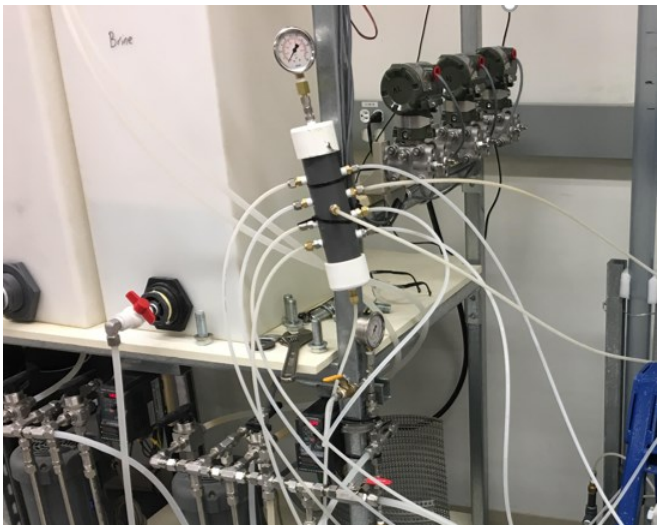

Figure 4-5. The photo illustration of the flow manifold

Figure 4-6 shows how pressure differential is distributed at A readings located at the same radial distance from the liner inside the sand pack. The figure displays a significant difference between these two locations, indicating that the flow distribution was not uniform. For instance, at Stage #6, the percentage difference between ports A3 and A2 is roughly 55%.

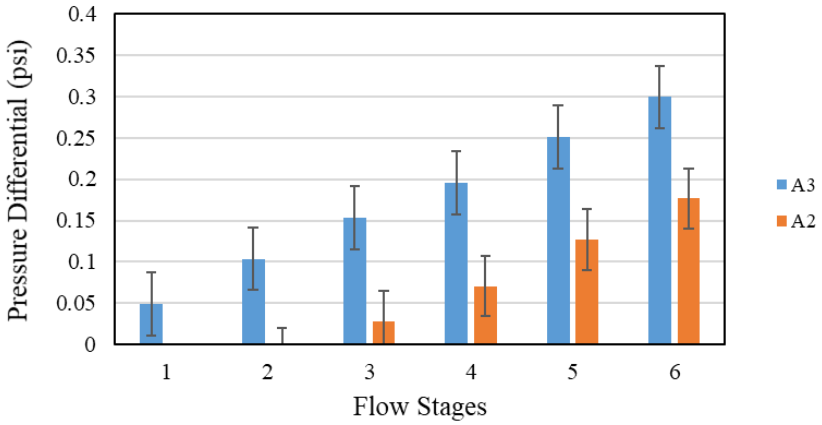

Figure 4-6. Pressure distribution around the liner at far readings.

When setting up the FCT cell for the first time, the position of injection ports with respect to the base plate was not noted. Essentially, the FCT cell is installed in a random direction that results in different relative positions of the injection ports and pressure ports, potentially impacting the comparison of test results. Further, most of the flow went to the flow manifold's bottom flowlines due to gravity. This observation raised a question about the manifold's necessity in the fluid injection system. Besides, it is necessary to record pressure changes at all pressure ports instead of only three ones.

To conclude, more pressure transducers were required. Further, the FCT cell needed to be appropriately set up to ensure a consistent position of the injection and pressure measurement ports to ensure the consistency in the comparisons. Fixing the non-uniform fluid injection due to the flow manifold was also necessary.

4.2.2.2 Test V2: DC-II with an increased number of pressure transducers

The problems related to Test V1 had to be addressed before running the following tests. Three more pressure transducers were added to address the limited number of differential pressure transducers. Six pressure transducers were installed in the system instead of only three transducers operating as the previous test. Concerning the relative positions of the injection inlets and the pressure ports, the base plate and the cell were marked to facilitate consistency. Lastly, the flow manifold was disconnected from the system, and the injection ports in the FCT cell were connected directly to the pumps to overcome the non-uniformity of the fluid injection (Figure 4-7).

The experiment employed the DC-II PSD. Still, several deficiencies were detected in the setup and testing procedure. One was that the pressure drop's magnitude was too small, making the assessments difficult (Figure 4-8). For the next experiments, the DC-I PSD was employed for its lower permeability instead of the DC-II. The far (A1, A2, and A3) and close (B1, B2, and B3) readings show the differential pressures are within 16 and 35%, respectively, indicating that the flow in the sand pack is not fully uniform yet (Figure 4-8).

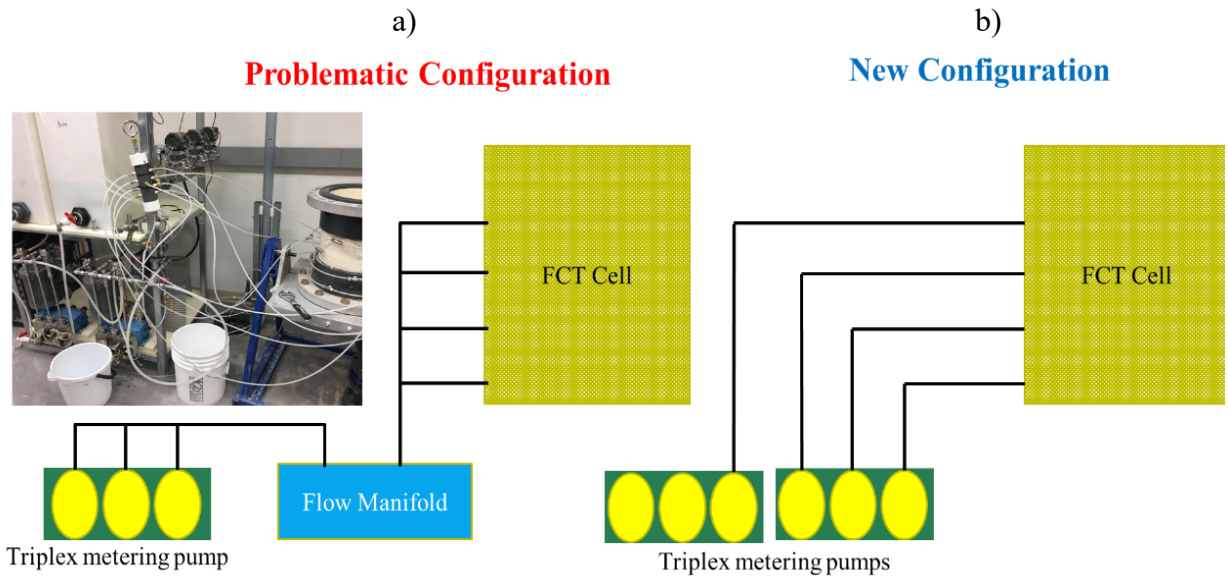

Figure 4-7. Schematic of the a) problematic, and b) new configurations of the fluid injection unit

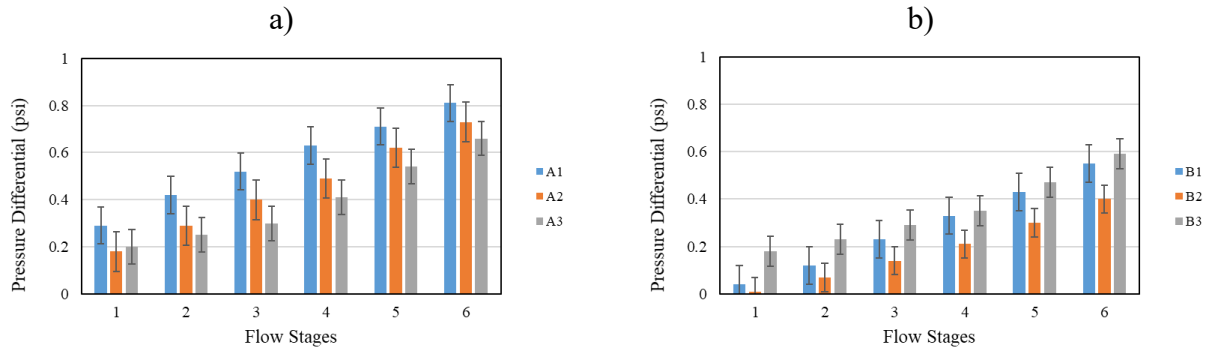

Figure 4-8. Pressure distribution around the liner at a) far readings, and b) close readings.

4.2.2.3 Test V3: DC-I

This test employed DC-I PSD for its low permeability to elevate the pressure differentials. One more modification was to wrap the mesh by two layers of geotextile rather than only one layer in

the previous tests, expecting to provide a more uniform fluid injection from the FCT cell's inner wall (Figure 4-9).

Figure 4-9. The photo illustration of the two geotextiles wrapping the mesh

The test was performed with the modifications mentioned above. Unfortunately, there might likely appear to be no flow at the top part of the sand pack. This was attributed to the sample not being fully de-aired (Figure 4-10). Regarding the saturation stage, all the injection ports were closed when brine came out from the ports. As the highest port was at the fourth level of the injection, there were no more ports to de-air the cell's top part. Therefore, a pipe was needed to be installed at the top of the sand pack in the next experiment to facilitate the de-airing of the sand pack when all the injection ports are closed. Another issue was that pressure measurement tubes had different lengths, affecting the measurements. Also, the differential pressures in the sand pack were still small (Figure 4-11), even with the DC-I PSD.

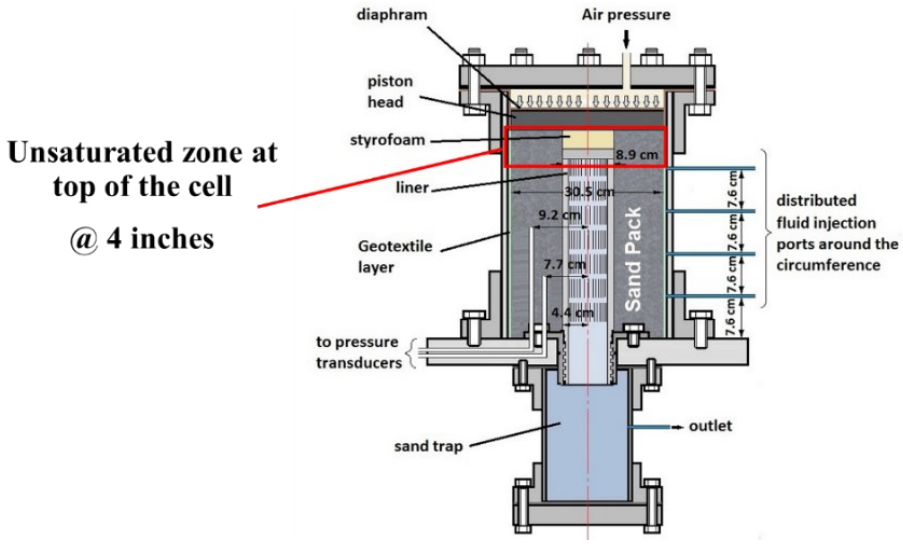

Figure 4-10. The unsaturated section at the top of the sand pack

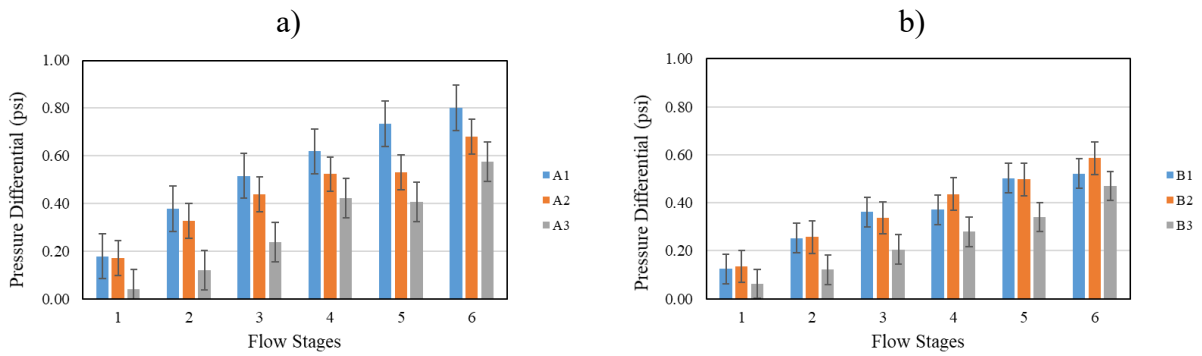

Figure 4-11. Pressure distribution around the liner at a) far readings, and b) close readings

4.2.2.4 Test V4: Installation of a pressure regulator

A pipe was installed at the sample top to facilitate the de-airing of the sand pack during the saturation phase to address the unsaturated part at the top of the sand pack (Figure 4-12). Further, the length of the pressure measurement tubes was set to be equal. A narrow tube was set up inside the sand trap beneath the central hole to immediately collect the outflow samples below the liner (Figure 4-13).

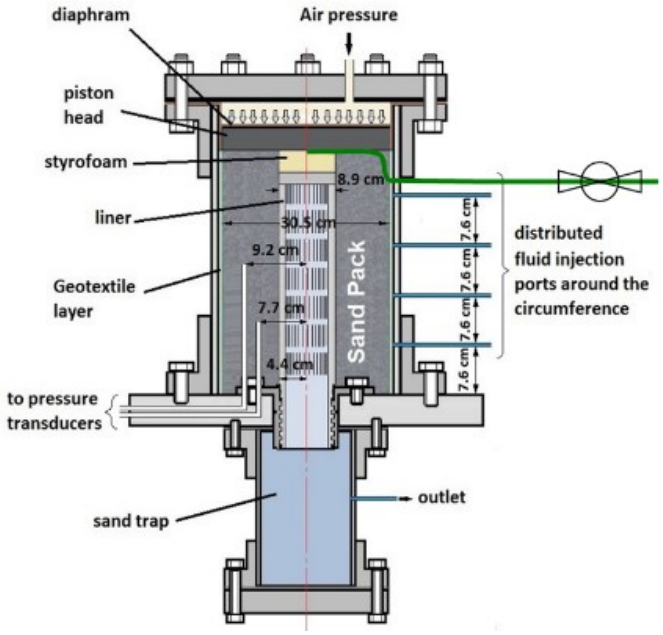

Figure 4-12. The FCT cell with the de-airing pipe indicated as a green line

Moreover, a pressure regulator was employed at the outlet to apply higher back-pressure in the sand pack (Figure 4-14). The pressure regulator allows increasing the back-pressure from 3.5 psi

to roughly 12 psi. The pressure regulator's opening can be manually manipulated based on the desired back-pressure.

Figure 4-13. The photo illustration of the sand trap with a narrow pipe

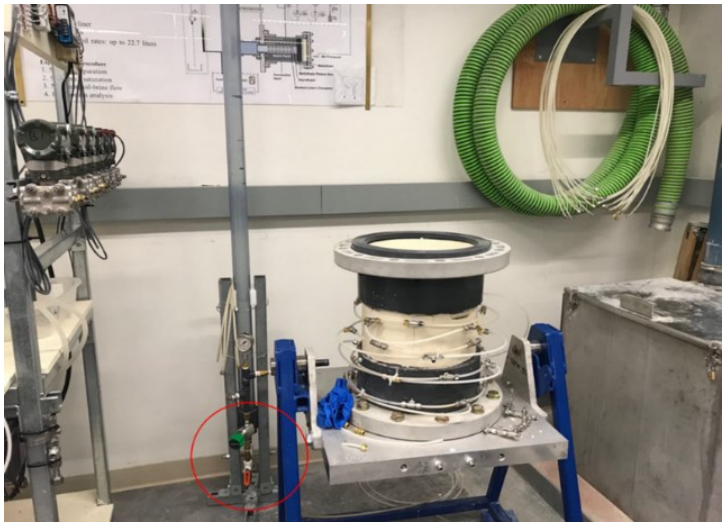

Figure 4-14. The photo illustration of the pressure regulator in the system, as highlighted in the red circle

The pressure differential during the injection Stage #3 at six pressure ports is displayed in Figure 4-15. As shown in the figure, there are large variations at the beginning of Stage #3, owing to manually adjusting the pressure regulator's opening to reach the target back-pressure of 12 psi. The same variation occurred at the start of other flow stages.

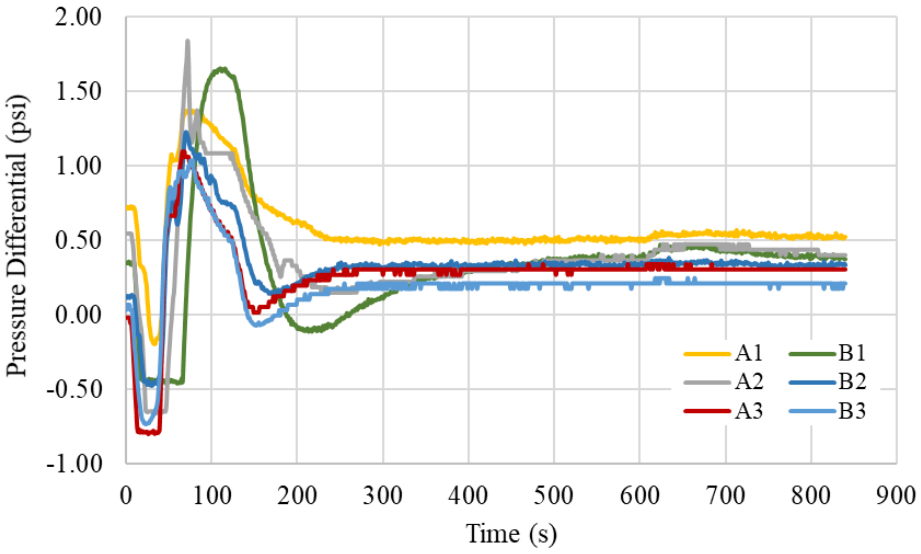

Figure 4-15. Pressure differentials during the third injection stage

Figure 4-16 shows the pressure differentials inside the sand pack. The magnitude of the differential pressure increases compared to the previous test. This can be explained by the fact that the higher pressure at the outlet was generated thanks to the pressure regulator, leading to the larger input pressure at the sand pack's outer side. The high-pressure injection reduced the effects of channeling and generated a more uniform inward flow through the sand pack towards the liner. For instance, the average pressure drops at Stage #2, #4, and #6 for ports A1, A2, and A3 in Test V4 are 111.5%, 73.5%, and 74% larger than the same in Test V3. More importantly, the pressure readings at A and B readings in Test V4 are within 5% and 6%, respectively. These variations indicate the uniformity of the flow inside the sand pack.

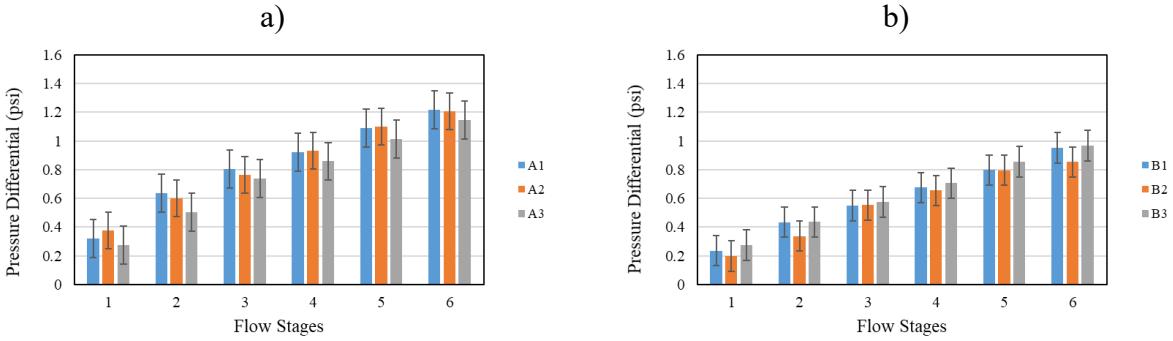

Figure 4-16. Pressure distribution around the liner at a) far readings, and b) close readings

The sand pack porosity in the first four tests was about 47%, which seems too high and one of the contributing factors in the low pressure differentials. Furthermore, it was noted that the sand pack's outer surface was not flat after removing the sample from the cell (Figure 4-17). Also, the high pressure differential variations at the beginning of each stage were concerning as it could affect the fines migration and testing results by the quick alteration of the flow and effective stress inside the sand pack. To summarize, the required improvements are to use the new packing method to compact the sand more to achieve lower porosity, replace the current mesh with the new one to render the more uniform surface of the sand pack, and resolve the pressure readings' fluctuations at the start of each flow stage.

Figure 4-17. The photo illustration of the sample surface of the sand pack

4.2.2.5 Test V5: Introduction of flow ramp-up

The first modification was to re-design the fluid injection unit by using the two pumps equally to ensure each pump delivers the same amount of brine. Figure 4-18 displays both the old and new configurations of the fluid injection unit.

The mesh and geotextile were also replaced by new ones to provide the sand pack a uniform surface, as illustrated in Figure 4-19. Another improvement of the sand trap was to employ a bigger line for collecting the fines samples, aiming to gather larger samples during the injection test and avoid any plugging in the line (Figure 4-20).

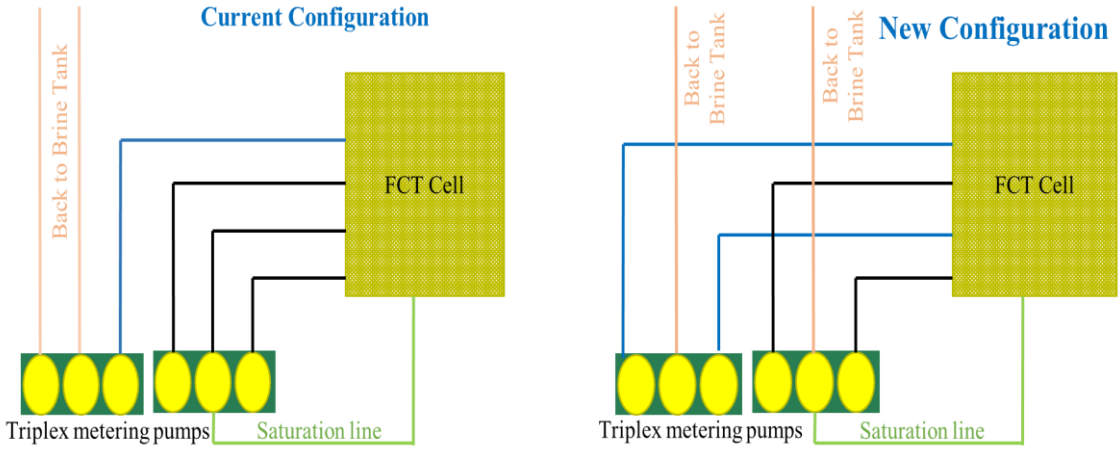

Figure 4-18. Schematic of the current and new configuration for the injection unit

Figure 4-19. The photo illustration of the sand sample surface with the new mesh

Figure 4-20. The photo illustration of the sand trap with the bigger line

Additionally, higher packing energy was applied over the sand pack during the sand packing phase to achieve a lower porosity of 37%. Consequently, the mass of the dry sand-mixture increased from 36 kg to around 38 kg, with the wet mass in the FCT cell being roughly 42 kg. The last improvement was introducing a flow ramp-up for the flow test to eliminate the abrupt jump of pressure differentials at the start of each flow stage.

The test was run with the modifications on the FCT setup and testing procedure detailed above. Figure 4-21 demonstrates the evolution of the pressure transducer's readings in Stage #1 with and without the flow ramp-up. The introduction of the flow ramp-up into the flow stages also facilitates the adjustment of the pressure regulator's opening. The large variations in the previous experiment without the flow ramp-up (Figure 4-21a) were reduced substantially (Figure 4-21b). Nevertheless, the pressure variations were still noticeable even with the flow ramp-up.

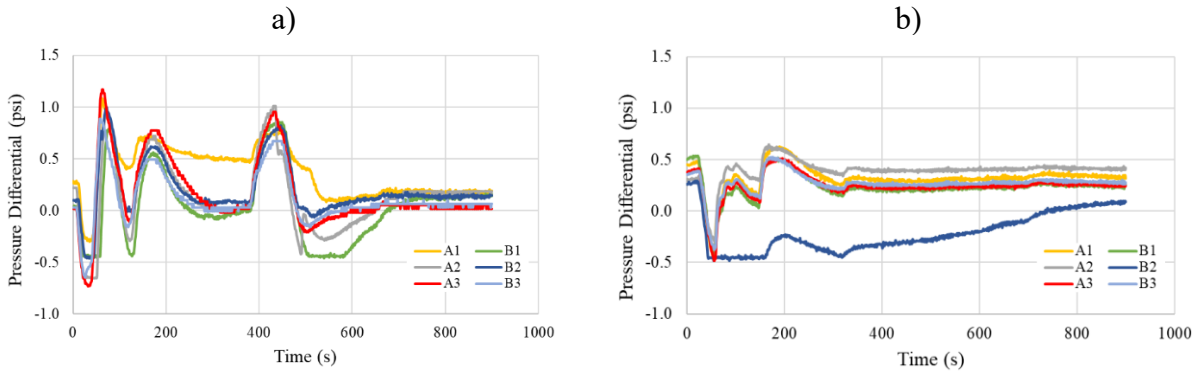

Figure 4-21. Pressure differentials in cases: a) without the flow ramp-up, and b) with the flow ramp-up during Stage #1

The far and close pressure readings in the experiment can be seen in Figure 4-22. As expected, by applying the new packing method to achieve a lower porosity of 37% compared to 47% in Test V4, the differential pressures around the liner increased substantially. For instance, the percentage increases of the pressure drop at ports A1, A2, and A3 between Test V5 and V4 for Stage #6 are around 83%, 78%, and 82%, respectively.

Nonetheless, the test was considered unsuccessful. The main problem that led to the test's failure was the noticeable variations observed at the flow stage's beginning in the pressure transducers' readings due to the pressure regulator manipulation, even after the flow ramp-up was introduced. The substantial pressure differential variations at each stage's commencement indicate that the pressure regulator's installation could highly disturb the sand pack, affecting the sand and fines

production. Since it was hard to control the regulator valve during the injection test consistently, it was necessary to remove the pressure regulator in the next experiment.

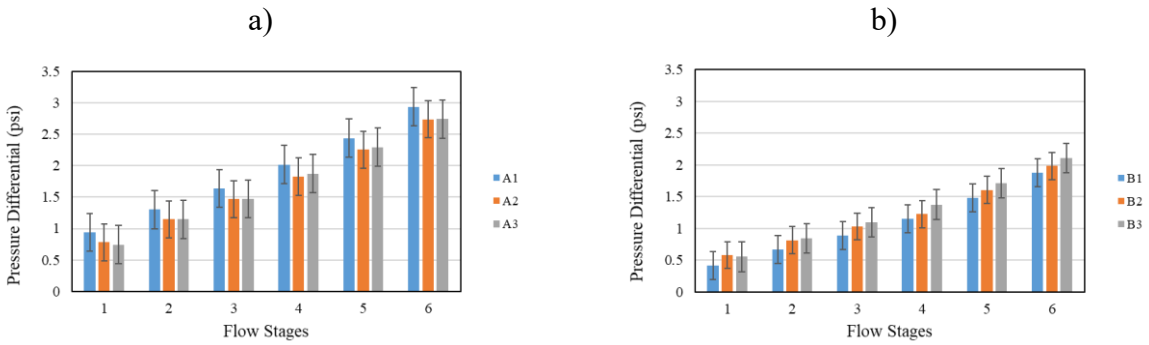

Figure 4-22. Pressure distribution around the liner at a) far readings, and b) close readings

4.2.2.6 Test V6: Removal of the pressure regulator

As described in Test V5, the pressure regulator was removed to address the substantial pressure variations at the beginning of each flow stage. The next improvement was to employ a mixer for mixing the dry commercial sands. The more uniform moist sand-mixture sample in the sand pack preparation can be achieved thanks to the mixer compared to manual mixing. Figure 4-23 demonstrates the pressure readings with and without the pressure regulator. The large variations in the pressure readings at the start of each stage disappeared after removing the pressure regulator. The pressure differential rises gradually during the ramp-up period before leveling off with minor oscillations (Figure 4-23b).

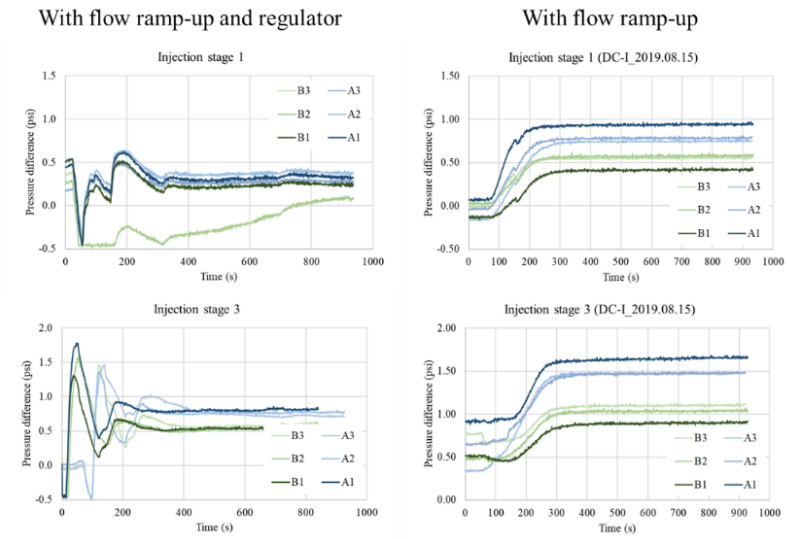

Figure 4-23. The pressure transducer readings with and without the pressure regulator

Figure 4-24 shows the pressure differentials at far and close readings, respectively. As shown in the figure, the differential pressures at far and close ports show less than 10% and 9% variations, respectively, which is reasonably close. In other words, the pressure distribution indicates the uniform flow distribution inside the sand pack.

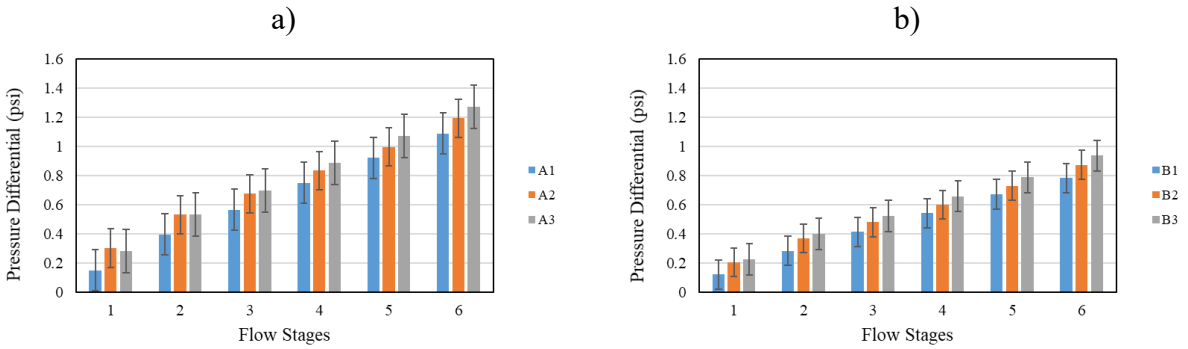

Figure 4-24. Pressure distribution at a) A readings, and b) B readings

Figure 4-25 displays the fines concentration in the horizontal samples extracted from the sand pack. The average values of the fines concentration in the samples at the far distance of 1.6-2.4'' and close distance of 0-0.8'' are 13.80 % and 13.77 %, respectively. The difference is not too significant, indicating the low amount of migrated fines.

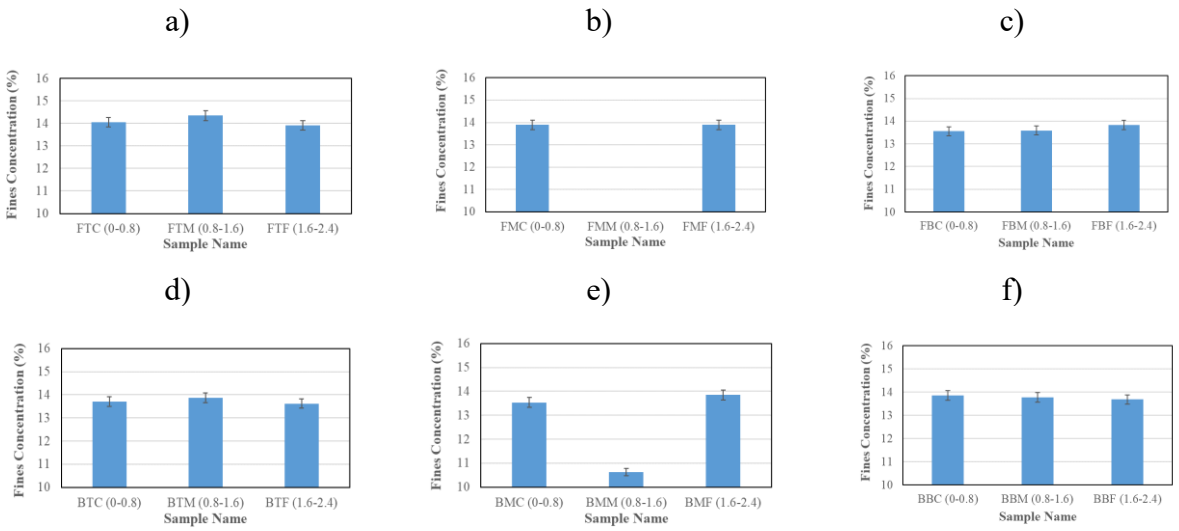

Figure 4-25. Fines concentration in the horizontal samples from the sand pack at a) front side-top, b) front side-middle, c) front side-bottom, d) backside-top, e) backside-middle, and f) backside-bottom

Figure 4-26 shows that the fines concentrations for the samples extracted from the vertical cores. The values are within 4 % and 3 % for the front and back samples, respectively, supporting the presence of the uniform flow in the sand pack.

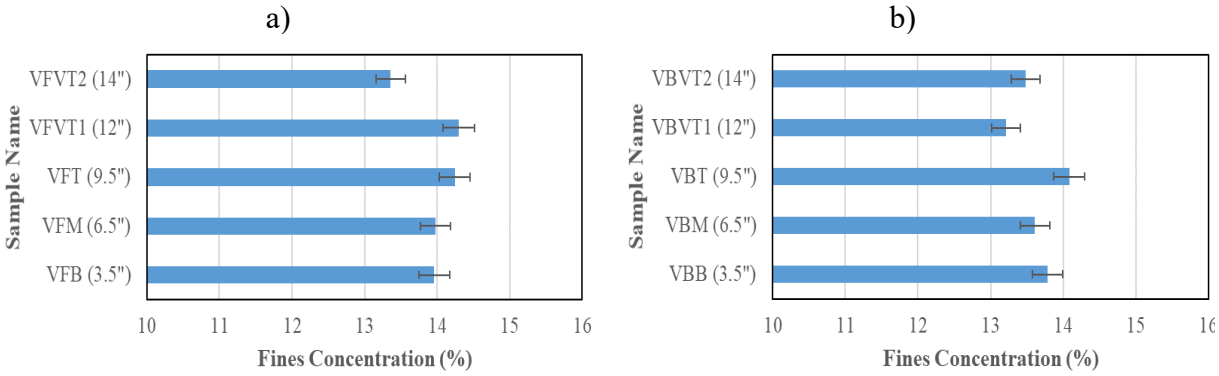

Figure 4-26. Fines concentration inside the vertical samples, a) front side-far from the liner, and b) backside-close to the liner

In summary, Test V6 was successful and achieved the uniform flow distribution inside the sand pack. Two different indicators, the pressure distribution and fines concentration inside the sand pack, were examined to confirm the flow distributed uniformly around the liner. However, this was the first time the mixer was used for the sand pack preparation. The dry sand with 10% wt brine (roughly 42kg in total) was mixed in the mixer that was higher than the mixer capacity. In the next experiments, the mixer was appropriately used by mixing two batches of sand to ensure uniform mixing.

4.2.2.7 Test V7 and Test V8: Assess the repeatability

Test V7 and V8 that are identical were carried out to identify the repeatability of the testing results and verify the uniformity of the flow inside the sand pack. For the sand pack preparation, the tested sand mixture was prepared in two batches, ensuring the mixer's functionality with the maximum capacity of 40kg.

Figure 4-27 displays the pressure differentials at different locations inside the sand pack for Test V8. As expected, the higher pressure differentials were measured as the flow rate went up. Moreover, at the same flow rate, differential pressures at the farther pressure ports (A1, A2, and A3) are higher than the pressure ports closer to the liner (B1, B2, and B3). A ports' pressure

readings are within 7%, and the differences for the B ports are less than 6%. These differences are within the acceptable range, indicating that the flow is distributed uniformly in the sand pack.

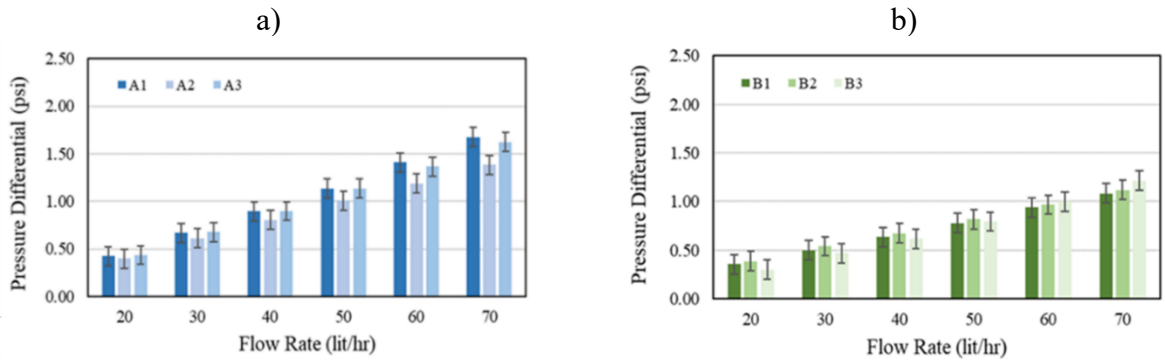

Figure 4-27. The pressure distribution at a) far, and b) close readings in Test V8

Fines particles were migrated from the sides towards the liner in Test V8, as shown in Figure 4-28. The horizontal samples located at the interval 1.6-2.4'' (distances from the liner) have lower fines concentration than the samples at the 0-0.8'' interval. The average value of the fines concentration in the far samples is about 12.5%, increasing to 12.7% in the close samples. Even when a general trend shows a decrease in fines concentration versus distance from the liner, the difference is insignificant.

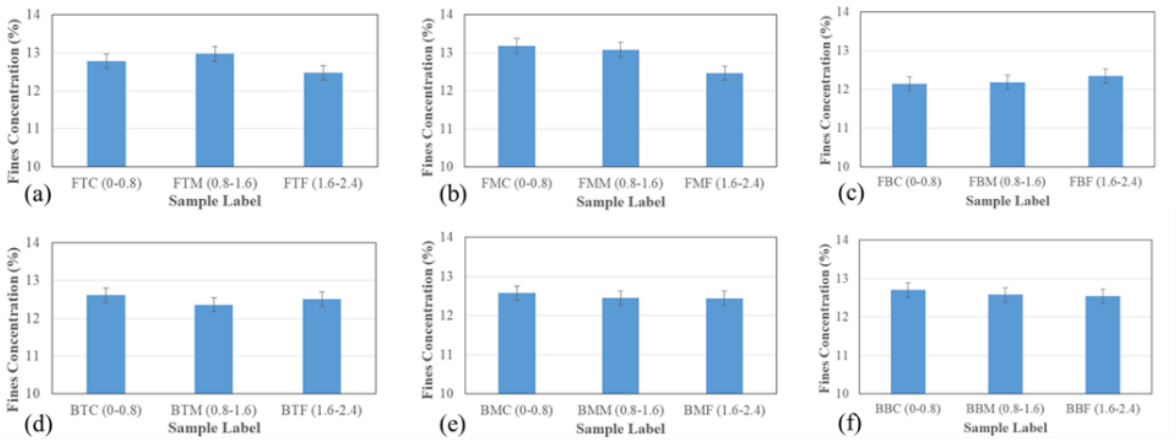

Figure 4-28. Fines concentration in the horizontal samples at a) front side-top, b) front side-middle, c) front side-bottom, d) backside-top, e) backside-middle, and f) backside-bottom in Test V8

The reason to explain the low amount of migrated fines can be attributed to brine's salinity level (roughly 400 ppm). Haftani et al. (2019) stated that the salinity around 400 ppm is insufficient to

mobilize fine particles. Another possible explanation for the low level of fines transportation is the flow velocity, which is not high enough in the sections far from the liner to detach the particles from grain surfaces and migrate them along the sand pack's entire length. For instance, Darcy velocities at the sand pack's outer boundary at the highest flow rate (70,000 cc/h) and the lowest flow rate (20,000 cc/h) are 23.98 cm/h and 6.85 cm/h, respectively.

Figure 4-29 displays the fines concentration in the horizontal samples located at equal radial distances, but with different elevations (top, middle, and bottom) and locations (front and backside). According to the bar diagrams, the variation is less than 4%, which is reasonably close.

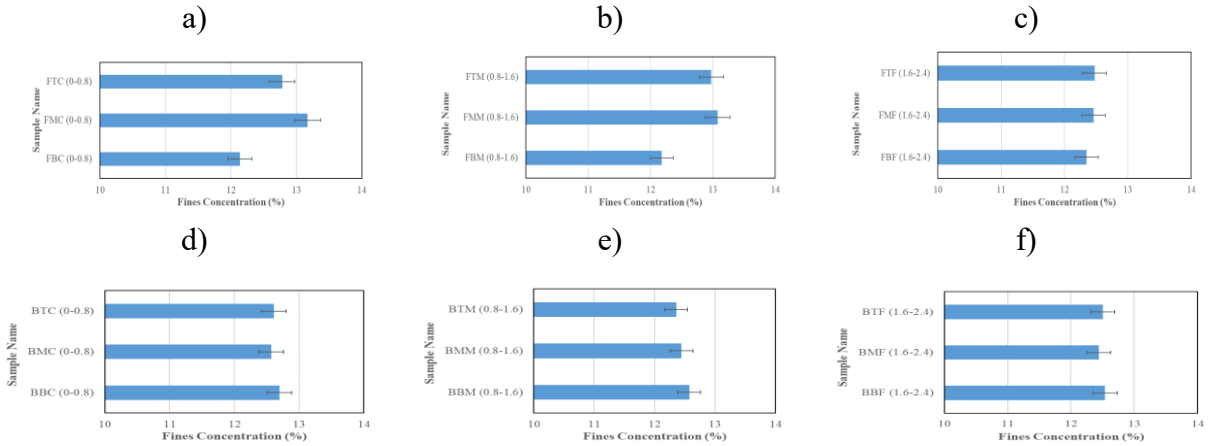

Figure 4-29. Fines concentration inside the samples located at different distances from the liner, a) front side-close to the liner, b) front side-middle distance to the liner, c) front side-far from the liner, d) backside-close to the liner, e) backside-middle distance to the liner, and f) backside-far from the liner in Test V8

The fines concentrations for the samples obtained from the vertical cores are shown in Figure 4-30. The bar diagrams display less than 4% and 2% variations for the front and back samples, respectively. The relative difference between the maximum and minimum fines concentrations is 9% for the front samples, while the difference is 4% for the back samples. At the large radial distances to the liner, the flow velocities are not sufficient to generate detachment and mobilization of the fines particles. When approaching the liner more closely, higher seepage forces cause more fines migration, resulting in more uniform fines distribution near the liner. The inconsiderable variations for fines concentration at the same radial distance for the vertical samples located backside and close to the liner support the existence of the uniform flow in the sand pack. To conclude, Test V8 identifies the presence of the uniform flow distribution in the sand pack.

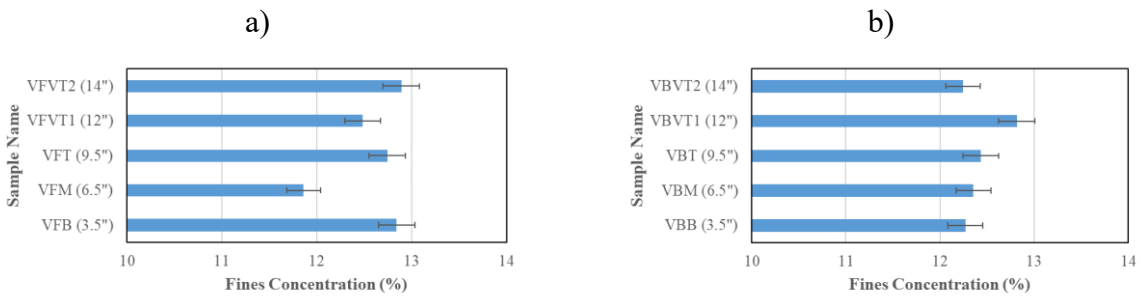

Figure 4-30. Fines concentration inside the vertical samples, a) front side-far from the liner, and b) backside-close to the liner

Figure 4-31 illustrates the comparison between Tests V7 and V8 regarding pressure differences around the liner at six pressure port locations. The pressure differentials follow similar trends for the two tests. Even though some variations exist, the differences between the two laboratory tests are within an acceptable range of 5%, which confirms the repeatability of the test results. A Standard Operating Procedure (SOP) is followed to ensure consistency in the experimental works. Therefore, instrument error is considered the maximum error in the pressure measurement shown as the error bars in Figure 4-31.

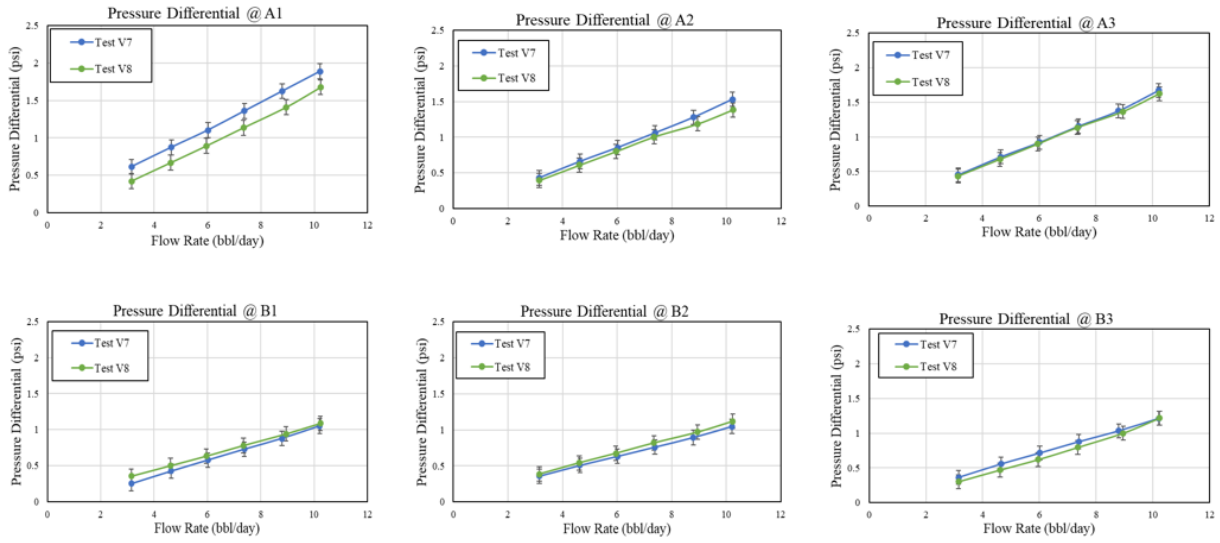

Figure 4-31. Comparing the pressure differentials between Test V7 and V8 at 6 locations

The next step in the post-mortem analysis is to calculate the permeability of the sand pack. It was reported that the pressure drop across the coupon was found to be less than 0.01 psi, which is negligible (Mahmoudi, 2017). Thus, the slotted liner is not included in the calculation of the

retained permeability. The following equation is used to determine the permeability for each interval (Ahmed, 2010):

$$Q_w = \frac{0.00708kh(p_e - p_w)}{\mu_w \ln\left(\frac{r_e}{r_w}\right)} \tag{4.1}$$

where Q_w is the brine flow rate (STB/day), p_e is the external pressure (psi), p_w is the liner pressure (psi), k is permeability (md), μ_w is viscosity (cp), h is the thickness (ft), r_e is the external radius (ft), and r_w is the hole radius (ft).

Figure 4-32 compares the permeability at different pressure port locations in the two experiments. As shown in the figure, the permeability is lower for higher flow rates, owing to the fines migration and pore plugging. Even though there is only a low amount of migrated fines through pore throats in the vertical FCT experiments, it plays a significant role in the plugging potential. Noticeably, both two tests display comparable permeability values for different intervals. Besides, the average retained permeability of the sand pack in the two experiments is about 94%. The parameter is calculated by dividing the permeability in the vicinity of the liner by the initial permeability at the beginning of the experiment.

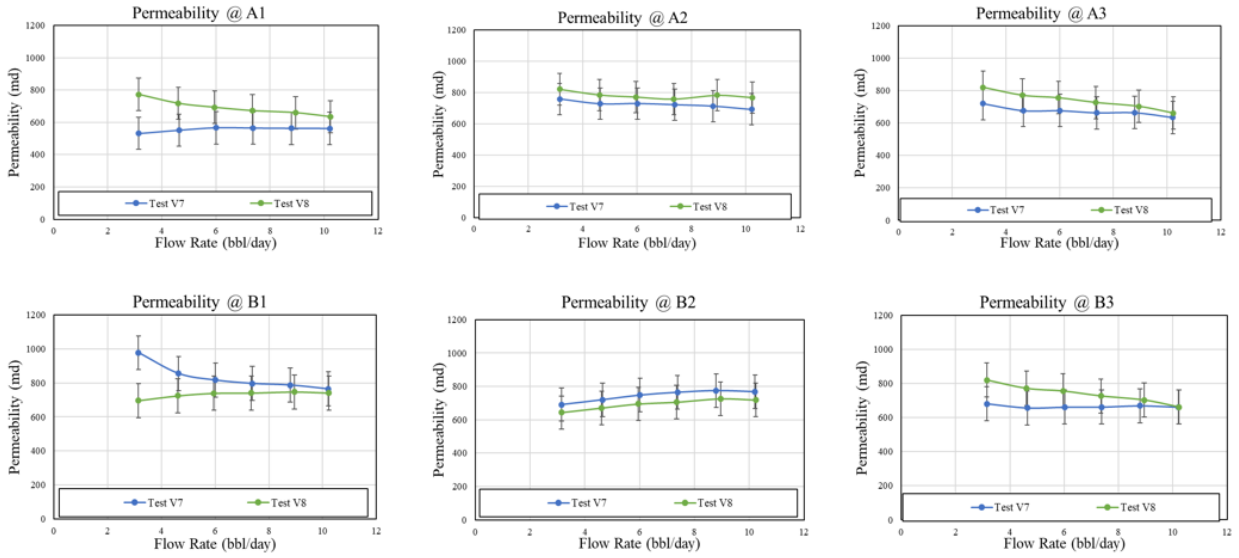

Figure 4-32. Comparing the permeability for Test V7 and V8 at six different locations

As mentioned in Chapter 3, for each testing flow rate, discharged brine samples were taken from the top part of the sand trap. Then the turbidimeter was employed to measure the turbidity of each sample. Subsequently, the produced fines concentration in the discharged brine was calculated

based on values measured from the turbidimeter. Figure 4-33 shows a comparison between the two tests in terms of cumulative fines production. Fines production for each test is reasonably close to each other, following a similar trend.

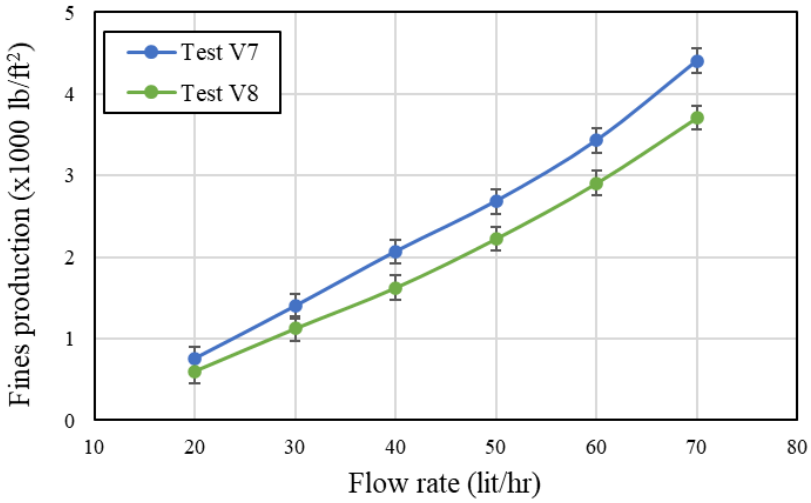

Figure 4-33. Cumulative production of fines in the discharge brine in Test V7 and V8

In addition to the cumulative fines production, the produced sand was also meticulously collected after the experiments. The produced sand was collected from the sand trap, inside the liner, and inside the slots. Figure 4-34 demonstrates the total produced sand in the two experiments. They are 8.9 and 6.8 g for Test V7 and V8, respectively. As the liner area is roughly 1 ft^2, the produced sands per area calculated are 0.02 and 0.015 lb/ft^2 for Test V7 and V8, respectively. These numbers are much lower than the reasonable threshold, which is 0.12 lb/ft^2 for SAGD producers suggested by Hodge et al. (2002). One practical explanation regarding the low amount of produced sand is attributed to liner corrosion during the test, resulting in slot plugging by solid particles. Corrosion in the slotted liner made of carbon steel is severe, as shown in Figure 4-35. Besides, the gravity force on sand particles adjacent to the liner helps the particles stay in their places with the liner being in the vertical position.

In conclusion, these two tests were successful, providing numerous valuable testing results. Comparing the testing results between the two experiments shows that differential pressures and permeability measurements follow similar trends with small variations. Produced fines concentration in the produced fluid for the two tests also shows reasonable agreement. Therefore,

it is concluded that test results are repeatable. Besides, the uniform flow distribution inside the sand pack was verified.

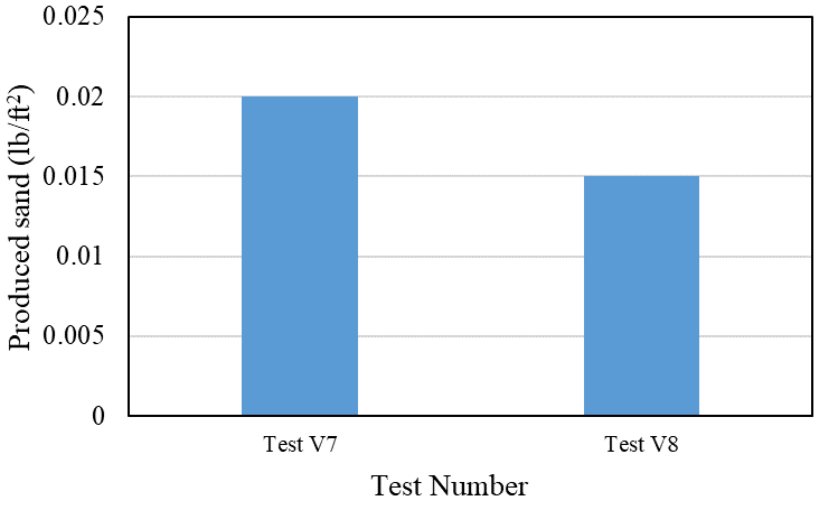

Figure 4-34. Total produced sand between Test V7 and V8

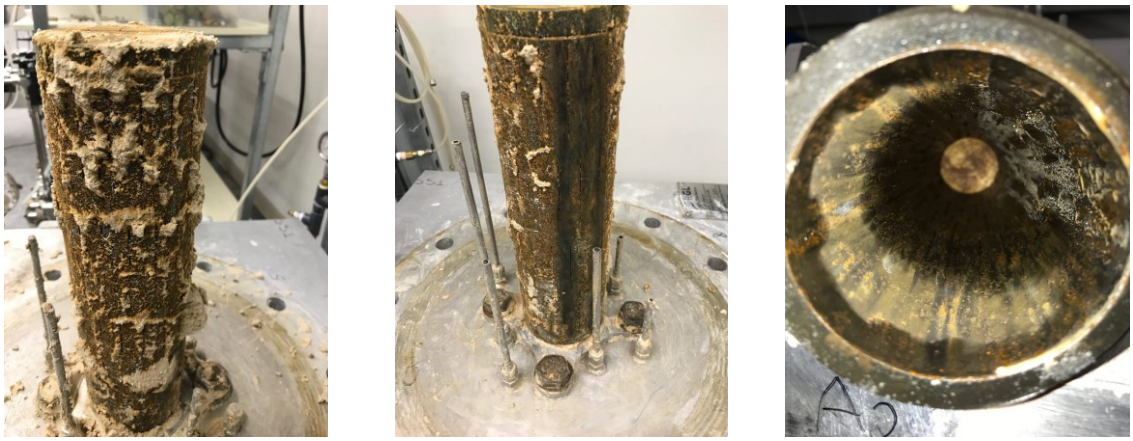

Figure 4-35. The photo illustration of the liner corrosion in the lab

4.2.3 Horizontal FCT

4.2.3.1 Test H9: Design a new configuration of the fluid injection unit

Test H9 was conducted in the horizontal direction. Previously, there were six pressure ports installed for the FCT experiments in the vertical position. Two additional pressure ports (A4 and B4) were supplemented to fully record the pressure distribution around the liner concerning the horizontal direction, as shown in Figure 4-36.

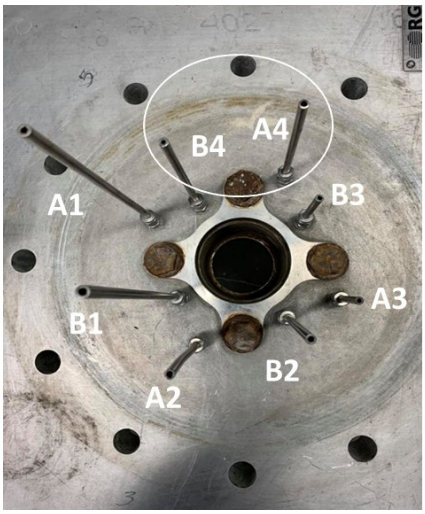

Figure 4-36. The photo illustration of the two new pressure ports in the base plate, as highlighted in the white circle (top view of the base plate where it is not rotated)

Initially, two added pressure transducers were connected to the new ports A4 and B4 in the monitoring system. However, one of eight pressure transducers could not function due to the problem of the DAQ device. Thus, seven pressure transducers connected to seven pressure ports were employed for the horizontal FCT tests. Since it is essential to keep track of pressures at the liner top and bottom, pressure ports A2, B2, A4, and B4 must be utilized. Accordingly, one pressure port at the liner right (either A3 or B3) could be eliminated. For Test H9, seven pressure ports comprising A1, B1, A2, B2, B3, A4, and B4 were employed, as depicted in Figure 4-37.

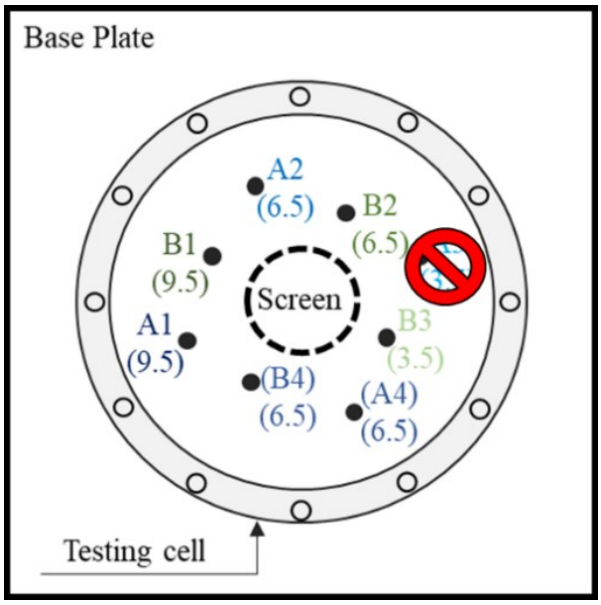

Figure 4-37. Schematic of the pressure ports (top view of the base plate where it is rotated)

Regarding performing the FCT test in the horizontal direction, it was required to devise a new configuration of the fluid injection unit. Five heads in total from the two triplex metering pumps, including three heads from the right pump and two heads from the left pump, were installed (Figure 4-38). The new horizontal FCT setup is illustrated in Figure 4-39. Each head from the right pump was connected to a set of four injection ports located at the same level by only one flowline. Likewise, each head from the left pump was connected to a set of two injection ports located at the same elevation by only one flowline. This configuration explains why the left pump's VFD frequency was set as half of the right pump, ensuring each injection inlet receives the same amount of fluid from the flowlines.

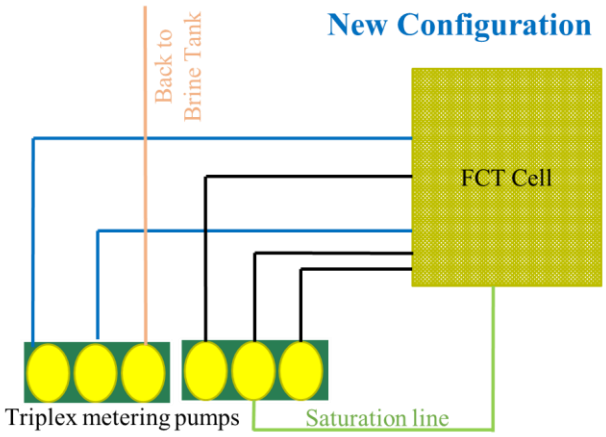

Figure 4-38. Schematic of the new configuration of the fluid injection unit

Figure 4-39. The photo illustration of the horizontal FCT setup

The horizontal FCT experiment's testing procedure followed the standard operating procedure of the vertical FCT test, except that the FCT cell was rotated horizontally. The pressure distribution at B readings is shown in Figure 4-40. The figure shows a noticeable gap in the pressure drops of close readings. The highest pressure differential is at the left side (B1) over six flow stages, while the lowest value is at the right side (B3). The percentage difference between B1 and B3 at Stage #6 is about 92%, which is significant.

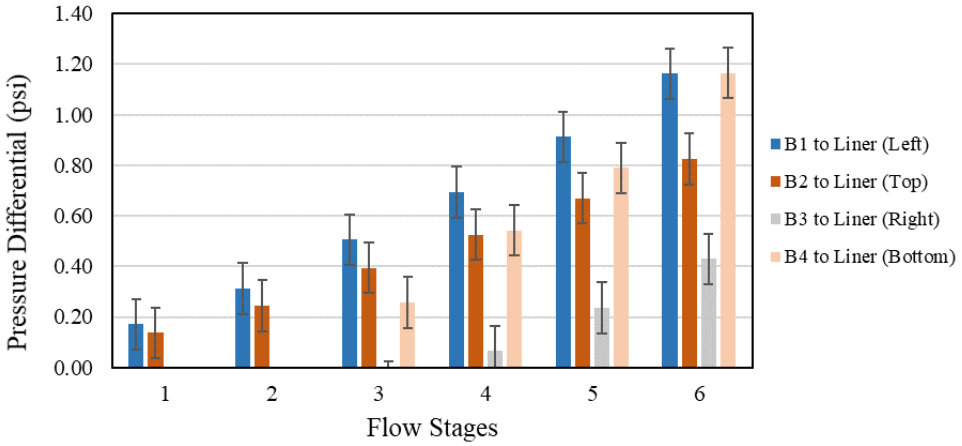

Figure 4-40. Pressure distribution at B readings

Figure 4-41 shows the flow potential variation between ports located close to the liner and the liner. The flow potential is defined as the sum of pressure and hydrostatic pressure. The distances between A and B ports and between B ports and the liner's outer wall are taken into account to calculate the flow potential. According to the figure, the percentage differences at B readings for Stage #4, #5, and #6 are 36%, 28%, and 23%, respectively, indicating non-uniform flow distribution inside the sand pack.

In conclusion, the test was unsuccessful since the uniform fluid injection was not achieved. The problem was the pumps. The two pumps were injecting brine at different rates under the same VFD frequency. Three heads from one pump were delivering a higher amount of fluid than the others under the same conditions. The issue can be attributed to rusted material inside the pumps and lines connected from the pumps to the heads. The next test was carried out to resolve the problem by washing out the rusted material stuck in the pumps. Another explanation for the test's failure is the non-uniform pressure buildup inside the sand pack, impacting the pump flow rates. The fluid injection unit's new configuration to address this problem will be presented later in Test H10.

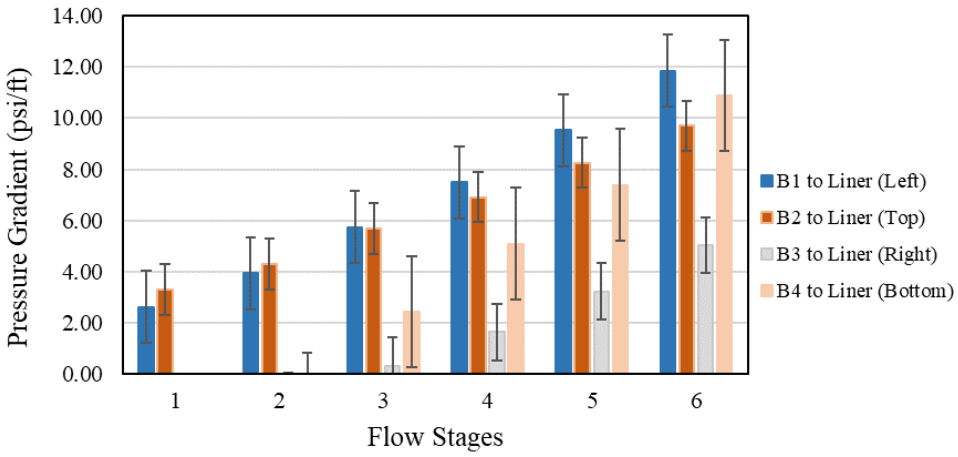

Figure 4-41. Flow potential variations between the ports located close to the liner and inside the liner

4.2.3.2 Flow Calibration Test: Check the pump operation

The pumps were cleaned carefully to wash out any rusted material stuck inside them. The main objective of the test was to determine how the two pumps were operating at three different pump frequencies. Ideally, each head should deliver the same amount of fluid at the same frequency and stroke length. Figure 4-42 displays the pumps in the experiment. The left and right pumps are referred to as P1 and P2, respectively. From the left to right of each pump, each head's label is H1, H2, and H3. Regarding complexity and time, the SRT equipment was utilized instead of the FCT (Figure 4-43).

Figure 4-42. The photo illustration of the two triplex metering pumps

Figure 4-43. The photo illustration of the SRT facility

Figure 4-44 displays a schematic diagram of the SRT facility. As shown in the figure, the SRT apparatus includes five units, namely: (1) sand pack cell, (2) fluid injection unit, (3) data acquisition and monitoring group, (4) sand and fines measurement unit, and (5) back-pressure unit. The SRT testing procedure involves: (1) the sand pack sample preparation by mixing the commercial sands to replicate the DC-I type, (2) assembly of the SRT cell, (3) the sand packing phase, (4) saturation of sand pack, (5) fluid injection, (6) pressure measurement, and (7) disassembly of the SRT cell. The dry commercial sands were mixed thoroughly by a mixer to achieve a uniform particle distribution. Next, 10 wt% of brine with 400 ppm and a pH of 7.9 was added and mixed with the dry sand mixture to produce a homogeneous moist sample in the box. The moist sample was then packed in a sequence of layers into the SRT cell by applying the moist tamping method to achieve a uniform porosity of roughly 37%. After the packing, a top platen was installed before applying an axial load of around 60 psi over the sand pack. The back-pressure column provided around 3 psi of back-pressure. Producing fluids were discharged through a back-pressure column and measured by employing graduated cylinders. The volume of produced fluid was measured in 2 minutes, and the flow rate was calculated by dividing the fluid volume by the interval. The flow rate was measured every 5 minutes to control the flow rate during the injection test.

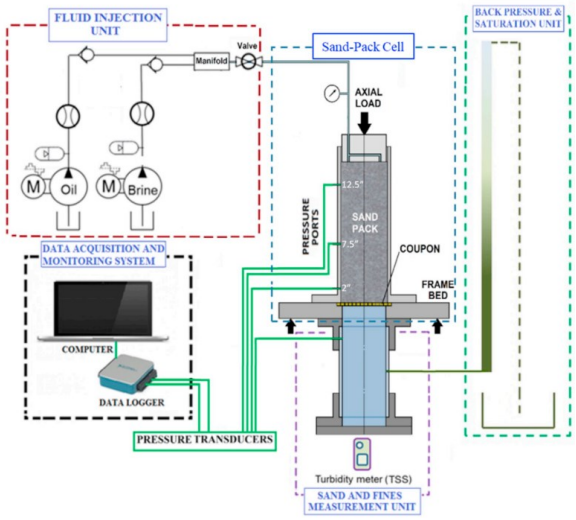

Figure 4-44. Schematic of the SRT setup, after Wang et al. (2020a)

Figure 4-45 shows flow rates of 6 heads from the pumps at three different VFD frequencies, indicating that the pump flow rate is pressure-dependent. The testing results are summarized in Table 4-2. The average difference goes down when increasing the pump frequency. Although each head from the two pumps cannot deliver the exact amount of fluid, the variations are within the acceptable range (less than 4% on average). It means that the pumps can function properly after the maintenance.

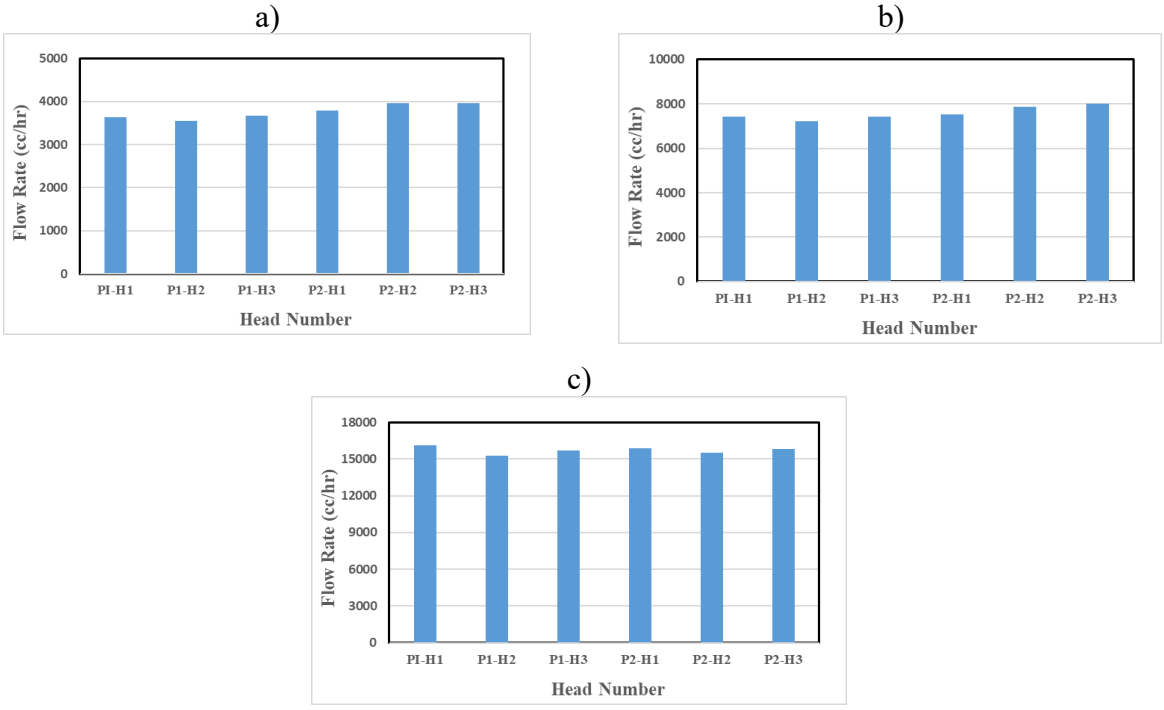

Figure 4-45. Flow rates at the VFD of a) 10, b) 20, and c) 40 from six heads from the two pumps

Table 4-2. The detailed summary of the flow calibration test

VFD	10	20	40
Max (cc/hr)	3960	8010	16125
Min (cc/hr)	3525	7215	15225
Average (cc/hr)	3755	7575	15695
Average Difference (%)	4.0	3.2	1.5

4.2.3.3 Test H10: Re-design the configuration of the fluid injection unit

The fluid injection's configuration was modified, attempting to provide improved uniformity of the fluid injection (Figure 4-46). A flow manifold was introduced into the fluid injection unit, and brine from the tanks was injected into the manifold before the injection ports in the FCT cells. There are eight flowlines on the flow manifold top. One flowline delivers brine to a set of two injection ports located at the same level. Besides, another sand trap that is more user-friendly was employed (Figure 4-47).

Figure 4-46. The photo illustration of the new horizontal FCT setup

Figure 4-47. The photo illustration of the new sand trap

Concerning the monitoring system, port B3 was excluded from the system (Figure 4-48). The reason to choose A3 rather than B3 was to capture a higher pressure difference based on a further distance from A ports to the liner, reducing the effects of the pressure transducer's error on the results.

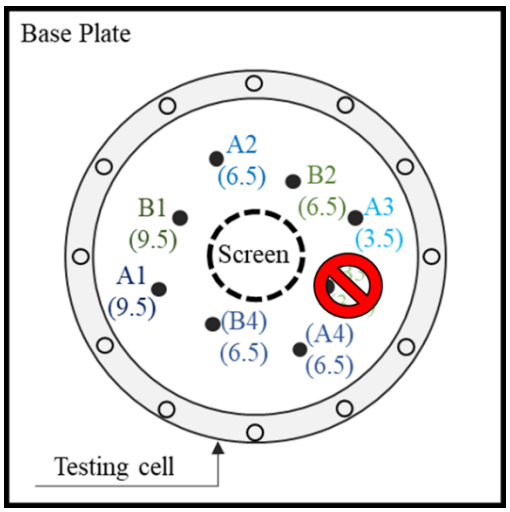

Figure 4-48. Schematic of the pressure ports around the liner

Figure 4-49 displays the pressure evolution in the six flow stages between the ports located far from and close to the liner and the port located inside the liner. The pressure differentials at different locations follow similar trends that are higher pressure drops correspond to higher flow rates. Further, the differential pressures at the farther pressure ports are higher than the ports located nearer the coupon.

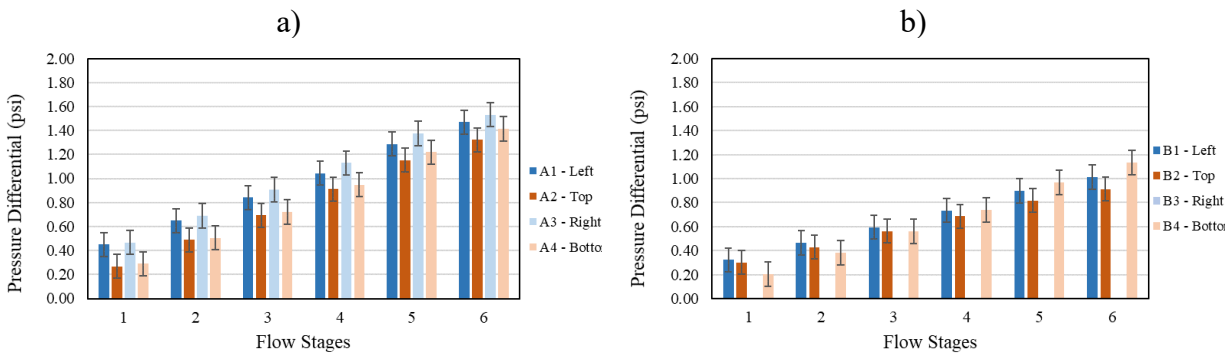

Figure 4-49. The pressure differentials between the ports located a) far from the liner, and b) close to the liner

The variation of the flow potential is shown in Figure 4-50. The differences in the ports located the most distant from the liner (A1, A2, A3, and A4) are less than 10% (Figure 4-50a). It is noticeable that the flow potentials for A ports show reducing differences with higher flow rates. For instance, the percentage differences at Stage #5 and #6 are 6% and 4%, while Stage #3 is 10%. These observations indicate that the flow is distributed relatively uniformly in the near-liner zones, especially at the high flow rates.

The flow potential differences between B ports and the liner at high flow rates, such as Stage #5 and #6, are almost identical, as shown in Figure 4-50b. For instance, the standard deviations at B ports for Stage #5 and #6 are 0.03 psi and 0.007 psi, respectively. More importantly, the difference at B ports displays less than 10% variation, indicating the presence of the uniform flow distribution in the sand pack. Noticeably, the flow manifold operates better at the higher pressure buildup inside the sand pack associated with higher flow injection rates.

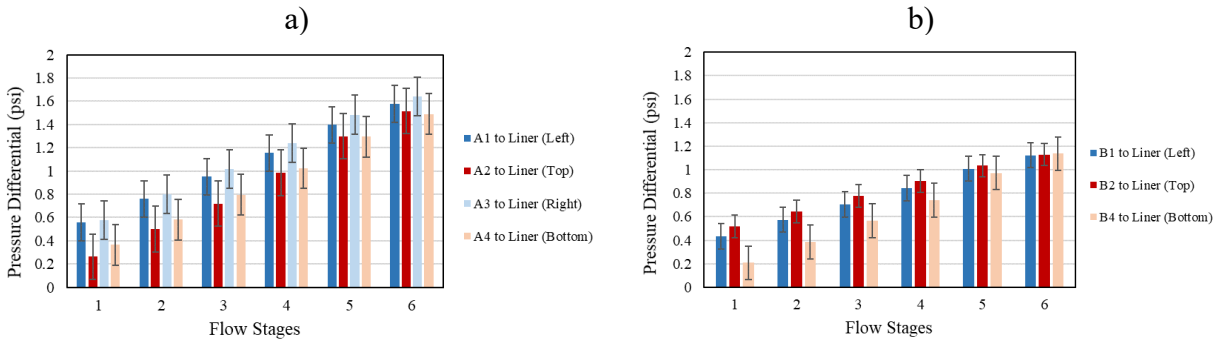

Figure 4-50. Flow potential variations between a) A ports located far from, and b) B ports located close to the liner and inside the liner

Figure 4-51 compares the fines concentration inside the horizontal samples at equal radial distances but different elevations from four sides around the liner. The average fines concentration at the intervals of 0-0.8'', 0.8-1.6'', and 1.6-2.4'' (distances from the liner) are 12.85 %, 12.7%, and 12.65%, respectively. Even when the general trend is a decreasing fines concentration with distance from the liner, the relative difference is not too significant. Also, fines contents at these zones are less than the original fines content (14.5%) since fine particles were migrated during the experiment.

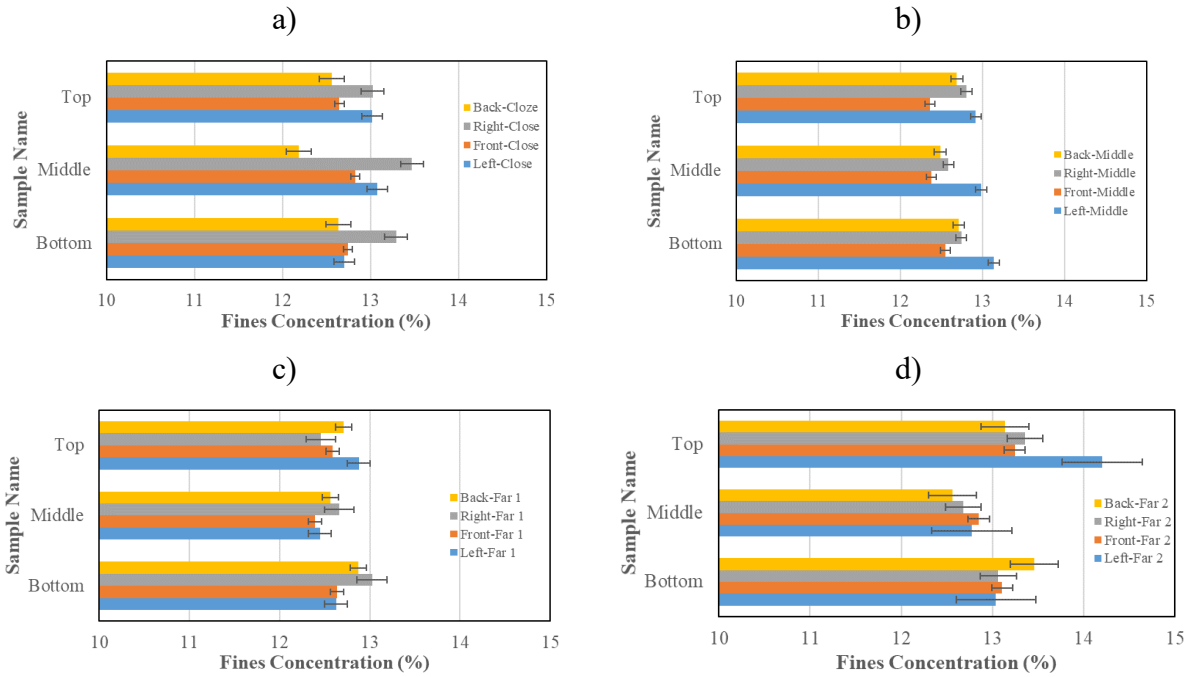

Figure 4-51. The fines concentration inside the horizontal samples at a) close (0-0.8), b) middle (0.8-1.6), c) far (1.6-2.4), and d) farthest (2.4-end) zones from the liner

Regarding the uniform radial flow condition, the expectation is to see similar fines content in the samples located at the same radial distances from the liner center. Figure 4-52 shows that the differences of fines concentrations for the samples obtained from the vertical cores are less than 4% and 5% for the front and back samples, respectively, supporting the existence of the uniform flow distribution along the liner.

In conclusion, the analyses of fines concentration and pressure evolution around the liner show that the flow distribution in the sand pack is uniform. Each flow stage during the injection test lasted roughly 15 minutes (Figure 4-53). As shown in the figure, the pressure differentials did not fully stabilize yet before moving to the next flow stage. For instance, the pressure differentials for

the six pressure ports were still increasing for Stage #4 right before being terminated. For the next experiment, each flow stage was extended for a more extended period.

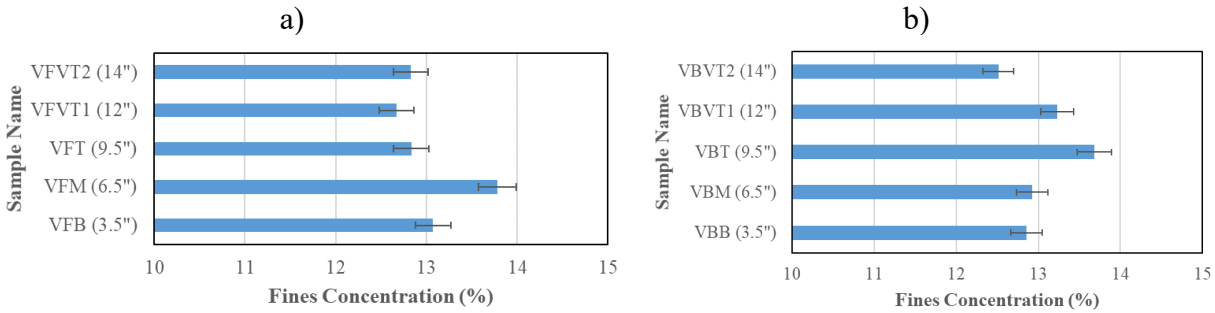

Figure 4-52. Fines concentration inside the vertical samples, a) front side-far from the liner, and b) backside-close to the liner

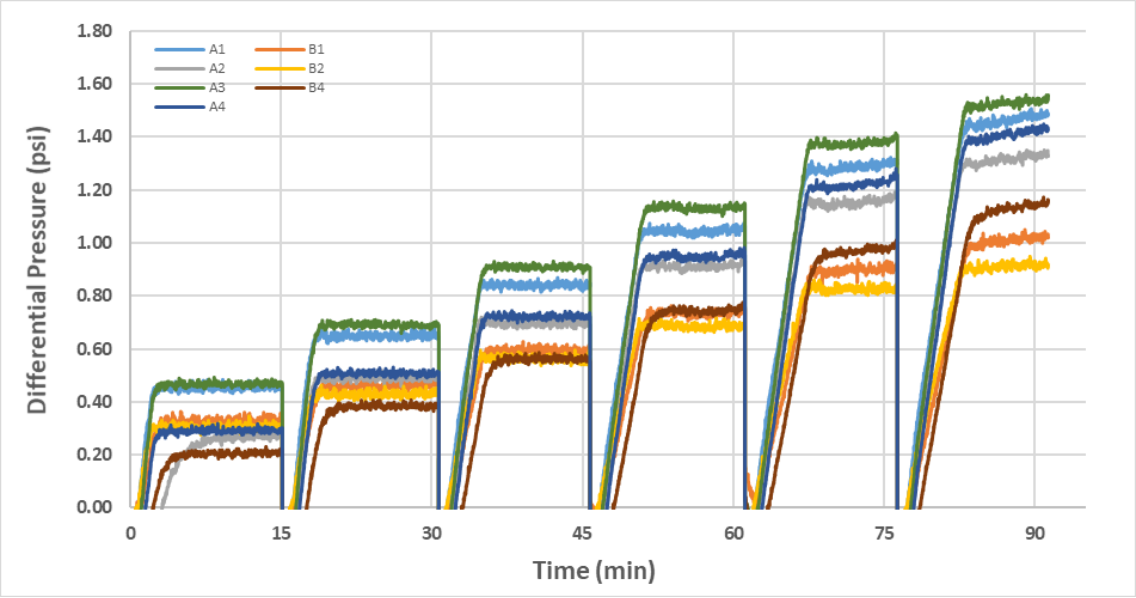

Figure 4-53. The recorded data during the flow test in the six flow stages

4.2.3.4 Test H11: Extend each flow stage of the injection test

For Test H11, the aim was to capture the pressure changes at all close readings. Therefore, port A3 was taken out of the system, as depicted in Figure 4-54. Rather than conducting each stage of the flow test in 15 minutes, the flow stages were extended for a longer time (Figure 4-55). It can be seen from the figure that the first two flow stages lasted 30 minutes; the third and fourth stages were 2 hours; the last two ones were one hour. Even though each flow stage lasted for a more extended period, the pressure readings still did not fully stabilize. For example, the pressure differentials for the pressure ports at Stage #4 were still decreasing when the flow stage ended.

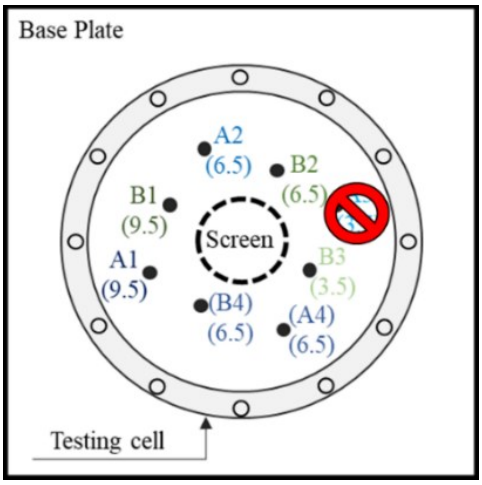

Figure 4-54. Schematic of the pressure ports

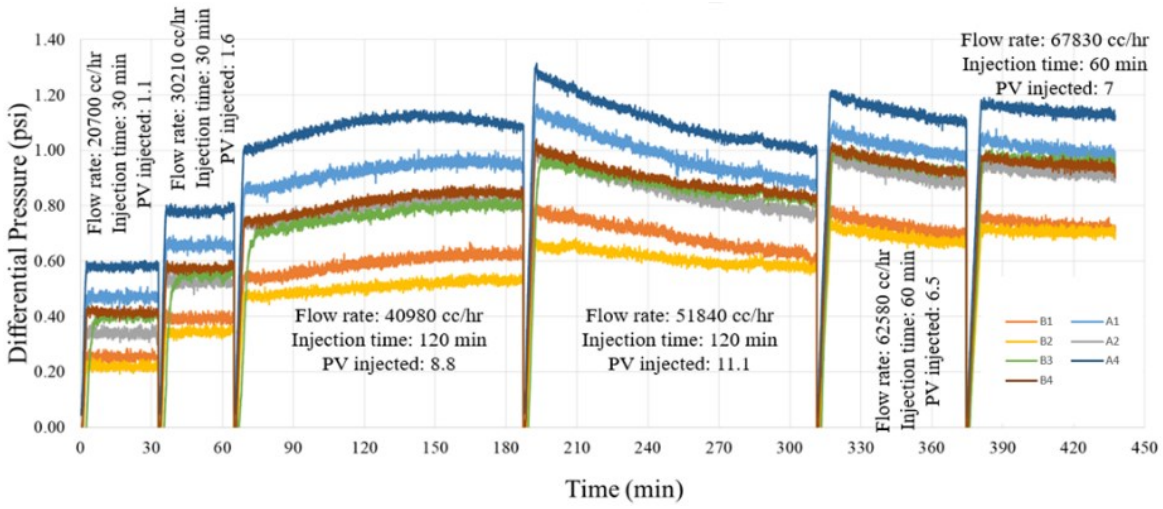

Figure 4-55. The recorded data during the flow test in the six flow stages

Figure 4-56 displays the differential pressures at different locations inside the sand pack. The pressure differentials for A ports in each flow stages are nearly similar (Figure 4-56a). For instance, Stage #1, #3, and #6 have standard deviations of 0.01, 0.03, and 0.02 psi, respectively. Figure 4-56b shows that pressure differences for B ports display less than 7% variation, which is reasonably close.

The variation of the flow potential around the liner is displayed in Figure 4-57. The flow potential differences between A and B ports go up to the peak at Stage #3 and then reduce at Stage #4 before varying insignificantly for the last two flow stages (Figure 4-57a). The flow potential variation is around 16%, which is relatively significant, indicating the non-uniform flow distribution for the regions between A and B ports.

Additionally, regarding the close readings, the most considerable flow potential difference is measured at the right side of the sand pack for the high flow rates, while the smallest one is at the bottom (Figure 4-57b). The differences between the highest and smallest values for Stage #5 and #6 are about 20.86 and 20.13 %, respectively, which are quite considerable, indicating the state of the non-uniform flow distributed around the liner. To conclude, the flow in the sand pack is not fully uniform.

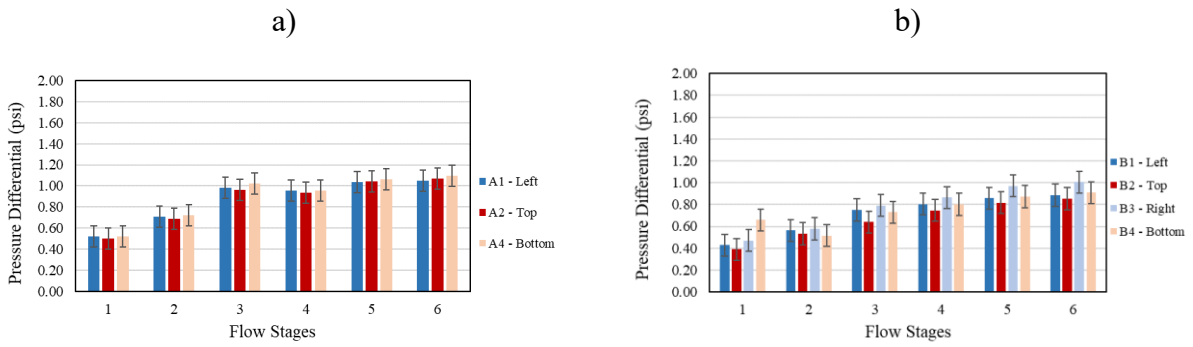

Figure 4-56. Pressure distribution at a) far, and b) close readings

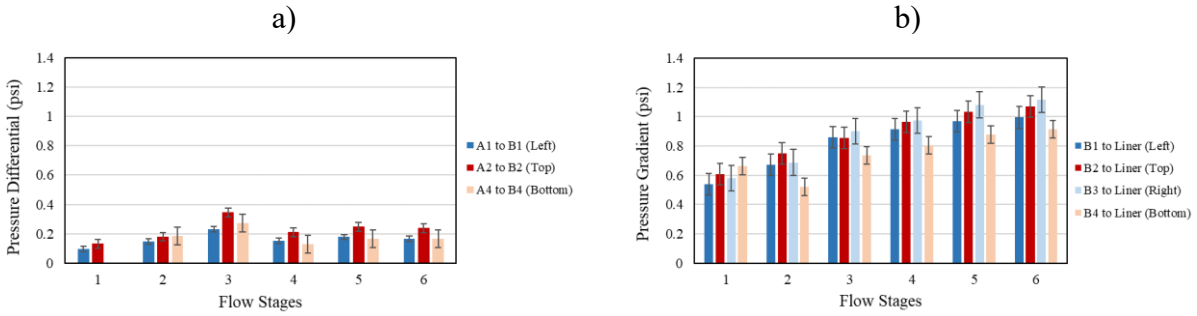

Figure 4-57. Flow potential variations between a) A and B ports, and b) B ports and the liner

Figure 4-58 compares the concentration of fines in the horizontal samples at the same elevation from different sides around the liner. According to the figure, there is no meaningful trend existing for the top, middle, and bottom parts of the sand pack. The fines concentrations are within 7%, 9%, and 7% for the top, middle, and bottom sections, respectively.

In summary, the flow potential shows a considerable variation between the pressure ports in the vicinity of the liner, which indicates that the flow is not uniformly distributed. Fines concentration in the samples measured after the testing does not exist any meaningful trend provided the uniform radial flow condition. The pressure readings did not wholly reach their stabilizations even though each flow stage lasted for a more extended period. It is necessary to extend each flow stage long enough for them to stabilize in the upcoming experiments.

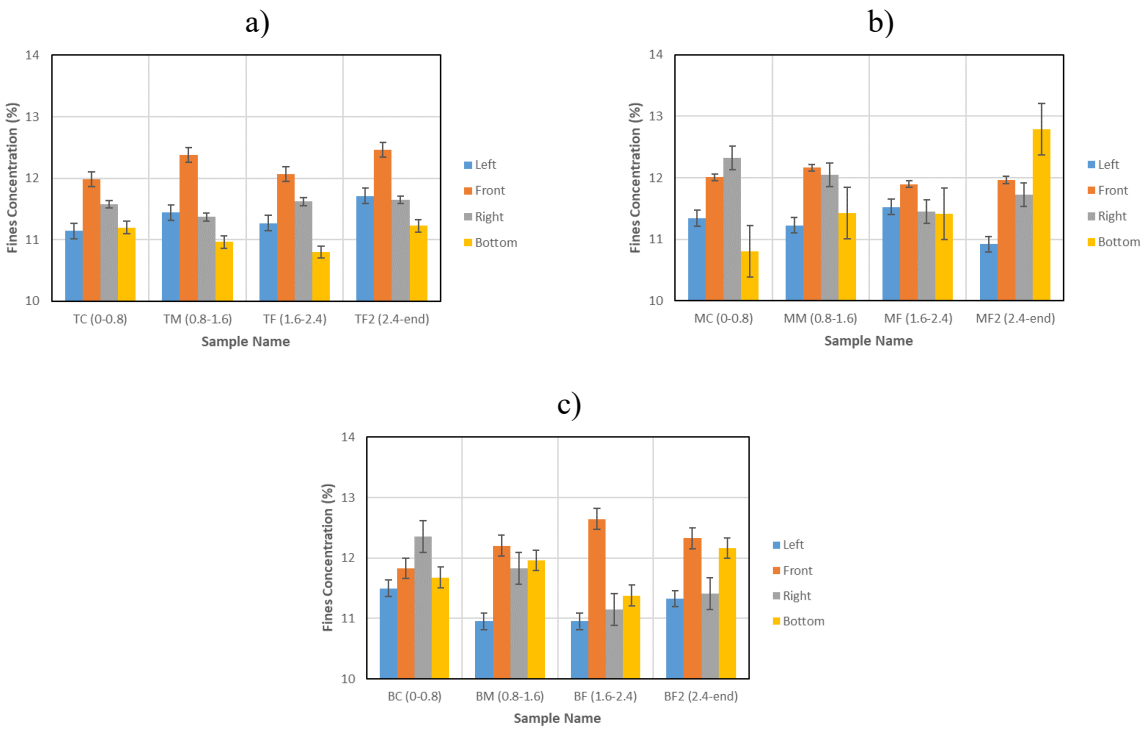

Figure 4-58. The fines concentration inside the horizontal samples at a) top, b) middle, and c) bottom parts of the sand pack

4.3 Comparison between the Vertical and Horizontal FCT Results

The comparison is performed between two vertical tests (Test V7 and V8) and one horizontal test (Test H10). The pressure differentials at four pressure ports located around the liner between these experiments are shown in Figure 4-59. It is noticeable that differential pressures from these experiments show similar variations. In detail, the pressure readings at ports A1, B1, A2, and B2 are within 10%, 5%, 8%, and 7%, respectively, which are within the acceptable range.

Figure 4-60 displays the permeability variations at different flow rates between Test V7, V8, and H10, showing comparable values for different intervals. The variations at ports A1, A2, A3, and A4 are less than 10%, 4%, 6%, and 4%, respectively. The error bars presented in Figure 4-59, and Figure 4-60 were calculated based on the transducer's maximum error as the experimental works follow the standard testing procedure to render consistent samples.

The total produced sand for these three experiments is demonstrated in Figure 4-61. The total amounts of produced sand in Test V7, V8, and H10 are 8.9, 6.8, and 6.4 g, respectively. Since the liner area is roughly 1 ft^2, the produced sands are roughly 0.02, 0.015, and 0.014 lb/ft^2 for Test V7,

V8, and H10, respectively, which are within the acceptable sanding level for the SAGD production well suggested by Hodge et al. (2012). The primary reason for the low produced sand for both directions is the aperture plugging by sand particles and corrosion, preventing sand from entering the sand trap. Another practical explanation is the combination of forces acting on sand particles near the liner. The gravity force keeps sand remaining in their places around the vertical liner and the left, right, and bottom of the horizontal liner.

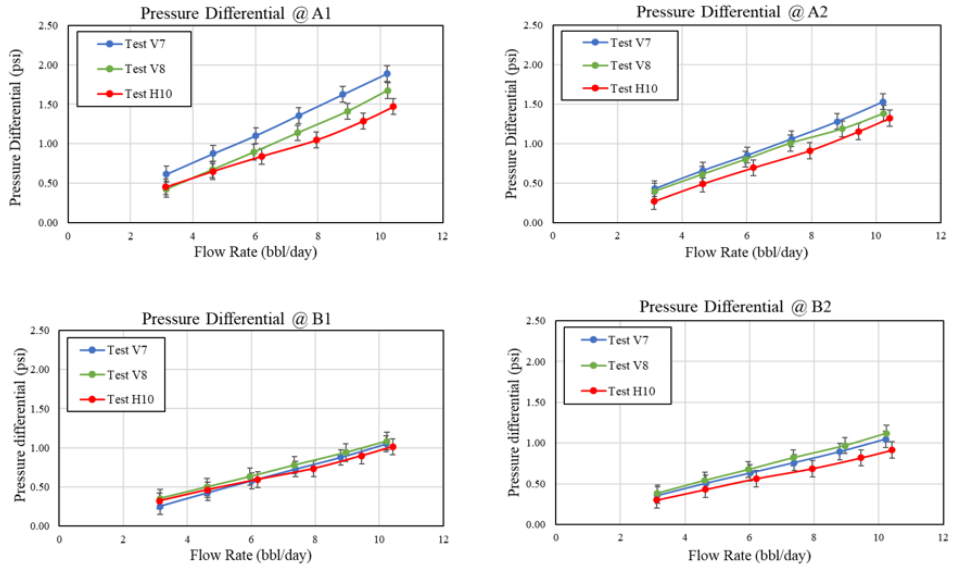

Figure 4-59. The comparison of the pressure differences between Test V7, V8, and H10

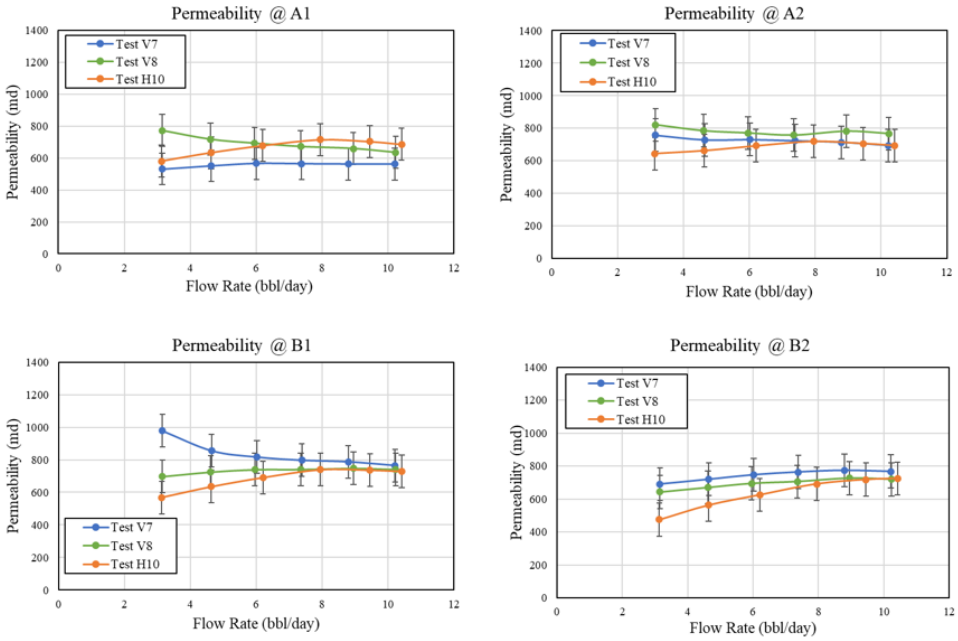

Figure 4-60. The comparison of the permeability between Test V7, V8, and H10

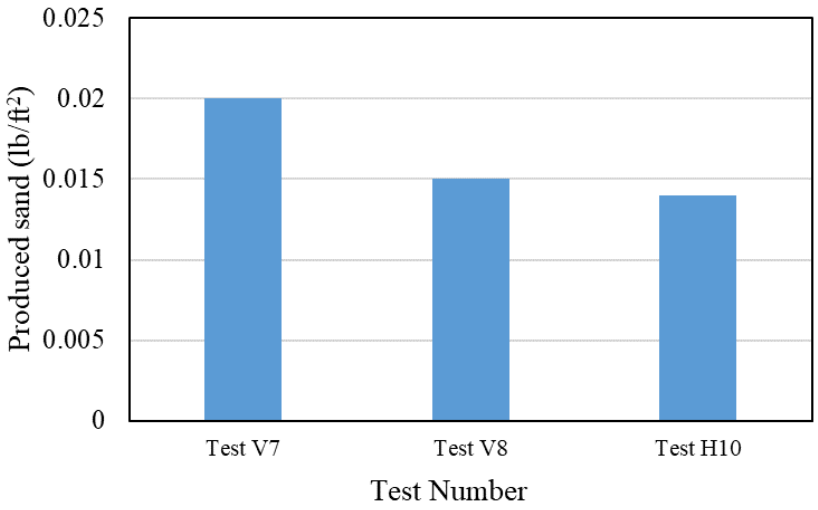

Figure 4-61. The comparison of the total produced sand between Test V7, V8, and H10

Figure 4-62 displays the cumulative fines production with the liner being in the vertical and horizontal positions. The cumulative produced fines' expectation is an exponential trend, which is reported in the literature (Mahmoudi et al., 2017b; Haftani et al., 2019). The slight increase observed in the produced fines in the discharged water at different flow stages can result from the low brine salinity level (400 ppm) and decreasing fluid velocity in the sand pack when moving farther from the liner, which reduces the fines transportation. Although the cumulative production of fines in Test H10 is lower than the others, the difference is insignificant.

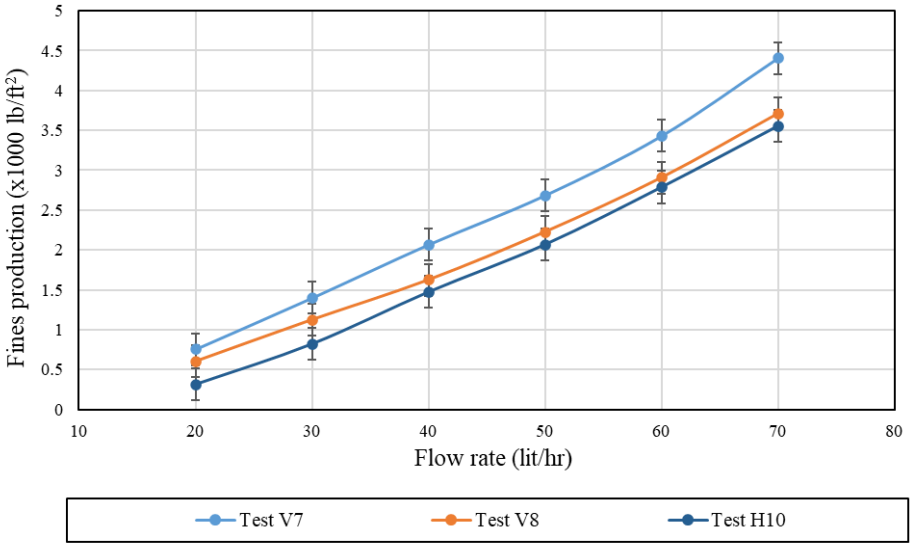

Figure 4-62. The comparison of the cumulative production of fines between Test V7, V8, and H10

To sum up, the comparisons between the vertical and horizontal positions show a reasonable agreement in terms of the pressure distribution and permeability. Even though the produced fines and sand production regarding the horizontal direction are lower than the vertical one, the difference is not too considerable.

4.4 Conclusion

This chapter presented how the FCT setup and testing procedure were modified and improved via the experimental works before reaching their final versions. Several single-phase experiments with brine flow were carried out to troubleshoot challenges and shortcomings in the setup and testing procedure. Two identical single-phase vertical FCT tests were performed, showing that the flow distribution is uniform around the liner, and the test results are repeatable. Produced sand, fines production, and permeability along the sand pack were measured to assess the slotted liner's performance.

The uniformity of the flow inside the sand pack was determined by analyzing two indicators: pressure distribution and fines concentration. The flow inside the sand pack was verified to be distributed uniformly in both the vertical and horizontal FCT experimental tests. Also, comparing the testing results in the vertical and horizontal directions is generally in agreement regarding the pressure differential, permeability, fines production, and sand production.

Chapter 5: Conclusions and Recommendations for Future Work

5.1 Main results and Contributions

The research elaborates on a novel large-scale sand control testing facility called Full-Scale Completion Testing (FCT). The apparatus is an advanced setup representing the SAGD well conditions more closely than the current testing setups such as the SRT equipment. The FCT facility was developed to investigate the effects of the radial flow regime around the liner instead of the linear flow in the SRT, which is more representative of the SAGD wells. The experimental testing results were processed to identify the uniformity of the flow distribution inside the sand pack and assess the test repeatability. The fines concentration was measured at different locations inside the sand pack, providing more insights about fines migration under the radial flow regime. The fines concentration and pressure evolution indicate the existence of the flow distributed relatively uniformly inside the sand pack. The injection scheme was also described in the study, which consists of several injection levels considering various levels of plugging conditions and non-contributing sections.

The work started by getting the FCT facility commissioned in the laboratory. Initially, the FCT experiment was unsuccessful due to many limitations in the testing setup and procedure. Several single-phase FCT tests with brine flow were carried out to troubleshoot challenges and shortcomings in the setup and testing procedure to improve the reliability and accuracy of the testing results. As a result of progressively modifying the testing setup and procedure, two identical single-phase vertical FCT tests were performed successfully. The uniformity of the flow was determined by analyzing the pressure evolution and fines concentration in the sand pack. The analyses indicate that the flow is uniformly distributed in the sand pack. The testing repeatability was also verified. Therefore, the testing procedure can confidently assess the sand control screen performance under the radial flow configuration.

The produced sand in the vertical FCT tests is much lower than the acceptable sanding threshold (less than 0.12 lb/ft^2) suggested by Hodge et al. (2002). The small amount of produced sand can result from liner corrosion, slot plugging induced by sand and fine particles, and the combination of physical forces acting on sand grains adjacent to the liner. The pressure differentials in the vertical FCT experiments at different pressure ports display similar trends with small variations,

indicating the uniform flow distribution. Furthermore, fines concentration measured after the flow tests also confirms the presence of the uniform flow distribution in the sand pack. The testing results show the facility's capability to simulate better the SAGD reservoirs concerning the radial-flow regime rather than the linear flow in the SRT experiment.

Additionally, three other FCT experiments were carried out in a horizontal position. The horizontal FCT experimental setup is more complicated than the vertical setup, especially in the fluid injection unit. Comparing the vertical and horizontal directions shows a reasonable agreement regarding the differential pressure, permeability, fines production, and sand production. Although there are existing problems in the horizontal FCT setup needed further investigation, the FCT facility shows a high practical application to simulate the conditions of the SAGD horizontal wells in the field more closely.

5.2 Experimental Testing Limitations

The limitations of the FCT setup and procedure are listed below:

- The current facility design only simulates the ideal field conditions of borehole collapse over the sand control screen at the early stages of the SAGD operations without incorporating the formation damage in the porous media such as asphaltene precipitation and mineral scaling. Also, concerning the liner made of carbon steel, erosion and corrosion phenomena cannot be included in the current setup.
- The FCT facility's current setup does not also allow the incorporation of high stress and high-temperature conditions. Currently, the maximum allowable stress applied over the sand pack is 40 psi. A further improvement to employ High Temperature-High Pressure (HT-HP) setup, which changes rock properties such as wettability and permeability, is essential.
- Concerning the horizontal FCT experiments, a flow manifold is installed to attempt to deliver the same amount of fluid through all FCT injection inlets from the FCT cell's inner wall towards the liner. However, the flow manifold does not seem to operate as expected under low injection rates. The flow manifold functions more appropriately with a high-pressure buildup inside the sand pack associated with high injection rates.

- It is necessary to correlate the laboratory results with field data. It is required to have sufficient reliable pressure and sand production field data in which the flow regime is radial.

5.3 Recommendation for Future Work

The following sections are proposed to investigate further the FCT facility, which is relatively new in the field. If these recommendations are studied, the facility will broaden its application.

5.3.1 Comparing between the SRT and the FCT

The SRT equipment prevents capturing the radial flow regime around the SAGD wellbores. It is expected to observe a higher pressure drop in the radial flow regime than linear flow, which might lead to an increase in sand production. Nonetheless, the gravitational force helps maintain the particles in their places in the vicinity of the vertical liner. The importance of each contributor to the sand production and fines migration is needed to investigate. Hence, it is essential to compare the testing results obtained from the FCT and SRT experiments to assess how much the flow regime could impact the performance of sand control screens.

5.3.2 Implementing FCT Experiments under the Horizontal Direction

The aim is to perform the FCT test in the horizontal direction, simulating the field cases more closely where SAGD wells are horizontal. Sand production and fines migration can be further investigated in the more representative testing conditions. Efforts to conduct the horizontal FCT experiment successfully are still ongoing in the research group.

5.3.3 Building a Numerical Model

The FCT facility is more like a black box. It is troublesome to understand what phenomena are taking place inside the FCT cell. Therefore, it is necessary to build a numerical model to get more insights into the nature of radial flow through slotted liners as well as flow upstream and downstream of the slots. Experimental works can be used to verify the numerical model, which can improve researchers' understanding regarding fines migration and plugging potential under the flow radial geometry.

5.3.4 Performing the Multi-Phase FCT Tests

There has been no effort so far given towards the multi-phase FCT experiment. Designing the fluid injection unit properly to generate the uniformly radial inward flow in the multi-phase experimental tests will be considerably challenging. The uniformity of the flow distribution in the sand pack has to be determined thoroughly by analyzing the pressure evolution and fines concentration. In return, carrying out the multi-phase experiments helps study the effects of capillary and relative permeability on sand production. The multi-phase FCT test also enables researchers to investigate fines migration in multi-phase flow conditions under the radial flow geometry, which will have high production engineering applications.

References

Natural Resources Canada. 2019. www.nrcan.gc.ca.

Adams, P.R., Davis E.R., Hodge R.M., Burton R.C., Ledlow L., Procyk A.D., and Crissman S.C. 2009. “Current State of the Premium Screen Industry: Buyer Beware, Methodical Testing and Qualification Shows You Don’t Always Get What You Paid For.” *SPE Drilling & Completion*, 24(03), 362-372. doi:10.2118/110082-PA.

AlBahlani, A.M., and Babadagli T. 2008. “A Critical Review of the Status of SAGD: Where Are We and What Is Next ?” *SPE Western Regional and Pacific Section AAPG Joint Meeting,* Bakersfield, California, USA: Society of Petroleum Engineers. doi:10.2118/113283-MS

Anderson, M. 2017. “SAGD Sand Control: Large Scale Testing Results.” *SPE Canada Heavy Oil Technical Conference,* Calgary, Alberta, Canada. doi:10.2118/185967-MS.

Ballard, T., and Beare S. 2006. “Sand Retention Testing: The More You Do, the Worse It Gets.” *SPE International Symposium and Exhibition on Formation Damage Control*, Lafayette, Louisiana, USA. doi:10.2118/98308-MS.

Ballard, T., and Beare S. 2003. “Media Sizing for Premium Sand Screens: Dutch Twill Weaves.” *SPE European Formation Damage Conference,* The Hague, Netherlands. doi:10.2118/82244-MS.

Ballard, T., Kageson-Loe N., and Mathisen A. 1999. “The Development and Application of a Method for the Evaluation of Sand Screens.” *SPE European Formation Damage* 111 *Conference*, The Hague, Netherlands. doi:10.2118/54745-MS.

Valdes, J. R., and Santamarina, J. C. 2006. “Particle Clogging in Radial Flow: Microscale Mechanisms.” *Society of Petroleum Engineers*. doi:10.2118/88819-PA

Bellarby, J. 2009. “Well Construction Design.” *Elsevier*, 56:129–239. doi:10.1016/S0376-7361(08)00203-3.

Bennion, D.B., Gupta, S., Gittins, S., and D. Hollies, D. 2009. “Protocols for slotted liner design for optimum SAGD operation.” *Journal of Canadian Petroleum Technology*. 48: 11, 21-26. doi:10.2118/130441-PA.

Bennion, D.B., Ma T., Thomas F.B., and Romanova U.G. 2007. “Laboratory Procedures for Optimizing the Recovery from High Temperature Thermal Heavy Oil and Bitumen Recovery Operations.” *Canadian International Petroleum Conference,* Calgary, Alberta. doi:10.2118/2007-206.

Brooks, R., and Tavakol H. 2012. “Experiences in Eliminating Steam Breakthrough and Providing Zonal Isolation in SAGD Wells.” *SPE Western Regional Meeting,* Calgary, Alberta, Canada. doi:10.2118/153903-MS.

Burton, R.C., Chin L., Davis E.R., Enderlin M.B., Fuh G., Hodge R., Ramos G.G., VanffhaDeVerg 112 P., Werner M., Mathews W.L., and Petersen S. 2005. “North Slope Heavy - Oil Sand – Control Strategy : Detailed Case Study of Sand Production Predictions and Field Measurements for Alaskan Heavy - Oil Multilateral Field Developments.” *SPE Annual Technical Conference and Exhibition,* Dallas, Texas, USA. doi:10.2118/97279-MS.

Butler, R.M. 1992. “Gravity Drainage to Horizontal Wells.” *Journal of Canadian Petroleum Technology***,** 31(4): 31-37. doi:10.2118/92-04-02.

CAPP. 2019. “Canada’s Oil Sands.” https://www.capp.ca/energy/canadas-energy-mix/.

CAPP. 2020. “Canada’s Oil Sands.” https://www.capp.ca/wp-content/uploads/2020/04/Introduction-to-the-Oil-Sands-360547.pdf.

RGL Reservoir Management Inc, 2018. “RGL Reservoir Management Inc” https://www.rglinc.com/solutions/sand-control/propunch/ (2018).

Chanpura, R.A., Hodge R.M., Andrews J.S., Toffanin E.P., Moen T., and Parlar M. 2011. “A Review of Screen Selection for Standalone Applications and a New Methodology.” *SPE Drilling & Completion*, 26(1): 84–95. doi:10.2118/127931-PA.

Chanpura, R. A., Mondal, S., Sharma, M. M. et al. 2012. “Unraveling the Myths in Selection of Standalone Screens and a New Methodology for Sand Control Applications.” *SPE Annual Technical Conference and Exhibition*, 8-10 October, San Antonio, Texas, USA. doi:10.2118/158922-MS.

Chenault, R.L. 1938. “Experiments on Fluid Capacity and Plugging of Oil-Well Screens.” *Drilling and Production Practice*. Amarillo, Texas: American Petroleum Institute.

Coberly, C.J. 1938. “Selection of Screen Openings for Unconsolidated Sands.” *Drilling and Production Practice*, API 37-189.

Constien, V.G., and Skidmore V. 2006. “Standalone Screen Selection Using Performance Mastercurves.” *SPE International Symposium and Exhibition on Formation Damage Control,* Lafayette, Louisiana, USA. doi:10.2523/98363-MS.

Qi, G. 2004. “Study on sand control mechanism and application of coated sand.” Southwest Petroleum University, Chengdu, China.

Cowie, B.R. 2013. “Stable Isotope and Geochemical Investigations into the Hydrogeology and Biogeochemistry of Oil Sands Reservoir Systems in Northeastern Alberta, Canada.” Ph.D. thesis at the University of Calgary. doi:10.11575/PRISM/27867.

Devere-Bennett, N. 2015. “Using Prepack Sand-Retention Tests (SRT’s) to Narrow Down Liner /Screen Sizing in SAGD Wells.” *SPE Thermal Well Integrity and Design Symposium,* Banff, Alberta, Canada. doi:10.2118/178443-MS.

Fattahpour, V., Azadbakht S., Mahmoudi M., Guo Y., Nouri A., and Leitch M. 2016. “Effect of Near Wellbore Effective Stress on the Performance of Slotted Liner Completions in SAGD Operations.” *SPE Thermal Well Integrity and Design Symposium*, Banff, Alberta, Canada. doi:10.2118/182507-MS.

Fattahpour, V., Mahmoudi M., Wang C., Kotb O., Roostaei M., Nouri A., Fermaniuk B., Sauve A., and Sutton C. 2018. “Comparative Study on the Performance of Different Stand-Alone Sand Control Screens.” *SPE International Conference and Exhibition on Formation Damage Control*, Lafayette, Louisiana, USA. doi:10.2118/189539-MS.

Fattahpour, V., Roostaei, M., Soroush, M., Hosseini, S. A., Berner, K., Mahmoudi, M., … Ghalambor, A. 2020. “Full-Scale Physical Modeling of Stand-Alone Screens for Thermal Projects.” *Society of Petroleum Engineers*. doi:10.2118/199239-MS.

Guo, Y. 2018. “Effect of Stress Build-up around SAGD Wellbores on the Slotted Liner Performance.” Master thesis at the University of Alberta. doi:10.7939/R3V98066B.

Guo, Y., Roostaei M., Nouri A., Fattahpour V., Mahmoudi M., and Jung H. 2018. “Effect of Stress Build-up around Standalone Screens on the Screen Performance in SAGD Wells.” *Journal of Petroleum Science and Engineering* 171: 325–339. doi:10.1016/j.petrol.2018.07.040.

Hodge, R.M., Burton R.C., Constien V., and Skidmore V. 2002. “An Evaluation Method for Screen-Only and Gravel-Pack Completions.” *International Symposium and Exhibition on Formation Damage Control,* Lafayette, Louisiana, USA. doi:10.2523/73772-MS.

Irani, M. 2013. “Understanding the Steam-Hammer Mechanism in Steam-Assisted-GravityDrainage Wells.” *SPE Journal* 18 (6): 1181–1201. doi:10.2118/165456-PA.

Jimenez, J. 2008. “The Field Performance of SAGD Projects in Canada.” *International Petroleum Technology Conference*, Kuala Lumpur, Malaysia. doi:10.2523/IPTC-12860-MS.

Jin, Y., Chen J., Chen M., Zhang F., Lu Y., and Ding J. 2012. “Experimental Study on the Performance of Sand Control Screens for Gas Wells.” *Journal of Petroleum Exploration and Production Technology* 2 (1): 37–47. doi:10.1007/s13202-012-0019-9.

Yang, D., and Macaraeg L. 2013. “Horizontal Well Completion Technology for Improved Heavy Oil Production.” *GeoConvention: Integration*, Calgary, Alberta, Canada.

Kaiser, T. M. V., Wilson, S., and Venning, L. A. 2002. “Inflow Analysis and Optimization of Slotted Liners.” *SPE Drilling & Completion*, 17 (4): 200-209. doi:10.2118/80145-PA.

Kaiser, T.M.V, Wilson S., and Venning L.A. 2000. “Inflow Analysis and Optimization of Slotted Liners.” *International Conference on Horizontal Well Technology*, Calgary, Alberta, Canada. doi:10.2118/65517-MS.

Layne, L.A., and F W Gerwick. 1973. “Wire Wrapped Well Screen.” U.S Patent Number: 3,709,293.

Lightbown, V. 2017. “New SAGD Technologies Show Promise in Reducing Environmental Impact of Oil Sand Production.” *Journal of Environmental Solutions for Oil, Gas, and Mining* 1 (2): 1–12.

Fermaniuk, B. 2013. “Sand Control in Steam Assisted Gravity Drainage (SAGD) Wellbores and Process of Slotted Liner Design and Process.” Master thesis at the University of Calgary. doi:10.11575/PRISM/27707.

Mahmoudi, M. 2016. “New Sand Control Design Criteria and Evaluation Testing for Steam Assisted Gravity Drainage (SAGD) Wellbores.” Ph.D. thesis at the University of Alberta. doi:10.7939/R3C824S55.

Mahmoudi M. 2017. “New sand control design criteria and evaluation testing for Steam Assisted Gravity Drainage (SAGD) wellbores.” Ph.D. thesis at the University of Alberta. https://doi.org/10.7939/R3C824S55.

Mahmoudi, M., Nejadi S., Roostaei M., Olsen J., Fattahpour V., Lange C.F., Zhu D., Fermaniuk B., and Nouri A. 2017a. “Design Optimization of Slotted Liner Completions in Horizontal Wells: An Analytical Skin Factor Model Verified by Computational Fluid Dynamics and Experimental Sand Retention Tests.” *SPE Thermal Well Integrity and Design Symposium*. Banff, Alberta, Canada. doi:10.2118/188167-MS.

Mahmoudi, M., Fattahpour, V., Nouri, A., and Leitch, M. 2017b. “An experimental evaluation of pore plugging and permeability reduction near SAGD sand control liners.” *SPE Canada Heavy Oil Technical Conference, Calgary, Alberta, Canada, 15-16 February 2017*. doi:10.2118/184999-MS.

Mahmoudi, M., Fattahpour V., Nouri A., and Leitch M. 2016. “An Experimental Investigation of the Effect of PH and Salinity on Sand Control Performance for Heavy Oil Thermal Production.” *SPE Canada Heavy Oil Technical Conference*. Calgary, Alberta, Canada. doi:10.2118/180756-MS.

Mahmoudi, M., Fattahpour, V., Roostaei, M. et al. 2018. “An Experimental Investigation into Sand Control Failure Due to Steam Breakthrough in SAGD Wells.” *SPE Canada Heavy Oil Technical Conference*, 13-14 March, Calgary, Alberta, Canada. doi:10.2118/189769-MS.

Markestad, P., Christie O., Espedal A., and Rorvik O. 1996. “Selection of Screen Slot Width to Prevent Plugging and Sand Production.” *SPE Formation Damage Control Symposium*. Lafayette, Louisiana, USA. doi:10.2118/31087-MS.

Matanovic, D., Cikes M., and Moslavac B. 2012. “Sand Control in Well Construction and Operation.” *Springer Science & Business Media*. doi:10.1007/978-3-642-25614-1.

Montero, J., Chissonde S., Kotb O., Wang C., Roostaei M., Nouri A., Mahmoudi M., and Fattahpour V. 2018. “Critical Review of Sand Control Evaluation Testing for SAGD Applications,” *SPE Canada Heavy Oil Technical Conference,* Calgary, Alberta, Canada. doi:10.2118/189773-MS.

Montero, J. 2019. “Design Criteria and Performance Evaluation of Wire-Wrapped Screens for Steam Assisted Gravity Drainage (SAGD) Wellbores.” Master thesis at the University of Alberta. https://doi.org/10.7939/r3-w32h-7192.

O'Hara, M. 2015. “Thermal Operations In The McMurray; An Approach To Sand Control.” *SPE Thermal Well Integrity and Design Symposium*, Banff, Alberta, Canada. doi:10.2118/178446-MS.

Penberthy, W.L., and Shaughnessy C.M. 1992. “Sand Control.” *Society of Petroleum Engineers*.

Peterson, D., West H.P.D., and Washington B. 2007. “Guidelines for Produced Water Evaporators in SAGD.” *IWC.* 7 (68): 1–16.

Romanova, U.G., Ma T. 2013. “An Investigation of the Plugging Mechanisms in a Slotted Liner from the Steam Assisted Gravity Drainage Operations.” *SPE European Formation Damage Conference and Exhibition,* Noordwijk, The Netherlands. doi:10.2118/165111-MS.

Romanova, U.G., Gillespie G., Sladic J., Ma T., Solvoll T.A., and Andrews J.S. 2014. “A Comparative Study of Wire Wrapped Screens vs. Slotted Liners for Steam Assisted Gravity Drainage Operations.” *World Heavy Oil Congress,* New Orleans, Louisiana, USA. WHOC14 - 113.

Sheng, J. 2013. “Enhanced Oil Recovery Field Case Studies.” *Gulf Professional Publishing.* 413–445. doi:10.1016/B978-0-12-386545-8.00017-8.

Sivagnanam, M., Wang J., and Gates I.D. 2017. "On the Fluid Mechanics of Slotted Liners in Horizontal Wells." *Chemical Engineering Science* 164: 23–33. doi:10.1016/j.ces.2017.01.070.

Zhang, Z. 2017. "An Advanced Sand Control Technology for Heavy Oil Reservoirs." Master thesis at the University of Calgary. doi:10.11575/PRISM/27963. doi:10.11575/PRISM/24806.

Zhang, W., Youn, S., and Doan, Q. T. 2007. "Understanding Reservoir Architectures and Steam-Chamber Growth at Christina Lake, Alberta, by Using 4D Seismic and Crosswell Seismic Imaging." *SPE Reservoir Evaluation & Engineering*, **10** (05): 446-452. doi:10.2118/97808-PA.

Spronk, E.M., Doan L.T., Matsuno Y., and Harschnitz B. 2015. "SAGD Liner Evaluation and Liner Test Design for JACOS Hangingstone." *SPE Canada Heavy Oil Technical Conference,* Calgary, Alberta, Canada. doi:10.2118/174503-MS.

Suman, G.O., Ellis R.C., and Snyder R.E. 1983. "Sand Control Handbook: Prevent Production Losses and Avoid Well Damage with These Latest Field-proven Techniques." *Gulf Publishing Company*, 2nd edition.

Suman, G., Ellis, R., and Snyder, R. 1985. "Sand Control Handbook." Houston: Gulf publishing company.

Sun, C., Shuang S., Zeng H., Fattahpour V., Mahmoudi M., and Luo J. 2018. "Investigation of Corrosion Properties of a High-Phosphorus Ni-P Coating and Corrosion Resistant Alloys in 3.5 Wt.% NaCl Solution." *Corrosion 2018,* Phoenix, Arizona, USA. NACE-2018-11526.

Williams, C.F., Richard B.M., and Horner D. 2006. "A New Sizing Criterion for Conformable and Nonconformable Sand Screens Based on Uniform Pore Structures." *SPE International Symposium and Exhibition on Formation Damage Control*, Louisiana, USA. doi:10.2118/98235-MS.

Haftani, M., C. Wang, Y. Pang, J.D. Montero, M. Mahmoudi, V. Fattahpour, and A. Nouri. 2019. "An investigation into the effect of brine salinity on fines migration in SAGD operations." *SPE Western Regional Meeting, San Jose, California, USA, 23-26 April 2019.* doi:10.2118/195370-MS.

Haftani, M., Kotb, O., Nguyen, P. H., Wang, C., Salimi, M., and Nouri, A. 2020. "A Novel sand control testing facility to evaluate the impact of radial flow regime on screen performance and its

verification.” *Journal of Petroleum Science and Engineering,* 107903. doi:10.1016/j.petrol.2020.107903.

Birks, J., J. Fennell, Y. Yi, J. Gibson, and M. Moncur. 2017. “Regional geochemistry study for the Southern Athabasca Oil Sands (SAOS) area.” *COSIA Hydrogeology Working Group*.

Dong, C., Gao, K., Dong, S., Shang, X., Wu, Y., Zhong, Y. 2017. “A new integrated method for comprehensive performance of mechanical sand control screens testing and evaluation.” *Journal of Petroleum Science and Engineering*. 158, 775-783.

Ma, C., Deng, J., Dong, X., Sun, D., Feng, Z., Luo, C., Xiao, Q., and Chen, J. 2020. “A new laboratory protocol to study the plugging and sand control performance of sand control screens.” *Journal of Petroleum Science and Engineering*. 184, 106548.

Nouri, A., Vaziri, H., Kuru, E., and Islam, R. 2005. “A laboratory study of the effect of installation of reticulated expandable liners on sand production in weakly consolidated sandstone formations.” *SPE Annual Technical Conference and Exhibition, Dallas, Texas, USA, 9 – 12 October 2005.* doi:10.2118/96151-MS.

Nouri, A., Vaziri, H. H., Belhaj, H. A., and Islam, M. R. 2006. “Sand-Production Prediction: A New Set of Criteria for Modeling Based on Large-Scale Transient Experiments and Numerical Investigation.” *Society of Petroleum Engineers*. doi:10.2118/90273-PA.

Abram, M., and Cain, G. 2014. “Particle-size analysis for the Pike 1 Project, McMurray Formation.” *Journal of Canadian Petroleum Technology.* 53: 06, 339-354. doi:10.2118/173890-PA.

Papamichos E., Vardoulakis, I., Tronvoll, J., and Skjvrstein, A. 2001. “Volumetric sand production model and experiment.” *International Journal for Numerical and Analytical Methods in Geomechanics*. 25, 789-808.

Taubner, S. P., Lipsett, M. G., Keller, A., and Kaiser, T. M. V. 2016. “Gravity Inflow Performance Relationship for SAGD Production Wells.” *Society of Petroleum Engineers*. doi:10.2118/180714-MS.

Furui, K., Zhu, D., and Hill, A. D. 2005. “A Comprehensive Model of Horizontal Well Completion Performance.” *Society of Petroleum Engineers*. doi:10.2118/84401-PA.

Furui, K. 2004. “A Comprehensive Skin Factor Model for Well Completions Based on Finite Element Simulations.” Master thesis at the University of Texas at Austin, Austin, Texas.

Wang, C., Montero, J.D., Haftani, M., and Nouri, A. 2020a. “Developing a methodology to characterize formation damage (pore plugging) due to fines migration in sand control tests.” *Journal of Petroleum Science and Engineering.* 186, 106793.

Wang, C., Pang, Y., Mahmoudi, M., Haftani, M., Salimi, M., Fattahpour, V., and Nouri, A. 2020b. “A set of graphical design criteria for slotted liners in steam assisted gravity drainage production wells.” *Journal of Petroleum Science and Engineering.* 185, 106608.

Wang, C., Montero, J.D., Haftani, M., and Nouri, A. 2021. “Protocol for optimal size selection of punched screen in steam assisted gravity drainage operations.” *Journal of Petroleum Science and Engineering*. 196, 107689.

Wang, C., Pang, Y., Montero, J.D., Haftani, M., Fattahpour, V., Mahmoudi, M., and Nouri, A. 2018. “Impact of anisotropic stresses on the slotted liners performance in steam-assisted gravity drainage.” *SPE Thermal Well Integrity and Design Symposium, Banff, Alberta, Canada, 27-29 November 2018.* doi:10.2118/193347-MS.

Edmunds, N. 2000. “Investigation of SAGD Steam Trap Control in Two and Three Dimensions.” *Journal of Canadian Petroleum Technology* 39 (1): 30–40. doi:10.2118/00-01-02.

Gates, I.D., and Leskiw C. 2010. “Impact of Steam Trap Control on Performance of SteamAssisted Gravity Drainage.” *Journal of Petroleum Science and Engineering* 75 (1–2). 215–222. doi:10.1016/j.petrol.2010.11.014.

Parlar, M., Tibbles R.J., Gadiyar B., and Stamm B. 2016. “A New Approach for Selecting SandControl Technique in Horizontal Openhole Completions.” *SPE Drilling & Completion* 31 (1): 4–15. doi:10.2118/170691-PA.

Hamid, S., and Ali, S. A. 1997. “Causes of Sand Control Screen Failures and Their Remedies.” *SPE European Formation Damage Conference*, 2-3 June, The Hague, Netherlands. doi:10.2118/38190-MS.

Gillespie, G., Beare, S. P., and Jones, C. 2009. “Sand Control Screen Erosion- When are you at Risk?.” *8th European Formation Damage Conference*, 27-29 May, Scheveningen, The Netherlands. doi:10.2118/122269-MS.

Toma, P., Livesey D., and Heidrick T. 1988. “New Sand-Control Filter for Thermal Recovery Wells.” *SPE Production Engineering* 3 (2): 249–257. doi:10.2118/15057-PA.

Ladd, R. 1978. “Preparing Test Specimens Using Undercompaction.” *Geotechnical Testing Journal, 1*(1), 16. doi:10.1520/gtj10364j.

Das, S. 2005. “Improving the Performance of SAGD.” *SPE International Thermal Operations and Heavy Oil Symposium*, Calgary, Alberta, Canada. doi:10.2118/97921-MS.

Dusseault, M.B. 2002. “CHOPS - Cold Heavy Oil Production with Sand in the Canadian Heavy Oil Industry.” *Alberta Department of Energy*.

Bybee, K. 2003. “Comparison of Cyclic Steam Stimulation and Steam Assisted Gravity Drainage.” *Journal of Petroleum Technology* 55 (06): 68–69. doi:10.2118/0603-0068-JPT.

Handfield, T.C., Nations T.E., and Noonan S.G.. 2009. “SAGD Gas Lift Completions and Optimization: A Field Case Study at Surmont.” *Journal of Canadian Petroleum Technology* 48 (11): 51–54. doi:10.2118/117489-PA.

Ahmed T. 2010. “Chapter 6: Fundamentals of reservoir fluid flow;” *Reservoir Engineering Handbook*. Elsevier Inc.

Appendix A: Standard Operating Procedure for the Vertical FCT

A.1 Brine Preparation

1) Check pH and EC from the DI water supplier, pH should be neutral (≈7), and EC should be less than 5 μs/cm.
2) The volume of the brine two tanks is close to 100L.
3) Prepare 100L brine for each test. The concentration of the brine is 400 ppm. For 100L water (100 kg, water density is 1Kg/L), 40g salt should be added.
4) Add adequate salt to the deionized water mix thoroughly to obtain a uniform mixture by using the driller (no deposit at the bottom).
5) The pH should be checked and calibrated using a pH meter whenever brine is prepared. The target pH is 7.9. If adjustment is necessary, sodium bisulfate (NaHSO4) and sodium carbonate (Na2CO3) can lower and increase the pH level, respectively. The addition of the small amount to the brine container is followed by mixing with a stirring drill so that another representative sample can be taken for the pH measurement.

A.2 Sand Pack Preparation

1) 38kg dry commercial sands should be prepared for each test. Prepare the sample in two batches (each one should be 19kg) to be ably mixing them in the mixer.
2) Carefully weigh all the commercial sands and clays following the recipe in Table A- 1. Pour samples slowly (to prevent loss of fine particles) and uniformly in a plastic mixing container and mixer.

Table A- 1. PSD of the commercial sands

Sand Type	Ind 50	Sil-1	Sil-4	Sil-7	LM 70	LM 125	Helmer Kaolinite
DC-I	-	15.5%	-	-	-	70.0%	14.5%
DC-II	-	13.2%	-	-	79.4%	-	7.4%
DC-III	-	66.1%	-	2.9%	25.7%	-	5.4%
DC-IV	-	-	36.5%	47.1%	6.9%	5.4%	4.2%

3) The dry sand samples are repeatedly mixed inside the mixer for 10 min.

4) Add 3.8 liters (1.9 liters per batch) brine to reach 10% water contain (water contain= total weight of water added / total weight of dry sand). Thoroughly mix all the dry sand and brine to achieve a homogenous moist sample in the sandbox.
5) Take four samples from two batches to define the PSD of the moist sand-mixture sample (beginning of batch 1, end of batch 1, beginning of batch 2, and end of batch 2).

A.3 Setup and liner assembly phase

1) Before the packing procedure, there is a verification of the cleanness of the apparatus parts. Clean the apparatus with water, air, and appropriate detergent in case of oil, precisely the following:
   a) The sand trap connection,
   b) Flowlines,
   c) Clean and gauge the size of the slots,
   d) The brine pump is connected to the back-pressure column to fill the tube, then the volume of brine is released to rinse the back-pressure pipe and the piping.
   e) Inspect, regrease and replace if damaged the O-rings on the liner,
2) Put the mesh inside the pressure ports.
3) Screw the liner to the FCT base plate.
4) Put a gasket to seal the cell and then place the cell on the base plate. Pay attention to adjust marks on the FCT cell to match with other marks on the base plate before tightening nuts in order from 1 to 12 (Figure A- 1a).

A.4 Sand packing phase

1) Wrap the mesh by two layers of geotextile and then put it inside the cell.
2) Pack 12 sand layers uniformly in sequence based on a modified approach of the moist tamping method (Ladd 1978) and compact them to reach the target porosity (for DC-I, target porosity is 37%).

   A small rod is used to flatten the surface of the sand. The weight of the layer is calculated based on the required porosity of the pack and the grain specific gravity. The mass of each layer is around 3656 g. After packing each layer, scratch the surface between the packed layers. Notably, use the file on the computer to record the packing process.
3) Do not forget to install the de-airing tube on the cell before packing layer No.#10 (Figure A- 1b).

4) After packing all layers, put the de-airing tube on top of the sand pack and place a specially designed diaphragm on top of the sand pack (Figure A- 1c).
5) Ensure the diaphragm edges are at the rim of the cell top gasket to secure the piston in place and prevent leaks (Figure A- 1c).
6) Install the top flange to seal the unit, and then tighten the nuts in a cross fashion to prevent over-torque and damage to the top flange (Figure A- 1d).

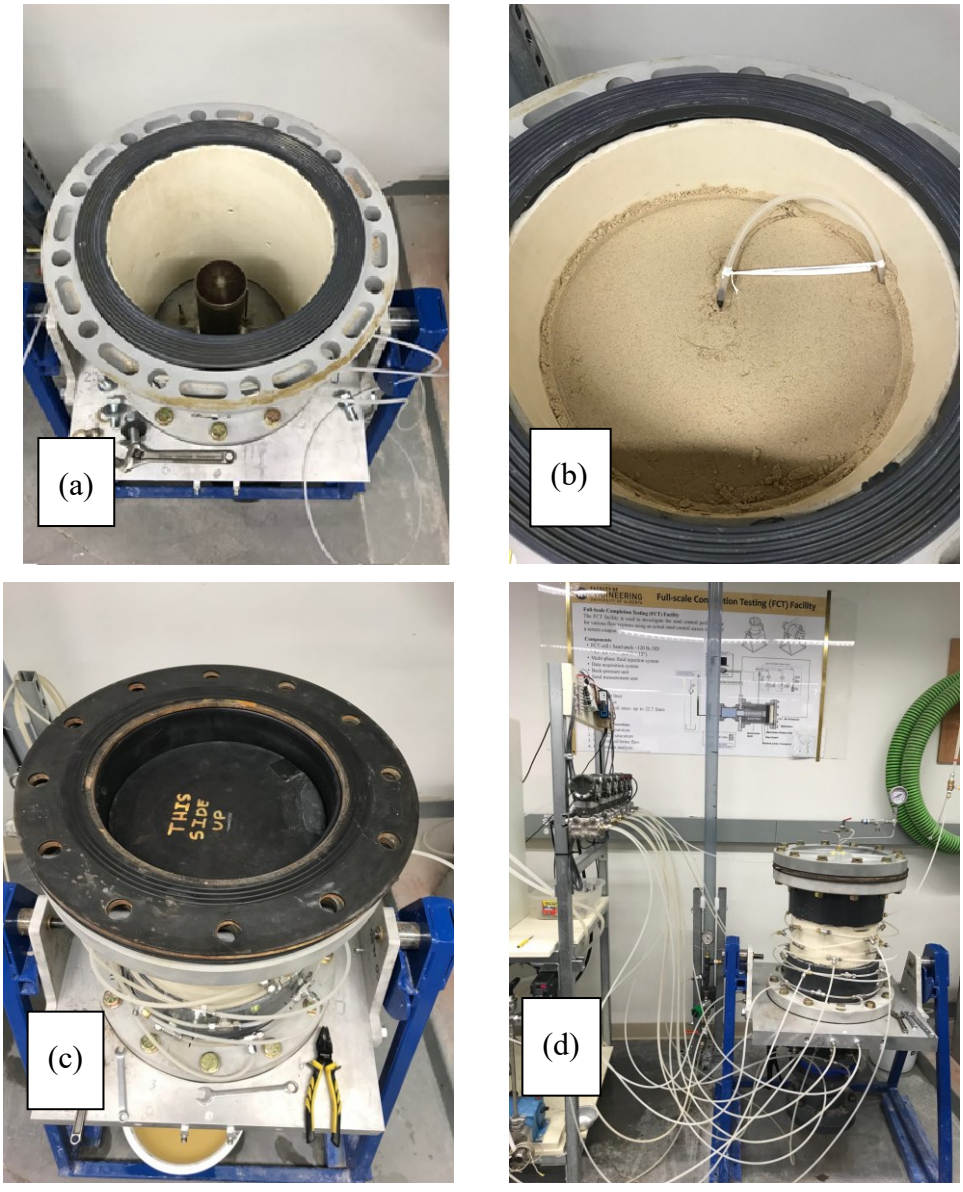

Figure A- 1. Sand packing phase and cell assembly

7) Pressurize the top flange with 20 psi with air using the air supply regulator.

8) Maintain the air pressure for 5 minutes. If the pressure drops more than one psi, then depressurize and remove the top flange.
9) Repeat and troubleshoot until the pressure can be maintained at the top.
10) Connect the sand trap to the base plate. Do not forget to put the gasket on top of the sand trap.
11) Connect the outlet of the pump to the inlet of the back-pressure column (second line on the right pump) (Figure A- 2), then connect the lines to the sand trap (3 lines) for the saturation.
12) Connect the pressure measurement lines to the ports on the base plate sides according to the labels.

A.5 Saturation phase

1) Ensure the connections of the pumps connected to the back-pressure column and the back-pressure column connected to the sand pack (check all three lines) (Figure A- 2).
2) Record the start time of fluid injection (samples have an initial brine saturation of about 60%). Brine is pumped to the back-pressure column at a minimum rate of 8000 cc/hr (5 on the VFD). Based on the past experimental works, it takes almost 3-4 hours to saturate the sand pack with brine thoroughly.
3) Once the water comes out from each FCT cell level through the injection ports, connect the injection lines to it.

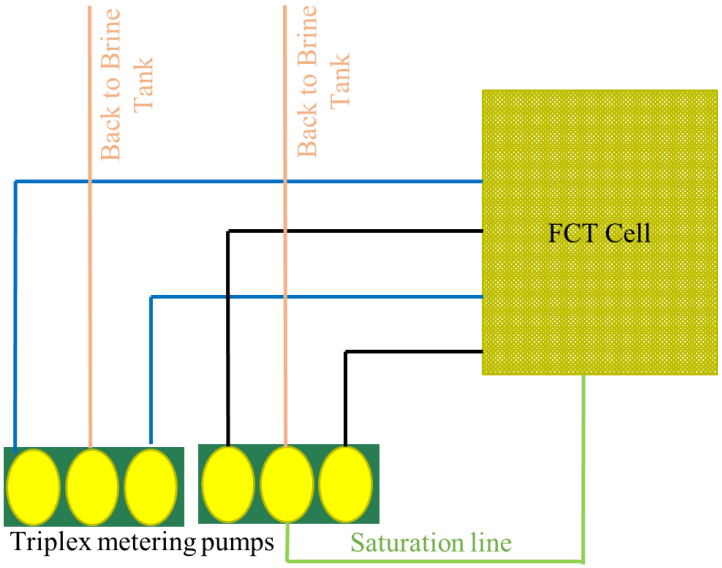

Figure A- 2. Schematic of the injection lines

4) Fully saturation checklist:

a) The outlet produces no bubbles
b) The water rate at the outlet is stabilized (steady-state flow)

5) De-air the connections of the transducers during the saturation.
6) Once the sand pack is saturated with brine, close the valve connecting the back-pressure column with the sand pack.
7) Close the butterfly valve on the sand trap to isolate the produced sand during the saturation and fluid injection.
8) Leave it overnight and then run the test on the next day.

A.6 Fluid Injection

1) Check the pressure inside the diaphragm; adjust it if dropped.
2) Connect the DAQ device to the computer and start the Labview for pressure measurement and recording during the injection. (Note: attach the higher pressure ports first, then the lower pressure ports to avoid damaging the transducers).
3) In the pressure-recording program, check that pressure transducers are working correctly and note the zero-point levels for the six transducers. Rather than focusing on value, the zero-point readings are based on the stabilized trend (zero point changes every time, but the whole tendency does not variate).
4) Set the VFD frequency on the required value for each stage (Table A- 2).

Table A- 2. Flow rate at each stage

Stage No.	1	2	3	4	5	6
Flow rate (cc/hr)	20000	30000	40000	50000	60000	70000
VFD	9	13.5	18.1	22.9	27.6	32.1
Ramp up time (min)	1.8	2.70	3.62	4.58	5.52	6.42

5) Start recording the data acquisition software.
6) Open the valves between the brine tanks and pumps.
7) Start the two pumps simultaneously.
8) Check the pumps; it may be required to shock the pump to be started.
9) During the flow period, do the following:
   a) Collect an effluent sample during the flow ramp-up,
   b) Record the pressure inside the cell and outlet once the flow becomes stable,

c) Record the injection rate once the flow becomes stable,
d) Collect an effluent sample after the flow rate measurement (record the duration that the sample is taken),

10) Continue each stage for 15 minutes and then stop the recording and stop the fluid injection by turning off the pumps and closing the valves.
11) Save the recording files on both computers.
12) Repeat stages 4 to 11 to complete all six injection stages.
13) Close the valves between the brine tanks and pumps.

A.7 Unload and Bleed

1) Start to drain the back-pressure column and then drain the cell.
2) Disconnect all the lines connected to the FCT cell (injection lines and pressure measurement lines) and clean them using water.
3) Release the axial load very slowly.
4) Open the top flange.

A.8 Sampling

1) Take core samples (vertical and horizontal) from the sand pack:
   a) 1 vertical core in front and far from the liner (Figure A- 3a),
   b) Open the nuts by the order and then remove the cell very slowly (lift the cell vertically) and remove the mesh slowly from the sand pack (Figure A- 3b),
   c) 3 horizontal cores from the front view of the sample at the elevations of 3.5”, 6.5”, 9.5” from the bottom. 3 samples should be taken from each core at the intervals with the following distances of 0-0.8’’, 0.8-1.6’’, 1.6’’-end cm from the outer liner surface (Figure A- 3c),
   d) Repeat step (c) for the backside of the sand pack,
   e) 1 vertical core in the back and close to the liner. 5 samples should be taken from each vertical core at the distances of 3.5”, 6.5”, 9.5”, 12” and 14” from the bottom (these locations are relevant to the pressure ports) (Figure A- 3d). The length of each sample taken from vertical cores is 1’’. For instance, sample 6.5 from bottom inches is taken from 6’’ to 7’’,
   f) Be careful not to mix up the samples; use the proper naming system for the samples (Figure A- 3e),

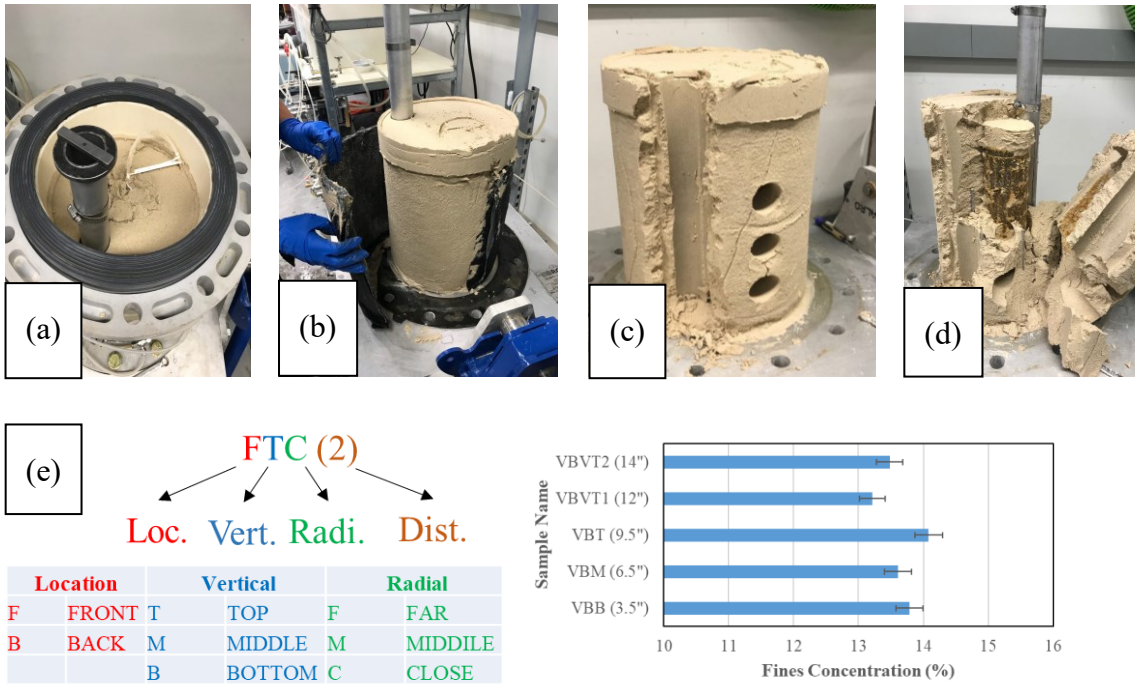

Figure A- 3. Taking core samples from the sand pack and labeling them

2) Disconnect the sand trap very carefully (two people are required for this task) and take the samples:
   a) Produced sand during the flow injection,
   b) Produced sand during the saturation,
3) Remove all the sands around the liner by shaving the liner (Figure A- 4).
4) Take a picture of the liner with a flashlight to check if there is any plugging inside the slots. In this regard, it is better to use a magnifier to check all slits for any plugging inside them (Figure A- 4).
5) Open the liner and take the following samples:
   a) Produced sand inside the liner,
   b) Produced sand inside the slots,
6) Clean everything using the water and compressed air;

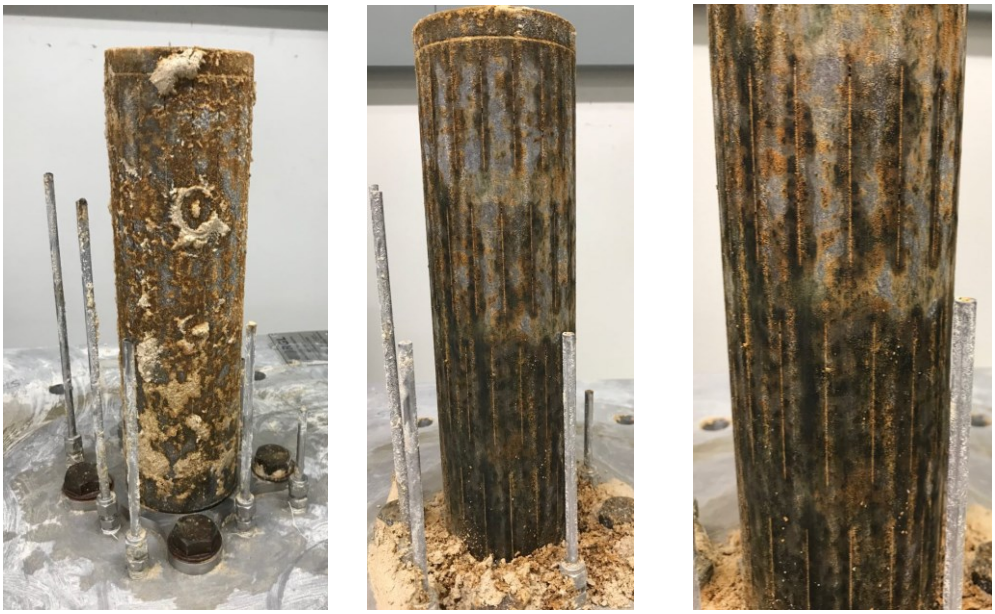

Figure A- 4. The photo illustration of the slotted liner before and after cleaning

A.9 Wet Sieving of Samples Taken from Sand Pack and Original Mixture

1) Leave sand samples in the oven to vaporize all the liquid inside the sand sample.
2) Record the weight of each part and the weight of their containers. Record them in a table shown below (Table A- 3).
3) Crash each part of the sample slowly by mortal and pastel (grinder) and mix with water. Use a blender to mix them thoroughly. Dump the mixture into a specially designed sieve (#325, 44 microns) to separate sand and fines.
4) Take some fluid samples (with washed fines) in small bottles and label them based on the labeling protocol.
5) Wash sand out of the sieve into a container and label the container based on the labeling protocol. Dry the sand in the oven (100°C) for at least 6 hours.
6) Weight the dry sand with the container and record the weight in Table A- 3.

Table A- 3. Wet sieving data recording table

Date:				
Sample Name	**Weight of container (gr)**	**Weight of sand & clay (gr)**	**Weight of dry sand & container (gr)**	**Weight of washed clay (gr)**

A.10 Produced Sand

1) Use the specially designed wet sieve to collect the produced sand.
2) Dry the sand inside the oven.
3) Collect the dry sand in small cups and weigh them.
4) Record the weight of produced sand and label the container based on the labeling protocol.

A.11 Produced Fines

Put the fluid sample into small bottles and put them into the chamber to measure each sample's turbidity. Be sure to shake them before measuring.

Appendix B: Standard Operating Procedure for the Horizontal FCT

B.1 Brine Preparation

1) Check pH and EC from the DI water supplier, pH should be neutral (≈7), and EC should be less than 5 μs/cm.
2) The volume of the brine two tanks is close to 100L.
3) Prepare 100L brine for each test. The concentration of the brine is 400 ppm. For 100L water (100 kg, water density is 1Kg/L), 40g salt should be added.
4) Add adequate salt to the deionized water mix thoroughly to obtain a uniform mixture by using the driller (no deposit at the bottom).
5) The pH should be checked and calibrated using a pH meter whenever brine is prepared. The target pH is 7.9. If adjustment is necessary, sodium bisulfate (NaHSO4) and sodium carbonate (Na2CO3) can lower and increase the pH level, respectively. The addition of the small amount to the brine container is followed by mixing with a stirring drill so that another representative sample can be taken for the pH measurement.

B.2 Sand Pack Preparation

1) 38kg dry commercial sands should be prepared for each test. Prepare the sample in two batches (each one should be 19kg) to be ably mixing them in the mixer.
2) Carefully weigh all the various commercial sands and clays following the recipe in Table B- 1. Pour samples slowly (to prevent loss of fine particles) and uniformly in a plastic mixing container and mixer.

Table B- 1. PSD of the commercial sands

Sand Type	Ind 50	Sil-1	Sil-4	Sil-7	LM 70	LM 125	Helmer Kaolinite
DC-I	-	15.5%	-	-	-	70.0%	14.5%
DC-II	-	13.2%	-	-	79.4%	-	7.4%
DC-III	-	66.1%	-	2.9%	25.7%	-	5.4%
DC-IV	-	-	36.5%	47.1%	6.9%	5.4%	4.2%

3) The dry sand samples are repeatedly mixed inside the mixer for 10 min.

4) Add 3.8 liters (1.9 liters per batch) brine to reach 10% water contain (water contain= total weight of water added / total weight of dry sand). Thoroughly mix all the dry sand and brine to achieve a homogenous moist sample in the sandbox.
5) Take four samples from two batches to define the PSD of the moist sand-mixture sample (beginning of batch 1, end of batch 1, beginning of batch 2, and end of batch 2).

B.3 Setup and liner assembly phase

1) Before the packing procedure, there is a verification of the cleanness of the apparatus parts. Clean the apparatus with water, air, and appropriate detergent in case of oil, precisely the following:
   a) The sand trap connection,
   b) Flowlines,
   c) Clean and gauge the size of the slots,
   d) The brine pump is connected to the back-pressure column to fill the tube, then the volume of brine is released to rinse the back-pressure pipe and the piping.
   e) Inspect, regrease and replace if damaged the O-rings on the liner,
2) Put the mesh inside the pressure ports,
3) Screw the liner to the FCT base plate,
4) Put a gasket to seal the cell and then place the cell on the base plate. Pay attention to adjust marks on the FCT cell to match with marks on the base plate before tightening nuts in order from 1 to 12 (Figure B- 1a),

B.4 Sand packing phase

1) Wrap the mesh by two layers of geotextile and then put it inside the cell.
2) Pack 12 sand layers uniformly in sequence based on a modified approach of the moist tamping method (Ladd 1978) and compact them to reach the target porosity (for DC-I, target porosity is 37%).

   A small rod is used to flatten the surface of the sand. The layer's weight is calculated based on the required porosity of the sand pack and the grain specific gravity. The mass of each layer is around 3656 g. After packing each layer, scratch the surface between the packed layers (use the computer file to record the packing process).
3) Do not forget to install the de-airing tube on the cell before packing layer No.#10 (Figure B- 1b).

4) After packing all the layers, put the de-airing tube on top of the sand pack and place the specially designed diaphragm on top of the sand pack (Figure B- 1c).
5) Ensure the diaphragm edges are at the rim of the cell top gasket to secure the piston in place and prevent leaks (Figure B- 1c).
6) Install the top flange to seal the unit, and then tighten the nuts in a cross fashion to prevent over-torque and damage to the top flange (Figure B- 1d).

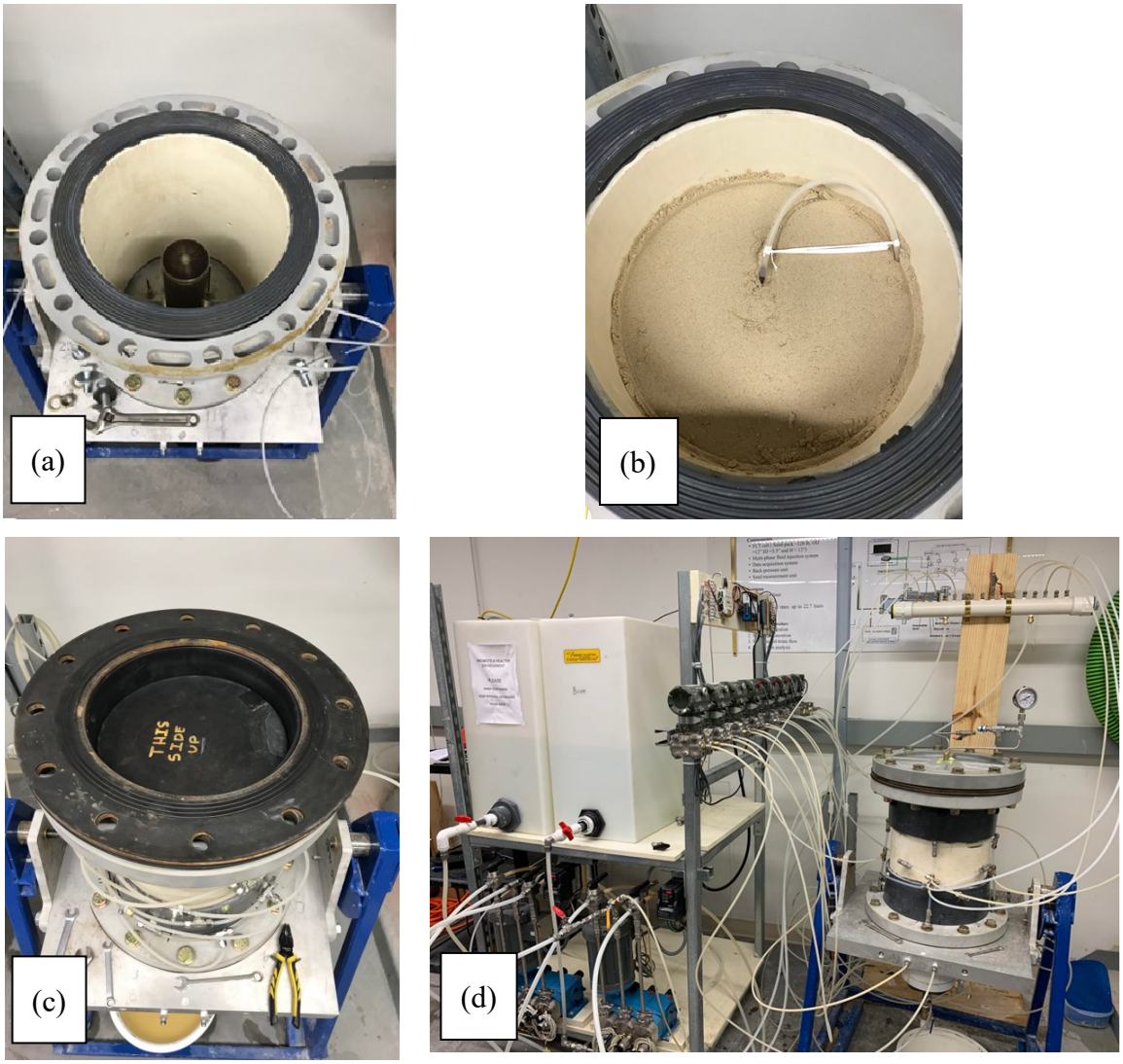

Figure B- 1. Sand packing phase and cell assembly

7) Pressurize the top flange with 20 psi with air using the air supply regulator.
8) Maintain the air pressure for 5 minutes. If the pressure drops more than one psi, then depressurize and remove the top flange.
9) Repeat and troubleshoot until the pressure can be maintained at the top.

10) Connect the sand trap to the base plate. Do not forget to put the gasket on top of the sand trap (two people are required to install the sand trap).
11) Connect the outlet of the pump to the inlet of the back-pressure column (second line on the right pump), then connect the lines to the sand trap (3 lines) for the saturation phase.
12) Connect the pressure measurement lines to the ports on the base plate sides according to the labels. For the horizontal tests, seven pressure transducers are used.

B.5 Saturation phase

1) Ensure that the pump's connections are connected to the back-pressure column, and the back-pressure column is connected to the sand pack.
2) Record the start time of fluid injection (samples have an initial brine saturation of about 60%). Brine is pumped to the back-pressure column at a minimum rate of 8000 cc/hr (5 on the VFD). The previous tests take almost 3-4 hours to saturate the sand pack with brine thoroughly.
3) Once the water comes out from each level of the FCT cell through the injection ports, connect the injection lines to each level. In horizontal FCT, brine flows into the manifold from the two pumps and then flows into the cell via the injection ports. There are eight injection lines from the flow manifold to deliver brine to 16 injection ports. A set of two ports located at the same level would be injected by only one flowline.
4) Fully saturation checklist:
    a) The outlet produces no bubbles,
    b) The water rate at the outlet is stabilized (steady-state flow)
5) De-air the connections of the transducers during the saturation.
6) Once the sand pack is saturated with brine, close the valve connecting the back-pressure column with the sand pack.
7) Close the butterfly valve on the sand trap to isolate the produced sand during the saturation and fluid injection.
8) Release the base plate's lock and rotate the cell very slowly to put it in the horizontal direction and then lock the base plate again (Figure B- 2).
9) Leave it overnight to saturate the whole sand pack fully.
10) De-air the connections of the transducers one more time on the next day
11) Run the test

Figure B- 2**.** The FCT cell assembly in the horizontal direction

B.6 Fluid Injection

1) Check the pressure inside the diaphragm; adjust it if dropped.
2) Connect the DAQ device to the computer and start the Labview for pressure measurement and recording during the injection. (Note: attach the higher pressure ports first, then the lower pressure ports to avoid damaging the transducers)
3) In the pressure-recording program, check that pressure transducers are working correctly and note the zero-point levels for the seven transducers. Rather than focusing on value, the zero-point readings are based on the stabilized trend (zero point changes every time, but the whole tendency does not variate).
4) Set the VFD frequency on each stage's required value (Table B- 2).

Table B- 2. Flow rate at each stage

Stage No.	1	2	3	4	5	6
Flow rate (cc/hr)	20000	30000	40000	50000	60000	70000
VFD	9	13.5	18.1	22.9	27.6	32.1
Ramp up time (min)	1.8	2.70	3.62	4.58	5.52	6.42

5) Start recording the data acquisition software.
6) Open the valves between the brine tanks and pumps.
7) Start the two pumps simultaneously.
8) Check the pumps; it may be required to shock the pump to be started.

9) During the flow period, do the following:
    a) Collect an effluent sample during the flow ramp-up,
    b) Record the pressure inside the cell and outlet once the flow becomes stable,
    c) Record the injection rate once the flow becomes stable,
    d) Collect an effluent sample after the flow rate measurement (record the duration that the sample is taken),
10) Continue each stage for 15 minutes and then stop the recording and stop the fluid injection by turning off the pumps and closing the valves.
11) Save the recording files on both computers.
12) Repeat stages 4 to 11 to complete all six injection stages.
13) Close the valves between the brine tanks and pumps.
14) Return the cell to the vertical position very slowly.

B.7 Unload and Bleed

1) Start to drain the back-pressure column and then drain the cell.
2) Disconnect all the lines connected to the FCT cell (injection lines and pressure measurement lines) and clean them using water.
3) Release the axial load very slowly.
4) Open the top flange.

B.8 Sampling

1) Take core samples (vertical and horizontal) from the sand pack:
    a) Open the nuts by the order and then remove the cell very slowly (lift the cell vertically) and remove the mesh slowly from the sand pack,
    b) 3 horizontal cores should be collected from the sample front view at the elevations of 3.5”, 6.5”, 9.5” from the bottom. 4 samples should be taken from each horizontal core at the intervals with the following distances of 0-0.8’’, 0.8-1.6’’, 1.6-2.4’’, and 2.4’’-end from the outer liner surface (Figure B- 3a),
    c) Repeat step (c) for the other sides (left, right, and back sides of the sand pack),
    d) 5 horizontal samples in front and far from the liner at the same radial distance; the samples should be taken at the elevation of 3.5”, 6.5”, 9.5”, 12” and 14” from the bottom (these elevations are relevant to the pressure ports) (Figure B- 3b). It is noted that these samples are the vertical samples in the vertical FCT test. The sample

locations are the same between the vertical and horizontal tests. The difference is the method to collect the sample. The length of each vertical sample is 1 inch,

e) Repeat step (d) for the back and close to the liner to collect 5 samples at the equal radial distance (Figure B- 3c),

f) Be careful not to mix up the samples; use the proper naming system for the samples (Figure B- 3d),

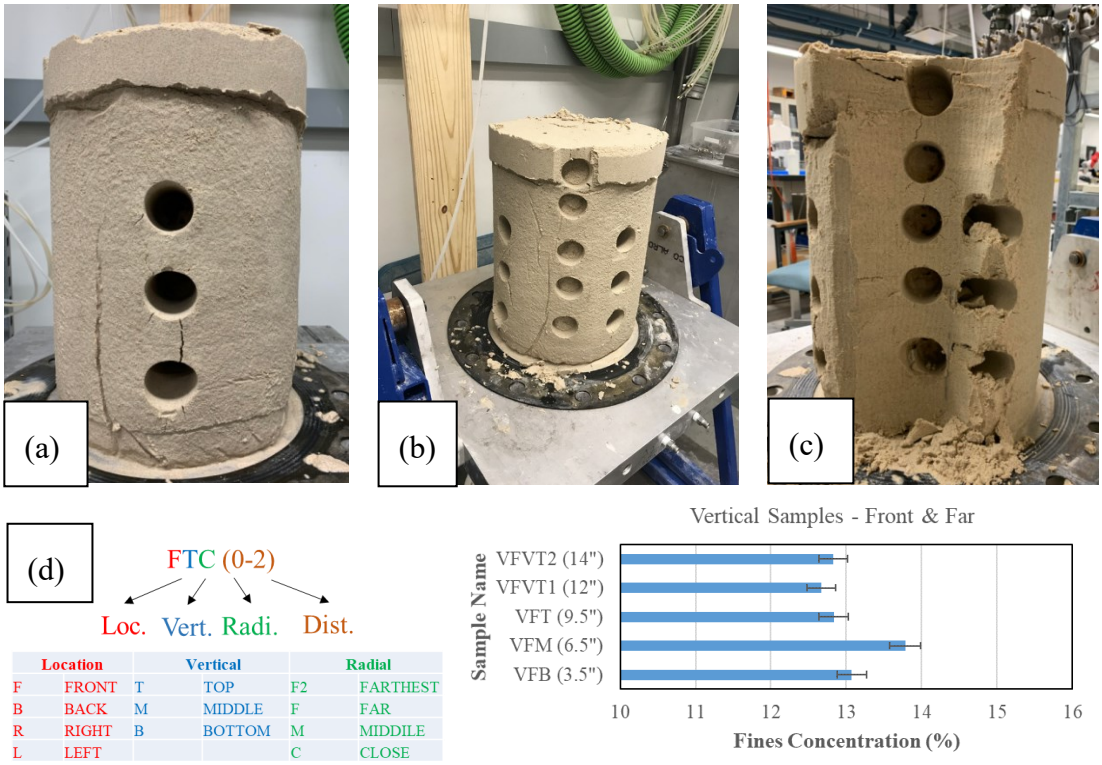

Figure B- 3. Taking core samples from the sand pack and labeling them

2) Disconnect the sand trap very carefully and take the samples:
   a) Produced sand during the flow injection,
   b) Produced sand during the saturation,
3) Remove all the sands around the liner by shaving the liner (Figure B- 4).
4) Take a picture of the liner with a flashlight to check if there is any plugging inside the slots. In this regard, it is better to use a magnifier to check all slits for any plugging inside them (Figure B- 4),
5) Open the liner and take the following samples:
   a) Produced sand inside the liner,

b) Produced sand inside the slot,

6) Clean everything using the water and compressed air;

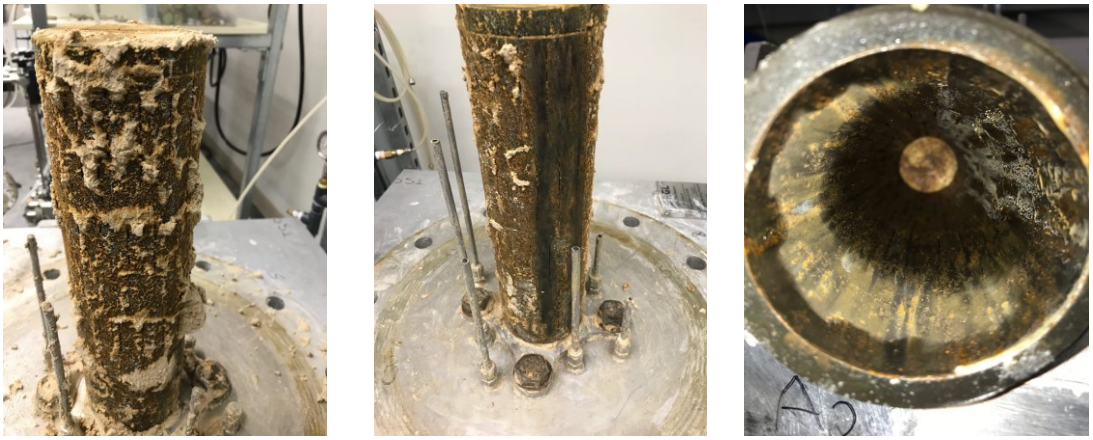

Figure B- 4. The photo illustration of the slotted liner before and after cleaning

B.9 Wet Sieving of Samples Taken from Sand Pack and Original Mixture

1) Leave sand samples in the oven to vaporize all the liquid in the sand sample.
2) Record the weight of each part and the weight of their containers. Record them in a table shown below (Table B- 3).
3) Crash each part of the sample slowly by mortal and pastel (grinder) and mix with water. Use a blender to mix them thoroughly. Dump the mixture into the specially designed sieve (#325, 44 microns) to separate sand and fines.
4) Take some fluid samples (with washed fines) in small bottles and label them based on the labeling protocol.
5) Wash sand out of the sieve into a container and label it based on the labeling protocol. Dry the sand in the oven (100°C) for at least 6 hours.
6) Weigh the dry sand with the container and record the weight in Table B- 3.

Table B- 3. Wet sieving data recording table

Date:				
Sample Name	**Weight of container (gr)**	**Weight of sand & clay (gr)**	**Weight of dry sand & container (gr)**	**Weight of washed clay (gr)**

B.10 Produced Sand

1) Use the specially designed wet sieve to collect the produced sand.
2) Dry the sand inside the oven.
3) Collect the dry sand in small cups and weigh them.
4) Record the weight of produced sand and label the container based on the labeling protocol.

B.11 Produced Fines

Put the fluid sample into small bottles and put them into the chamber to measure each sample's turbidity. Be sure to shake them before measuring.